Remarks

Claims 1-13, 32-57, and 60-69 are pending in the subject application. By this Amendment, Applicant has canceled claims 33-35 and 67 and amended claim 1. Entry and consideration of the amendments presented herein is respectfully requested. Accordingly, claims 1-13, 32, 36-57, 60-66, 68,and 69 are currently before the Examiner. Favorable consideration of the pending claims is respectfully requested.

Claim 67 is objected to because of informalities. The Examiner indicates that claim 67 depends from itself. Applicant gratefully acknowledges the Examiner's careful review of the claims. By this Amendment, Applicant has canceled claim 67. Accordingly, reconsideration and withdrawal of the objection is respectfully requested.

Claims 33-35 are rejected under 35 USC §112, second paragraph, on the grounds that the limitation "said host cell" lacks antecedent basis. Applicant has canceled claims 33-35, thereby rendering the rejection moot. Accordingly, reconsideration and withdrawal of the rejection under 35 USC §112, second paragraph, is respectfully requested.

Claims 62, 63, 66, 67, and 69 are rejected under 35 USC §112, first paragraph, as lacking sufficient written description. The Examiner asserts that the specification does not teach any mutations in CFTR polypeptides that do not also include the ΔF508 mutation. Applicant respectfully traverses this rejection.

Applicant respectfully asserts that the subject specification does provide written description for CFTR polypeptides having mutations other than the ΔF508 mutation and not in combination with the ΔF508 mutation. Applicant notes that the subject application, at page 21, lines 14-24, does disclose individual mutations (ΔI507, S549R, and G551D) within a CFTR polypeptide that are not in combination with the ΔF508 mutation. In addition, many mutations in CFTR other than ΔF508, and not in combination with ΔF508, were known in the art as of the filing date of the subject application. As the Examiner is undoubtedly aware, there is no requirement that a specification teach that which is well known in the art. *Hybritech, Inc. v. Monoclonal Antibodies, Inc.*, 231 USPQ 81 (Fed. Cir. 1986) citing *Lindemann Maschinenfabrik v. American Hoist and Derrick*, 221 USPQ 481 (Fed. Cir. 1984), (". . . a patent need not teach, and preferably omits, what is well known in the art."). Moreover, the claims encompass any mutation in a CFTR polypeptide other than the ΔF508

mutation. Thus, any amino acid substitution, deletion, *etc.* other than the ΔF508 mutation is contemplated. This encompasses millions of possible mutations of a CFTR polypeptide. While each possible mutation could be recited in the subject application, doing so would not be an efficient use of Applicant's resources or the Patent Office's resources. Applicant notes that the claim language does not require that the effect of the mutation on CFTR function or activity be known or disclosed; therefore such disclosure in the application is not required in order to satisfy the written description requirement of 35 USC §112. In view of the above remarks, reconsideration and withdrawal of the rejection under 35 USC §112, first paragraph, is respectfully requested.

Claims 1-3, 5-10, 13, 32-34, 36-41, 44-47, 49-54, and 57 are rejected under 35 §USC 103(a) as obvious over Zerhusen *et al.* (1999) in view of Fields *et al.* (U.S. Patent No. 5,667,973). Claims 1-10, 13, 32-41, 44-54, and 57 are also rejected under 35 USC §103(a) as obvious over Zerhusen *et al.* (1999) and Fields *et al.,* and in further view of Payan *et al.* (U.S. Patent No. 6,316,223). Claims 1-3, 5-13, 32-34, 36-47, and 49-57 are rejected under 35 USC §103(a) as obvious over Zerhusen *et al.* (1999) and Fields *et al.*, and in further view of Neville *et al.* (1998). Claims 1-3, 5-10, 13, 32-34, 36-41, 44-47, 49-54, 57, 60, 64, and 68 are rejected under 35 USC §103(a) as obvious over Zerhusen *et al.* (1999) in view of Fields *et al.*, and in further view of Serebriiskii *et al.* (1999). Claims 1-3, 5-10, 13, 32-34, 36-41, 44-47, 49-54, 57, 61, 65, and 67 are newly rejected under 35 USC §103(a) as obvious over Zerhusen *et al.* (1999) in view of Fields *et al.* and Neville *et al.* (1998), and in further view of Brown *et al.* (1997). Applicant will address these rejections together as each rejection relies on the primary references of Zerhusen *et al.* and Fields *et al.*

Zerhusen *et al.* is cited as teaching that CFTR forms dimers. Fields *et al.* is cited as teaching that the interaction of two polypeptides can be detected by the method of the yeast two-hybrid system. The Neville *et al.* reference is cited as teaching that CFTR interaction occurs at the NBD1 domain and is affected by the ΔF508 mutation. The Serebriiskii *et al.* reference is cited as teaching a two-hybrid method performed with a LexA binding domain and a transcriptional activator for *lacZ.* The Brown *et al.* reference is cited as teaching incubating a host cell containing a ΔF508 mutation in CTFR at a non-permissive temperature. The Examiner states that these references taken together would have made it obvious to one skilled in the art at the time of Applicant's invention to detect the interaction of CTFR proteins in the yeast two-hybrid system. Applicant respectfully traverses these

grounds of rejection.

Applicant respectfully asserts that the cited references do not teach or suggest the claimed invention. The Zerhusen *et al.* reference is the primary reference for each of the §103 rejections. The Examiner asserts that the Zerhusen *et al.* reference teaches a dimer. However, the Examiner further points out that the Zerhusen *et al.* reference also teaches that "more information is needed to determine which portions of the CFTR molecule are involved in the contact interaction." If "more information" was needed to determine which portions of the molecule are involved in the contact interaction as indicated by Zerhusen *et al.*, then it cannot have been obvious which CFTR domains were involved in the interaction. More specifically, it was not obvious that NBD1 domains would be involved in the formation of a CFTR dimer. Applicant notes that the claimed method requires that the NBD1 domain of the first CFTR polypeptide interact with the NBD1 domain of the second polypeptide in order for the detector gene to be expressed.

Neither the Fields *et al.* patent, nor the Payan *et al.* patent, nor the Serebriiskii *et al.* reference, nor the Brown *et al.* reference teach or suggest anything regarding the domains involved in CFTR dimer formation and, therefore, these references do not teach or suggest that CFTR NBD1 domains interact in the formation of CFTR dimers.

Applicant maintains that the Neville *et al.* reference does not teach or suggest CFTR protein-protein interaction, nor does it teach that CFTR NBD1 domains interact; therefore, the Neville *et al.* reference does not cure the deficiency of the Zerhusen *et al.* reference. Rather, the Neville *et al.* reference only teaches that the R-domain of CFTR interacts with the NBD1 domain. In the instant Office Action, the Examiner did not address any of Applicant's comments regarding the teachings of Neville *et al.* and the deficiencies thereof. There is no data in the Neville *et al.* reference that teaches or suggests that NBD1 domains form dimers. The Neville *et al.* reference is focused solely on the effect of the NBD1 domain on phosphorylation of the R-domain in an NBD1/R-domain fusion. If anything, the focus of the Neville *et al.* reference on the R-domain interaction with the NBD1 domain teaches away from Applicant's claimed invention. Thus, none of the references cited in the §103 rejections teach or suggest that NBD1 domains can interact and are involved in the formation of CFTR dimers.

Kiser *et al.* publicly disclosed the following abstract at the 1996 International Cystic Fibrosis meeting:

Kiser GL, Chang XB, and Riordan JR. (1996) "Two-hybrid analysis of CFTR domain interactions"(Abstract). *Pediatr. Pulmonol. Suppl.* 13: 213.

The public disclosure by Kiser *et al.*, which is evidence as to the state of the art in 1996, described numerous two-hybrid constructs that were made to detect intramolecular interactions between various CFTR cytosolic domains. Although interactions were detected between various cytosolic CFTR domains (the amino terminus and cytosolic loops) and the R-domain, there was no evidence provided to suggest an interaction between two NBD1 domains (*i.e.*, dimerization of NBD1), even though constructs were made to specifically test for such an interaction. Presumably, the particular segment of NBD1 chosen for construction of the GAL4 fusion constructs in the Kiser *et al.* experiments did not properly old in a manner that would allow dimer formation *in vivo*. This presentation demonstrated that other CFTR intramolecular interactions occur and could be involved in forming CFTR dimers and thus, taught away from NBD1 dimerzation. Prior art that teaches away from a claimed invention has long been accepted as indicia of non-obviousness of the invention. *United States v. Adams*, 383 U.S. 39, 52 (1966).

The Kiser *et al.* abstract is referenced in a publication in Wang *et al.* (Wenlan Wang, Zhaoping He, Thomas J. O'Shaughnessy, John Rux and William W. Reenstra (2002) "Domain-domain associations in cystic fibrosis transmembrane conductance regulator." *Am. J. Physiol. Cell Physiol.* 282:1170-1180). In the Wang *et al.* publication, the authors state therein that "Yeast two-hybrid studies suggest the presence of interactions between intracellular domains and intracellular loops in the transmembrane domains . . .." Since the Wang *et al.* reference is principally concerned with CFTR domain-domain interactions, the authors would undoubtedly have highlighted any result from Kiser *et al.* indicating NBD1 dimerization. The absence of any reference to NBD1 dimerization demonstrates that the art at the time of these references (1996-2002) taught interactions between domains <u>other</u> <u>than</u> <u>NBD1</u> dimerization.

Applicant also notes that the Examiner is not convinced that there was uncertainty in the field as to whether CFTR formed dimers or existed as a monomer. The Examiner cites Eskandari *et al.*

(1998) as a reference that offers evidence that CFTR forms dimers and further comments that only one reference was provided by Applicant that supports CFTR as a monomer. Two additional references are listed below that specifically argue that CFTR exists as a monomer and not as a dimer.

> M Ramjeesingh, C Li, I Kogan, Y Wang, LJ Huan, CE Bear (2001) "A monomer is the minimum functional unit required for channel and ATPase activity of the cystic fibrosis transmembrane conductance regulator." *Biochemistry* 40: 10700-6.
>
> JH Chen, XB Chang, AA Aleksandrov, JR Riordan (2002) "CFTR is a monomer: biochemical and functional evidence." *J. Membr. Biol.* 188: 55-71.

If there was no controversy regarding the monomer vs. dimer state of CFTR at the time of the filing of the subject application, then why were two major CFTR laboratories pursuing research that led them to conclude that CFTR was a monomer? Clearly these research groups held a view that CFTR did not form dimers (in October 1999) and thus pursued experiments to support their view.

Applicant also respectfully asserts that if a protein forms a dimer, it cannot be predicted in advance which domains of the protein will be involved in the protein:protein interaction required for dimer formation. In other words, the domains of a protein that are involved in dimerization can only be determined empirically. For example, in the Pak1 protein kinase of *Schizosaccharomyces pombe*, the regulatory domain of PAK1 protein binds to the PAK1 kinase catalytic domain, forming an inactive dimer (Tu H and Wigler M. (1999) "Genetic evidence for Pak1 autoinhibition and its release by Cdc42." *Mol. Cell Biol.* 19:602-11). The use of two-hybrid constructs showed that the kinase is released from autoinhibition by Cdc42, which disrupts the dimer. In this example, the dimer forms results from the interaction of two different parts of the Pak1 protein. There was no way of predicting this is the absence of the research studies performed to investigate what parts of the protein were involved. Likewise, a person of ordinary skill in the art at the time of Applicant's invention could not have predicted, but could have speculated the dimer formation of CFTR to involve different domains of the CFTR polypeptide, particularly in view of the results of Kiser *et al.* discussed above.

In summary, even if one were to acknowledge, *arguendo*, that the Zerhusen *et al.* reference teaches CFTR dimers, this was not universally accepted at the time of the filing of the present application as indicated by the Ramjeesingh *et al.* and Chen *et al.* references. A person of ordinary

skill in the art was just as likely to have believed that CFTR did not form as dimers as he or she was to have believed that CFTR did form dimers. Thus, a person of ordinary skill in the art at the time of Applicant's invention would not have had the requisite "reasonable expectation of success" in arriving at the claimed invention. As the Examiner is aware, it is well established in patent law that in order to support a *prima facie* case of obviousness, a person of ordinary skill in the art must find both the suggestion of the claimed invention, and a reasonable expectation of success in making that invention, solely in light of the teachings of the prior art. *In re Dow Chemical Co.*, 5 USPQ2d 1529, 1531 (Fed. Cir. 1988).

Moreover, even if a CFTR dimer was assumed to have been known in the art (which Applicant maintains is not the case), there would be no reason to expect the CFTR dimer would involve CFTR NBD1 interaction, which is an explicit element of the claimed invention. All claim limitations must be considered and all claim limitations must be found in the prior art; claim limitations missing from the prior art cannot be ignored. *In re Evanega*, 4 USPQ2d 1249 (Fed. Cir. 1987). As noted above, Kiser *et al.* presented data in 1996 that argued against CFTR NBD1 self interaction and argued in favor of interactions between intracellular loops and other intracellular domains such as the R-domain. Thus, the state of the art at the time of Applicant's invention taught that intramolecular CFTR interactions other than NBD1 self-association occur and would be the most likely interactions to be involved in CFTR dimer formation. This is also consistent with the Tu *et al.* reference which showed homodimer formation as result of the interaction of dissimilar domains.

In view of the above remarks, Applicant respectfully asserts that the cited references do not teach or suggest the claimed invention and a person of ordinary skill in the art would not have had a reasonable expectation of success in arriving at Applicant's claimed invention. Thus, Applicant maintains that the claimed invention is not obvious over the cited references. Accordingly, reconsideration and withdrawal of the rejections under 35 USC §103(a) is respectfully requested.

It should be understood that the amendments presented herein have been made solely to expedite prosecution of the subject application to completion and should not be construed as an indication of Applicant's agreement with or acquiescence in the Examiner's position.

J:\fsu\100C2XC1\pTO-Misc\Amd2.doc/DNB/kmm

In view of the foregoing remarks and amendments to the claims, Applicant believes that the currently pending claims are in condition for allowance, and such action is respectfully requested.

The Commissioner is hereby authorized to charge any fees under 37 CFR §§1.16 or 1.17 as required by this paper to Deposit Account No. 19-0065.

Applicant invites the Examiner to call the undersigned if clarification is needed on any of this response, or if the Examiner believes a telephonic interview would expedite the prosecution of the subject application to completion.

Respectfully submitted,

Doran R. Pace
Patent Attorney
Registration No. 38,261
Phone No.: 352-375-8100
Fax No.: 352-372-5800
Address: P.O. Box 142950
Gainesville, FL 32614-2950

DRP/kmm
Attachments: Wang *et al.* (2002); Chen *et al.* (2002); Ramjeesingh *et al.* (2001); Tu and Wigler (1999).

MOLECULAR AND CELLULAR BIOLOGY, Jan. 1999, p. 602–611 Vol. 19, No. 1
0270-7306/99/$04.00+0

Genetic Evidence for Pak1 Autoinhibition and Its Release by Cdc42

HUA TU[1,2]† AND MIKE WIGLER[1]*

Cold Spring Harbor Laboratory, Cold Spring Harbor, New York 11724,[1] and Department of Biochemistry and Cell Biology, State University of New York at Stony Brook, Stony Brook, New York 11794[2]

Received 4 June 1998/Returned for modification 6 July 1998/Accepted 15 September 1998

Pak1 protein kinase of *Schizosaccharomyces pombe*, a member of the p21-GTPase-activated protein kinase (PAK) family, participates in signaling pathways including sexual differentiation and morphogenesis. The regulatory domain of PAK proteins is thought to inhibit the kinase catalytic domain, as truncation of this region renders kinases more active. Here we report the detection in the two-hybrid system of the interaction between Pak1 regulatory domain and the kinase catalytic domain. Pak1 catalytic domain binds to the same highly conserved region on the regulatory domain that binds Cdc42, a GTPase protein capable of activating Pak1. Two-hybrid, mutant, and genetic analyses indicated that this intramolecular interaction rendered the kinase in a closed and inactive configuration. We show that Cdc42 can induce an open configuration of Pak1. We propose that Cdc42 interaction disrupts the intramolecular interactions of Pak1, thereby releasing the kinase from autoinhibition.

The p21-GTPase-activated protein kinase (PAK) family is present in all eukaryotes. Genetic evidence suggests that STE20, one of three *Saccharomyces cerevisiae* homologs of PAK, mediates signaling of pheromone response from receptor-coupled heterotrimeric G proteins to the mitogen-activated protein kinase (MAPK) cascade, which includes STE11, STE7, and the pair FUS3 and KSS1 (13, 14, 28). STE20 can phosphorylate STE11 in vitro (25, 36). Another homolog, CLA4, appears to regulate normal localization of cell growth and cytokinesis (7), and a third, SKM1, has broad functions in morphogenesis and growth (20). In the fission yeast, *Schizosaccharomyces pombe*, Pak1 (also known as Shk1) seems to be involved in both sexual differentiation and morphogenesis (17) and has a structural and functional homolog, Shk2 (26, 37). Pak1 has been shown to release the intramolecular and, presumably, autoinhibitory interactions of Byr2, the *S. pombe* homolog of STE11 (31). Mammalian PAK proteins have three major isoforms, and they appear to be mediators of signaling from members of the p21-GTPase family such as Rac1 and Cdc42 to the MAPKs including Jun kinase and p38 MAPKs (1, 3, 6, 11, 23, 27, 38).

All PAKs have an N-terminal regulatory domain and a conserved C-terminal kinase catalytic domain. The regulatory domains are poorly conserved except for a 70-amino-acid stretch, named CRIB (Cdc42-Rac interactive binding) domain, which is known to bind the small Rho-family GTPases (4). Cdc42 can activate PAK proteins in vitro, inducing a PAK autophosphorylation event (16). Two mechanistic models are consistent with the in vitro biochemical data: Cdc42-Rac directly induces an active conformation of the catalytic region, or the GTPases antagonize an autoinhibitory mechanism.

We have been utilizing genetic analysis and the two-hybrid system of Fields and Song (8) to probe the regulatory mechanisms of kinases in the RAS signaling pathways of yeast and mammalian systems (2, 5, 17, 18, 31, 32, 35). Byr2, one of the *S. pombe* Ras1 effectors that is required for sexual differentiation, has been analyzed in this way (31). The regulatory domain of Byr2 was found to bind to the kinase catalytic domain, and mutants in the regulatory domain that abolish this interaction were activating. Two-hybrid analysis has shown that this autoinhibitory intramolecular interaction also keeps the kinase in a closed configuration. With further analysis, we demonstrated that dominant activated Pak1 induced the open configuration of Byr2. Previous studies had strongly suggested a role for Pak1 in the integrity of the sexual differentiation pathways (17).

Using methods similar to those we have described previously, we have discovered an intramolecular interaction between the regulatory and catalytic domains of Pak1. The catalytic domain binds to the same highly conserved region on the regulatory domain that also binds Cdc42, and we have shown that wild-type Pak1 exists in a closed configuration with the kinase catalytic domain masked. We used these observations to isolate Pak1 mutants that are in an open configuration, with an accessible catalytic domain. Binding analysis of the regulatory domains of these Pak1 mutants has shown that they all have lost the ability to bind the catalytic domain. These results demonstrate that the intramolecular interaction keeps the kinase in a closed configuration. Moreover, in three different genetic assays, we have shown that most of these Pak1 mutants are more active than the wild-type kinase. Therefore, an autoinhibitory role for the intramolecular interaction is strongly suggested. Consistent with the in vitro result that Cdc42 induces PAK autophosphorylation (16), we have found that Cdc42 can induce the open configuration of Pak1 in vivo. Based on the conservation among PAK proteins, we propose that kinase autoinhibition and Cdc42 release of autoinhibition are general regulatory mechanisms for these protein kinases.

MATERIALS AND METHODS

Yeast, media, and genetic manipulations. *S. cerevisiae* L40, a *lexA*-based two-hybrid reporter strain with both *HIS3* and *lacZ* as reporter genes (33), was used to study two-hybrid interactions. AN43-5A has a *FUS1-lacZ* reporter system and was used to measure the activity of the *S. cerevisiae* mating signaling pathway (17). *S. cerevisiae* cultures were grown in YPD (2% peptone, 1% yeast extract, 2% glucose) or in dropout (DO) synthetic minimal medium (0.67% yeast nitro-

* Corresponding author. Mailing address: Cold Spring Harbor Laboratory, Cold Spring Harbor, NY 11724. Phone: (516) 367-8376. Fax: (516) 367-8381. E-mail: wigler@cshl.org.

† Present address: Tularik, Inc., South San Francisco, CA 94080.

gen base without amino acids, 2% glucose) with appropriate auxotrophic supplements. The lithium acetate protocol was used for yeast transformation (12).

Generating Pak1 and Cdc42 clones. PCR (24) was used to generate all constructs. Pak1-Cat, the kinase catalytic domain of Pak1 that encodes the C-terminal 385 amino acids, was made previously (31). Pak1-Reg, which encodes the N-terminal 284 amino acids, was made with the following pair of oligonucleotides (boldfacing indicates restriction enzyme sites): AAGGATCCGATGGA AAGAGGGACTTTACAA, which contains a *Bam*HI site, and GGGGGGTT GTCGACTAGCATTAGAGGTAGTAGTTTTAAC, which contains a *Sal*I site. The PCR product was digested with *Bam*HI and *Sal*I and cloned into pGAD and pLBD vectors. Full-length Pak1 was made by fusing Pak1-Reg to the C-terminal 375 amino acids of Pak1, which was generated by PCR with the following pair of oligonucleotides: CCCCCCAGTCGACAACCTTCTCCATTAGTTTCCAGC AAG and AAGGATCCCTGCACGTATTTACCAGAATGATGTATGGA. The 658-amino-acid full-length Pak1 clone thus had a new *Sal*I site but was identical to wild-type full-length Pak1 at the amino acid level. $Cdc42^{wt}$ and $Cdc42^{V12}$ were made by PCR with the primer pair GGGGATCCGATGCCC ACCATTAAGTGTGTCGTAGTA, which contains a *Bam*HI site, and CCCTT GGGTCGACTGCAGTTACAGTACCAAACACTTTGACTTTTT, which contains an overlapping *Sal*I site and a *Pst*I site. The templates for the PCRs were pREP-$Cdc42^{wt}$ and pREP-$Cdc42^{V12}$ (kindly provided by Doug Johnson, University of Vermont). Cdc42 sequences were cloned into pGAD and pLBD. Cdc42 clones with a C189S mutation were made by PCR with the primer pair GGGGATCCGATGCCCACCATTAAGTGTGTCGTAGTA, which contains a *Bam*HI site, and CCCCGTCGACAGTACCAAAGACTTTGACTTTTTCTTGT GAGGAAC, which contains the C189S mutation and a *Sal*I site. $Cdc42^{C189S}$ sequences were cloned into pGAD, pLBD, and pLS104.

Detection of protein complex formation by the yeast two-hybrid system. To determine if GAD fusions interact with LBD fusions in the two-hybrid system, the two fusions were transformed into L40 by the standard lithium acetate yeast transformation procedure. Cells were plated onto synthetic medium lacking leucine and tryptophan (DO-LT). Transformants were patched out on fresh DO-LT plates and examined for histidine prototrophy and β-galactosidase synthesis, since two-hybrid interactions result in transactivation of *lexA-HIS3* and *lexA-lacZ*. Histidine prototrophy was tested by replicating patches onto medium lacking leucine, tryptophan, and histidine (DO-LTH) and was evident by growth on the His^- plates. β-Galactosidase filter assay and liquid assay were conducted as previously described (32). 5-Bromo-4-chloro-3-indolyl-β-D-galactopyranoside (X-Gal) was used as the substrate in the β-galactosidase filter assay. *o*-Nitrophenyl-β-D-galactopyranoside (ONPG) was used as the substrate in the β-galactosidase liquid assay for quantitative measurement.

Making Pak1 regulatory segment fusions by PCR. Four Pak1 regulatory segments, each about 70 amino acids long, were made by PCR. The DNA fragment that encodes the first 70 amino acids of Pak1 was made by PCR with the oligonucleotide pair of AAGGATCCGATGGAAAGAGGGACTTTACAA and GGGGGTCGACTAGGATTGAGATAAAGGGAAACCGGA; the second 70-amino-acid fragment was made with the oligonucleotide pair of GTGGATCCA ATGCGTACAACTGTATCTAGGGTTTCA and GGGGGTCGACTAGCTG GCAGAGCCTGACCCATAGGA; the third 70-amino-acid fragment was made with the oligonucleotide pair of GTGGATCCAATGCCTCGCAAATCGACT GTCATCTCT and GGGGGTCGACTAAAGATATTTCTTGGATTGGGAA TA; and the last fragment, which is 74 amino acids long, was made with the oligonucleotide pair of GTGGATCCAATGGAGGAGGGAGCAAAGCCACC CTTT and GGGGGGTTGTCGACTAGCATTAGAGGTAGTAGTTTTAAC. The fragments were excised with *Bam*HI and *Sal*I and cloned into pGAD.

To map more precisely the domains mediating Cdc42 and Pak1-Cat interaction, we generated further segment fusions within the stretch of amino acids 141 to 210. Segments starting from amino acids 149, 153, 157, and 161 were made with the oligonucleotides GTGGATCCAATGTCTCCATTTGATCCGAAGCA TGTC, GTGGATCCAATGCCGAAGCATGTCACTCACGTTGGT, GTGGA TCCAATGACTCACGTTGGTTTTAATTATGAT, and GTGGATCCAATGT TTAATTATGATACTGGGGAATTT, respectively. The segments ending at amino acids 194, 198, 202, and 206 were made with the oligonucleotides GGGGG TCGACTACTGTGGAGTTTGTACTTGTTCCGA, GGGGGTCGACTAGTC CAAAACGGCCTGTGGATGTTG, GGGGGTCGACTAAAAAGCCATAGC GTCCAAAACGGC, and GGGGGTCGACTAGGATTGGGAATAAAAAGC CATAGC, respectively. The PCR products were excised with *Bam*HI and *Sal*I and cloned into the pGAD vector.

Creating and screening two-hybrid mutant libraries. We constructed a library of Pak1 regulatory mutants by PCR mutagenesis of this region (40). We used the oligonucleotide pair AAGGATCCGATGGAAAGAGGGACTTTACAA and GGGGGGTTGTCGACTAGCATTAGAGGTAGTAGTTTTAAC, described above, to amplify and mutagenize wild-type Pak1 template. The PCR product was gel purified and digested with *Bam*HI and *Sal*I, and full-length Pak1 was reconstructed by ligation of the PCR products into the LBD fusion vector containing the C-terminal 375 amino acids of Pak1, as we described above. This mutant library had a complexity of over 10^4.

For screening, the pLBD-Pak1 mutant library was transformed into L40 containing pGAD-Pak1-Reg. Cells were plated onto DO-LTH to select for interacting pairs. A total of 3×10^4 clones were screened, and His^+ transformants were patched out on fresh DO-LT for β-galactosidase filter assays. Twenty-five independent clones were both His^+ and $LacZ^+$. pLBD fusion plasmids were recovered, amplified, and tested individually with GAD-Pak1-Reg and GAD for binding specificity and reproducibility. Nineteen independent clones were found to bind Pak1-Reg specifically.

Recovery and amplification of plasmids from yeast cells. To recover plasmids from yeast cells of interest, the yeast cells were collected and resuspended in 200 μl of lysis buffer (2% Triton X-100, 1% sodium dodecyl sulfate, 0.1 M NaCl, 0.01 M Tris [pH 8], 0.001 M EDTA) and vortexed with equal volumes of glass beads and phenol-chloroform-isoamyl alcohol (25/24/1 [vol/vol/vol]) at 4°C for 5 min. After vortexing, cell extracts were centrifuged for 10 min, and the supernatants were used for electroporation into *Escherichia coli*. Plasmids were extracted from *E. coli* by standard DNA preparation procedures (Qiagen).

RESULTS

A conserved region of the Pak1 regulatory domain interacts with the catalytic domain. Many protein kinases have a regulatory domain that binds to and inhibits the kinase catalytic domain (29, 31), and we tested if Pak1 has domains capable of such intramolecular interaction, detectable by two-hybrid interaction. Pak1-Reg, the regulatory domain of Pak1, was fused to GAD (*GAL4* transcription activation domain). The fusion was tested for interaction with LBD-Pak1-Cat, which is an LBD (*lexA* DNA binding domain) fusion of the kinase catalytic domain of Pak1. LBD-$Cdc42^{V12}$, which had been shown elsewhere to bind GAD-Pak1-Reg (17, 26), was used as a positive control. GAD and LBD-Ras1 were employed as negative controls. The two-hybrid interaction was determined by histidine prototrophy and β-galactosidase production (see Materials and Methods). As shown in Fig. 1, GAD-Pak1-Reg was able to bind LBD-Cdc42 and LBD-Pak1-Cat, but not LBD-Ras1, while LBD-Pak1-Cat failed to bind GAD. This result established the specific binding between Pak1-Reg and Pak1-Cat. In keeping with this conclusion, we also tested and found that GAD-Pak1-Cat can bind LBD-Pak1-Reg faithfully as well (data not shown). We note in passing that the regulatory domain can even bind to a mutant, inactive catalytic domain.

To identify the region on Pak1-Reg that is responsible for binding Pak1-Cat, we generated several Pak1-Reg deletion mutants by PCR and tested their ability to bind Pak1-Cat (see Materials and Methods). We found that a 70-amino-acid stretch from residues 141 to 210 is able to bind both Cdc42 and Pak1-Cat specifically (see Fig. 2). This region contains CRIB (Cdc42-Rac1 interactive binding) domain, the most conserved region on PAK proteins outside the kinase catalytic domain. Thus, Pak1-Cat binds to the same region on Pak1-Reg known to bind Cdc42.

To map more precisely the regions on Pak1-Reg that mediate Cdc42 and Pak1-Cat interactions, several more deletion mutants within $Pak1^{141-210}$ were made by PCR (see Materials and Methods). These deletion mutants were then tested for binding $Cdc42^{V12}$, Pak1-Cat, and Ras1, the negative control. The two-hybrid binding results are also presented in Fig. 2. We found that truncation from the N-terminal portion of $Pak1^{141-210}$ abolished binding to Cdc42 before affecting binding to Pak1-Cat, whereas truncation from the C terminus abolished binding to Pak1-Cat before binding to $Cdc42^{V12}$. These experiments suggest that, in theory, $Pak1^{160-206}$ should be the shortest peptide that can bind Pak1-Cat specifically. The experiments described below use slightly larger fragments that do not bind Cdc42.

Pak1 regulatory domains block truncated and activated Pak1 in vivo. The standard autoinhibition model for protein kinases predicts that the regulatory domain inhibits the catalytic activity, and for Pak1, this is supported by the truncation experiments that have been performed and reported by others (17, 28). If our two-hybrid data correctly identifies the region of the regulatory molecule that binds to the catalytic domain, and the truncated Pak1 is activated because of the loss of the

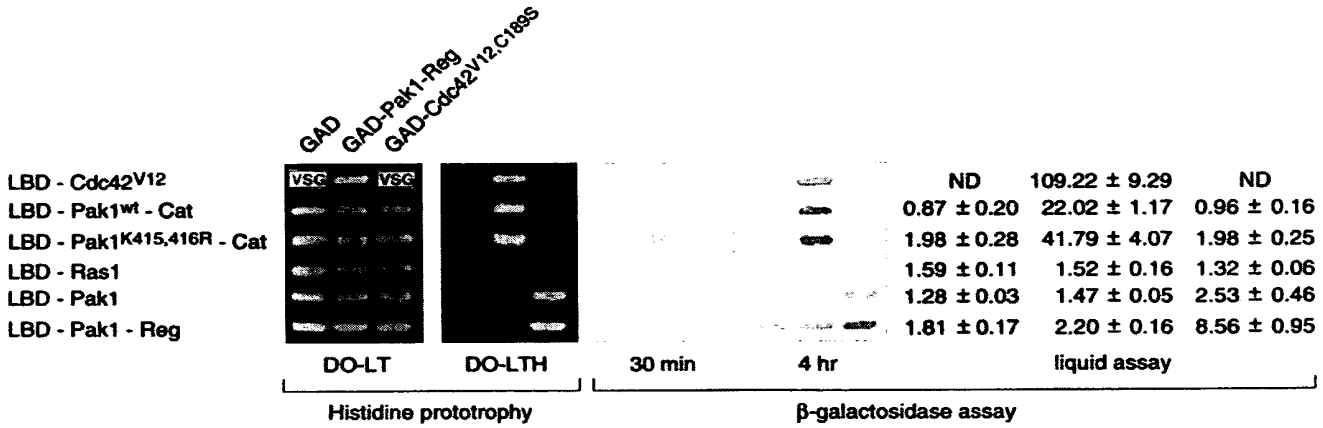

FIG. 1. Binding between the separated regulatory and catalytic domains of Pak1. L40 was transformed with either pGAD, pGAD-Pak1-Reg, or pGAD-Cdc42^{V12,C189S} and either pLBD-Cdc42^{V12}, pLBD-Pak1-Cat, pLBD-Pak1^{K415,416R}-Cat, pLBD-Ras1, pLBD-Pak1, or pLBD-Pak1-Reg. Transformants were tested for growth on medium lacking histidine (DO-LTH) and assayed for β-galactosidase production. VSG, very slow growth. Values shown are relative levels (means ± standard deviations). DO-LT is the medium lacking leucine and tryptophan. ND, not determined.

inhibitory influence of the regulatory domain, then expression of that domain should inhibit the activity of the truncated Pak1 when it is expressed in *trans*. To test this prediction, we exploited the observation that expression of the truncated Pak1 is somewhat toxic to *S. cerevisiae*. We thus performed an expression toxicity assay. L40 was transformed with either GAD-Pak1-Reg, GAD-Pak1$^{149-210}$, GAD-Pak1$^{157-210}$, or GAD alone, all carrying the *LEU2* marker, and either pLS104-Pak1-Cat or pLS104 vector alone, each carrying *ADE2*. Cells were plated on medium lacking leucine and adenine (DO-LA), and transformants were patched out on fresh DO-LA plates. The patches were then replica plated and grown for several days on the nonselective medium, YPD, before being replica plated back on the selective medium. Cells expressing toxic *ADE2* plasmids will tend to lose the same, which we can assay in two ways: by failure to thrive on the selective plates and by the red color characteristic of cells lacking ADE2. Cells with Pak1-Cat and GAD alone failed to grow effectively on the selective medium, and the patches displayed a red color. However, those with Pak1-Cat with either GAD-Pak1-Reg, GAD-Pak1$^{149-210}$, or GAD-Pak1$^{157-210}$ grew more effectively, and the patches displayed a pink to white color (Fig. 3). These studies confirm that the region we have identified not only binds to the catalytic domain but also inhibits it, even when expressed in *trans*.

Regulatory and catalytic interaction keeps wild-type, full-length Pak1 in a closed configuration. Since Pak1, like Byr2, contains a regulatory domain capable of interacting with its catalytic domain, we suspected that full-length Pak1, like full-length Byr2, would exist in a closed configuration in which the catalytic domain is occupied by the regulatory domain. In support of this hypothesis, we found that although we could readily detect binding between Pak1-Reg and Pak1-Cat, we could not detect the binding of Pak1-Reg to full-length Pak1, even though the latter was perfectly capable of binding Cdc42^{V12,C189S} (Fig. 1). (Note: in these experiments, the Cdc42^{V12,C189S} protein, lacking the farnesylation site, was used because the combined expression of Pak1 and Cdc42^{V12} is toxic.) These results suggest that an intramolecular interaction exists between the regulatory and catalytic domains in full-length Pak1. This hypothesis is further strengthened by the experiments, described below, in which we searched for, found, and analyzed mutants of Pak1 that were in an open configuration.

If we correctly surmise that wild-type Pak1 failed to bind Pak1-Reg because of intramolecular interactions, we should be able to readily isolate Pak1 mutants that gain the ability to bind Pak1-Reg, and such mutants should have regulatory and catalytic domains that are no longer able to interact.

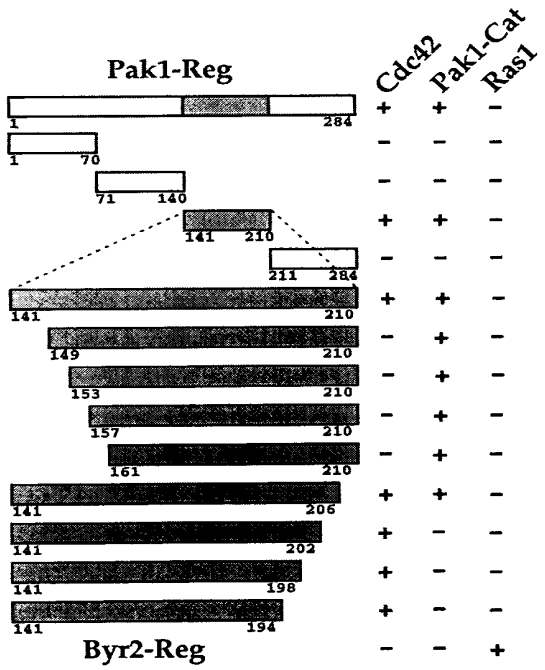

FIG. 2. Regions on Pak1-Reg mediating the interaction with the kinase catalytic domain. Pak1-Reg deletion mutants were made by PCR and fused to GAD. The GAD fusion to the regulatory domain of Byr2 was included as a control (last row). These fusions were assayed for interactions with LBD fused to Cdc42, Pak1-Cat, or Ras1 as a negative control. A plus sign represents a two-hybrid interaction; a minus sign represents no detectable two-hybrid interaction. The positive interactions were all of about similar intensities. The amino acid positions of the peptide sequences expressed as GAD fusions are shown. The conserved region of the Pak1 regulatory domain is shown in gray.

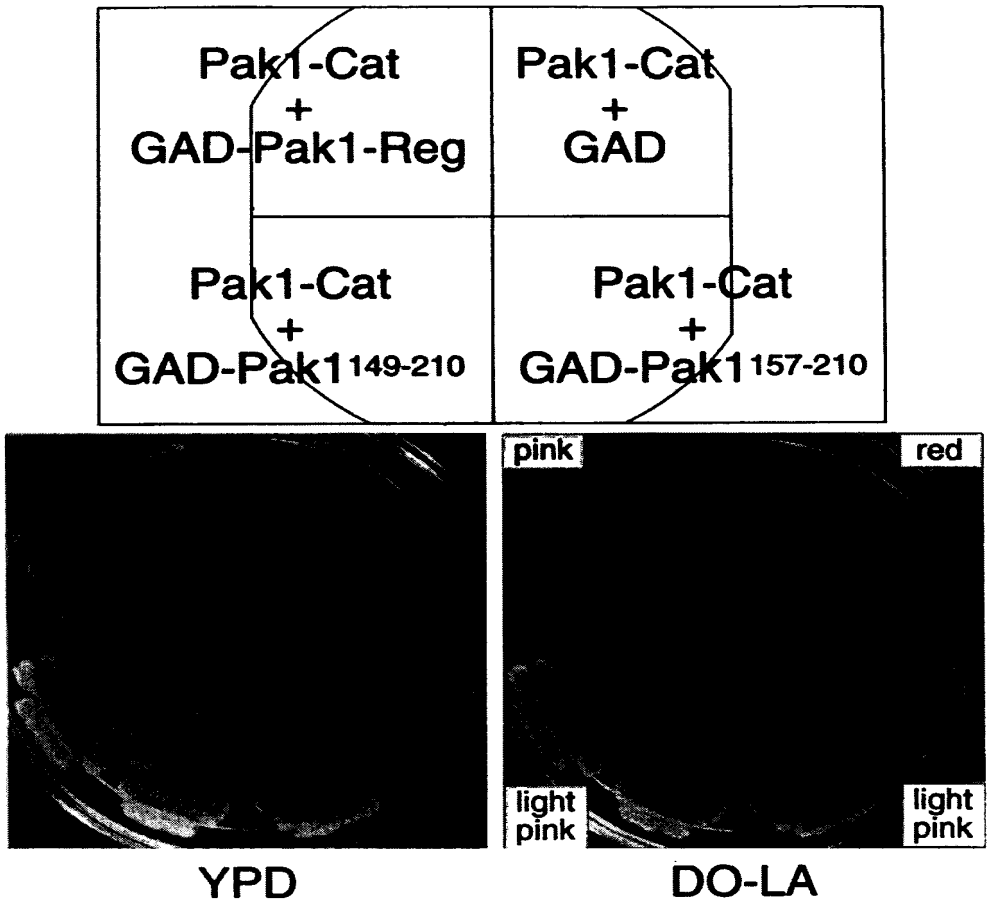

FIG. 3. Effect of expressing the Pak1 regulatory domain on the toxicity of Pak1-Cat. L40 was transformed with pLS104-Pak1-Cat and either pGAD, pGAD-Pak1-Reg, pGAD-Pak1$^{149-210}$, or pGAD-Pak1$^{157-210}$. Transformants were initially plated and streaked on medium lacking leucine and adenine (DO-LA). The Leu$^+$ and Ade$^+$ cells were then grown for several days in the nonselective medium, YPD, before being replica plated on the selective medium, DO-LA. Pictures were taken of the patches, and the color of the patches was noted.

Pak1-Reg was randomly mutagenized by PCR and fused to Pak1-Cat in to form a library of LBD fusions of full-length, mutagenized Pak1. The DNA of this mutant library was transformed into L40 together with GAD-Pak1-Reg, and cells were plated in the absence of histidine to select for mutant, full-length Pak1 capable of interacting with the isolated regulatory domain. Colonies that grew on the His$^-$ plates were patched out and tested for the production of β-galactosidase. Twenty-five colonies that were both His$^+$ and LacZ$^+$ were isolated, and the LBD plasmids from these cells were recovered, amplified, and transformed back into L40 together with GAD-Pak1-Reg or GAD. Nineteen of the 25 LBD-Pak1 plasmids interacted with GAD-Pak1-Reg but not with GAD. Figure 4 shows the two-hybrid interactions of the 19 LBD-Pak1 mutants with GAD-Pak1-Reg and with the negative control. Since these Pak1 mutants can bind Pak1-Reg, we call them Pak1^{open} mutants hereafter.

The regulatory domains of the 19 Pak1^{open} mutants were sequenced. All of them contain a single mutation between residues 161 and 200, that is, within the CRIB domain, the highly conserved region that binds both Cdc42 and Pak1-Cat (Table 1). Several mutations were encountered more than once, and the mutants fell into 13 groups. All mutations except M200T and M200R were mapped to residues conserved among PAK proteins. Figure 5 shows the multiple alignments of this conserved region with representative homologs, with the sites of mutation indicated.

As the first step towards characterizing these Pak1^{open} mutants, we tested the binding of the Pak1-Reg of these mutants to Pak1-Cat and Cdc42. The Pak1-Regs were excised and fused to GAD, and the GAD fusions were tested with LBD-Pak1-Cat and LBD-Cdc42, individually. GAD-Pak1^{wt}-Reg and GAD were tested alongside. The two-hybrid results are presented in Fig. 6. Significantly, but not surprisingly, the regulatory domains of all of the Pak1^{open} mutants failed to bind LBD-Pak1-Cat, while all still bound Cdc42 to varying degrees.

These results demonstrate that all 19 Pak1^{open} mutants contain mutations in the CRIB domain that abolish binding to the catalytic domain Pak1 and argue strongly that the loss of intramolecular interaction is the cause for the open configuration.

Genetic characterizations of Pak1^{open} mutants. If the disruption of the regulatory-catalytic interactions were sufficient to activate Pak1, we would expect the Pak1^{open} mutants to be

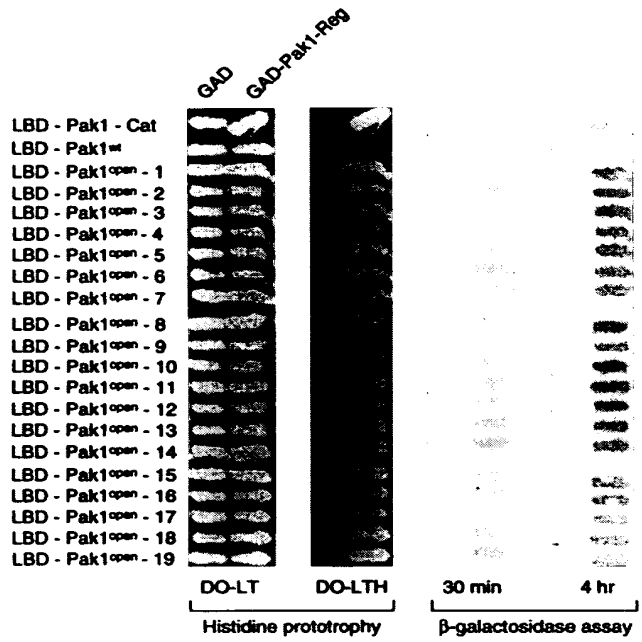

FIG. 4. Binding of the separated regulatory domain to Pak1^{open} mutants. L40 was transformed individually with either pGAD or pGAD-Pak1-Reg and either pLBD-Pak1-Cat, pLBD-Pak1, or the 19 pLBD-Pak1^{open} mutants. Transformants were tested for growth on medium lacking histidine (DO-LTH) and assayed for β-galactosidase production. DO-LT is the medium lacking leucine and tryptophan.

activated. To test this, we examined the activity of Pak1^{open} mutants in comparison with that of the wild-type Pak1. Three phenotypes associated with the dominant activated Pak1, Pak1-Cat, were assayed: toxicity (references 17 and 26 and as described above), activation of the *FUS1-lacZ* reporter system (17), and the induction of the open configuration of Byr2 (31).

The format for expression toxicity assays was described above. Pak1, Pak1^{open} mutants, Pak1-Cat, and Pak1^{K415,416R}-Cat were cloned under an alcohol dehydrogenase promoter into an *ADE2*-based 2 μm plasmid, pLS104. L40 cells transformed with various pLS104 clones were plated on Ade$^-$ plates. Transformants were then patched onto fresh Ade$^-$ plates and replica plated on nonselective medium and then again on Ade$^-$ plates. Cells that grow well while carrying the pLS104 derivatives grow robustly as white patches on Ade$^-$ plates, while cells with pLS104 derivatives that cause toxicity or slower growth will not grow as well on Ade$^-$ plates and have a red to pink color, indicative of defective adenine biosynthesis. The patches of cells expressing Pak1-Cat, Pak1^{K415,416R}-Cat, Pak1, or Pak1^{open} mutants are shown in Fig. 7. As expected, cells containing pLS104-Pak1-Cat failed to grow efficiently on Ade$^-$ plates after being replica plated, and the patches displayed a red color; those containing pLS104 or pLS104-Pak1^{K415,416R}-Cat grew perfectly well in the absence of adenine, and the patches displayed a white color. Cells containing pLS104-Pak1 grew well in the absence of adenine, and patches were light pink, suggesting a very mild toxicity resulting from the expression of wild-type Pak1. Cells expressing various Pak1^{open} mutants displayed varying ranges between these two extremes. Those containing Pak1^{F161S}, Pak1^{G166W}, Pak1^{E167G}, or Pak1^{F168S} grew well, and their patches exhibited a light pink color, much like cells with wild-type Pak1; cells with Pak1^{W175R}, Pak1^{P193S}, Pak1^{P193Q}, Pak1^{A195V}, or Pak1^{M200R} grew, but their patches were pink; cells with Pak1^{M200T} were dark pink; and cells with Pak1^{L179P}, Pak1^{I184T}, or Pak1^{A195T} grew poorly after being replica plated back to the Ade$^-$ plates, and the patches had a red color, much like those with dominant activated Pak1. From this, we conclude that the majority of Pak1^{open} mutants have higher activity than wild-type Pak1, and the results support the model that Pak1 intramolecular interaction is responsible for autoinhibition.

The *FUS1-lacZ* reporter system provides an indicator for the activity of the *S. cerevisiae* mating signaling pathway (10). We have shown previously that dominant activated forms of STE20 and Pak1 can activate this pathway in an STE11-dependent manner (17). It was noted then that full-length wild-type Pak1 failed to activate the pathway. Therefore, we asked if any of the Pak1^{open} mutants could activate the *S. cerevisiae* mating pathway and stimulate β-galactosidase production by the reporter system. Pak1^{open} mutants were cloned under a galactose-inducible *GAL1* promoter, as described in Materials and Methods, to avoid the potential complications due to the toxicity of the expressed gene. Cells containing the plasmids were patched on medium rich in glucose and then replica plated to medium depleted of glucose but rich in galactose (2%). The amount of β-galactosidase in these cells was monitored by the conversion of X-Gal, and the results are presented in Fig. 8. As expected, cells with Pak1-Cat expressed produced more β-galactosidase than did cells with the vector alone or cells with Pak1^{K415,416R}-Cat, the kinase-defective Pak1-Cat. While cells containing wild-type Pak1 were unable to activate the reporter system detectably, several of the strains carrying Pak1^{open} mutants were able. In fact, some produced β-galactosidase as well as did cells carrying Pak1-Cat. These results demonstrate that some Pak1^{open} mutants are more active than wild-type Pak1 and further confirm that intramolecular interaction is autoinhibitory.

The third assay for Pak1 activation was based on its ability to induce the open configuration of Byr2. We have previously shown that expression of the dominant activated Pak1, Pak1-Cat, but not the wild-type full-length kinase, induced the two-hybrid interaction between GAD-Byr2-CBD (the GAD fusion to the smallest subregion of the regulatory domain of the Byr2 kinase sufficient to bind to its catalytic domain) and LBD-Byr2 (31). We therefore tested if Pak1^{open} mutants were more effective than wild-type Pak1 at inducing this interaction. L40 was transformed with pGAD-Byr2-CBD, pLBD-Byr2, and either pLS104-Pak1-Cat, pLS104-Pak1^{K415,416R}-Cat, pLS104-Pak1, pLS104-Pak1^{I184T}, pLS104-Pak1^{L179P} (the two Pak1 mu-

TABLE 1. Mutations in Pak1^{open} mutants

Mutant group	Mutation	Member(s)
I	F161S	Pak1^{open}-1
II	G166W	Pak1^{open}-9
III	E167G	Pak1^{open}-17
IV	F168S	Pak1^{open}-11
V	W175R	Pak1^{open}-5, Pak1^{open}-10
VI	L179P	Pak1^{open}-6, Pak1^{open}-18
VII	I184T	Pak1^{open}-3, Pak1^{open}-12, Pak1^{open}-13, Pak1^{open}-15
VIII	P193S	Pak1^{open}-2
IX	P193Q	Pak1^{open}-19
X	A195V	Pak1^{open}-4
XI	A195T	Pak1^{open}-7, Pak1^{open}-8
XII	M200T	Pak1^{open}-14
XIII	M200R	Pak1^{open}-16

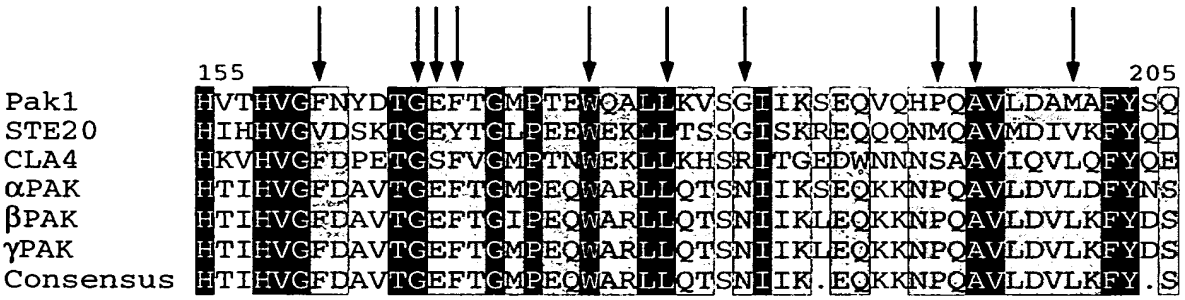

FIG. 5. Location of the altered amino acid residues of the Pak1^{open} mutants in the highly conserved region of PAK proteins. The highly conserved regions on Pak1 (17, 26), STE20 (28), CLA4 (7), and three major mammalian PAK isoforms (3, 16, 21) are aligned, with identical residues in black boxes, conserved residues in grey boxes, and the residues altered in the Pak1^{open} mutants indicated by arrows.

tants that were most active in the previous assays), or just pLS104 vector alone. Transformants were tested quantitatively for the production of β-galactosidase. The results are presented in Fig. 9. As expected, Pak1^{wt}-Cat induced the interaction between GAD-Byr2-CBD and LBD-Byr2 to about six times above the background level, while kinase-defective Pak1-Cat, Pak1^{K415,416R}-Cat, failed to enhance this interaction. Wild-type full-length Pak1 also failed to increase this interaction, but both Pak1^{open} mutants were able to induce levels twofold over the background level. These results once again confirm that the intramolecular interaction is autoinhibitory.

Cdc42 promotes the open configuration of Pak1. It has been shown in vitro, with a gel overlay assay, that purified Rac-Rho-Cdc42 can induce an autophosphorylation and activation event of Pak1 (16). Cdc42 is now known to be an upstream activator of Pak1 in vivo (17, 26), although the activation mechanism remains unknown. We have shown that Cdc42 and Pak1-Cat interact with a tightly overlapping region on Pak1-Reg. Moreover, we failed to find evidence for a trimeric complex among Cdc42^{V12}, Pak1-Reg, and Pak1-Cat, detectable by the two-hybrid system, suggesting that the three-way interaction is sterically forbidden (data not shown). Therefore, we speculated that Cdc42 activates Pak1 by directly relieving Pak1 of

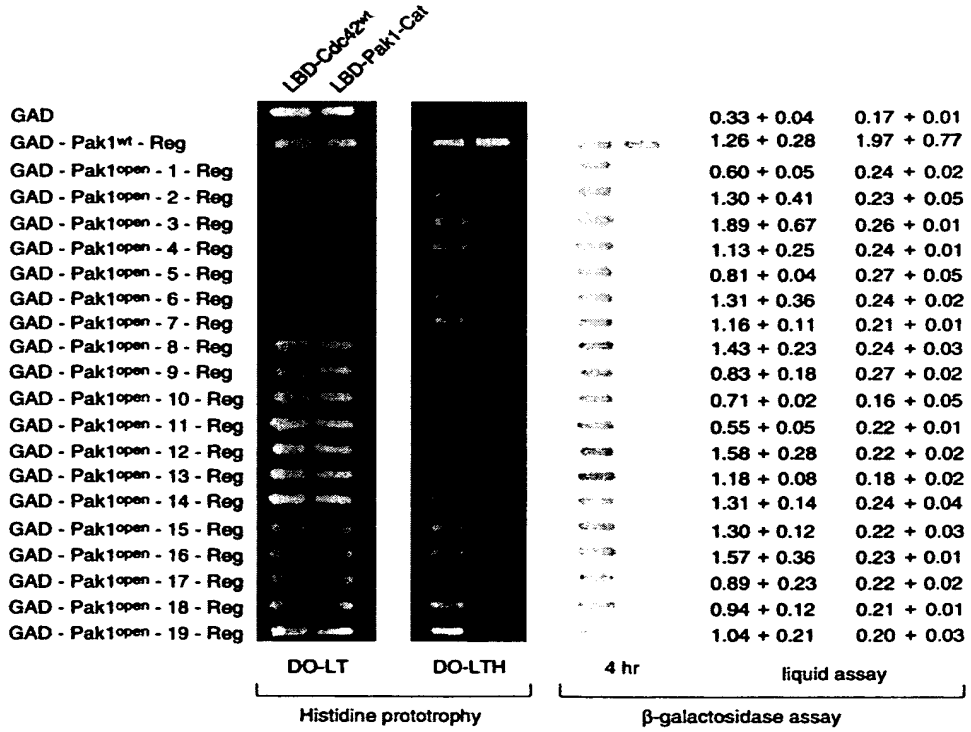

FIG. 6. Failure of the separated Pak1^{open} regulatory domains to bind the catalytic domain. L40 was transformed individually with either pLBD-Cdc42 or pLBD-Pak1-Cat and either pGAD, pGAD-Pak1-Reg, or 19 pGAD-Pak1^{open}-Reg. Transformants were tested for growth on medium lacking histidine (DO-LTH) and assayed for β-galactosidase production. DO-LT is the medium lacking leucine and tryptophan.

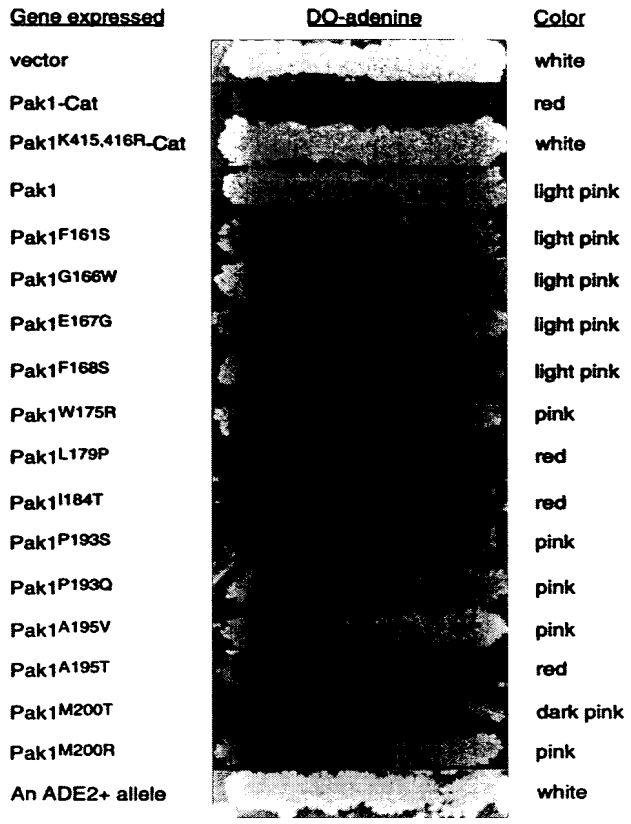

FIG. 7. Expression toxicity assay with Pak1^{open} mutants. L40 was transformed with either pLS104, pLS104-Pak1-Cat, pLS104-Pak1^{K415,416R}-Cat, pLS104-Pak1, or 13 pLS104-Pak1^{open} mutants. Transformants were initially plated and then patched in groups of four on medium lacking adenine. The Ade$^+$ cells were then replica plated on the nonselective medium, YPD, for several days, before being replica plated on medium lacking adenine (DO-adenine). Pictures were taken of the patches on DO-adenine, and the color of the patches was noted. The wild-type *ADE2* allele was included for comparison.

the autoinhibition that results from the intramolecular binding of the regulatory and catalytic domains. This speculation led us to predict and test whether Cdc42 could induce the open configuration of Pak1.

We have successfully used the two-hybrid system to identify signaling components that can induce the open configuration of Byr2 (31), and we applied the same principles to Pak1. The Pak1 opening assay was performed in the following fashion: L40 was transformed with (i) either GAD-Pak1-Reg, GAD-Pak1$^{149-210}$, GAD-Pak1$^{157-210}$, or GAD alone; (ii) either LBD-Pak1 or LBD-Ras1 as a control; and (iii) either pLS104-Cdc42^{V12,C189S}, pLS104-Pak1-Cat, pLS104-Pak1^{K415,416R}-Cat, or pLS104. Cells were patched on medium lacking leucine, tryptophan, and adenine (for pLS104 plasmid selection) (DO-LTA). Patches were replica plated on medium lacking histidine to test the transactivation of the *HIS3* reporter gene. Transformants were also tested for *lacZ* expression, by both filter overlay and liquid assays. As shown in Fig. 10, only two kinds of cells displayed an interaction between GAD and LBD fusions: those expressing GAD-Pak1$^{149-210}$, LBD-Pak1, and Cdc42^{V12,C189S} and those expressing GAD-Pak1$^{157-210}$, LBD-Pak1, and Cdc42^{V12,C189S}. All other cells failed to display two-hybrid interactions. These results demonstrate that Cdc42^{V12,C189S} can effectively and specifically induce the open configuration of Pak1.

Cells expressing GAD-Pak1-Reg, LBD-Pak1, and Cdc42^{V12,C189S} did not yield a positive interaction. We attribute this to the fact that Pak1-Reg, unlike GAD-Pak1$^{149-210}$ or GAD-Pak1$^{157-210}$, also binds Cdc42^{V12,C189S} and thus competes for its binding.

These experiments suggest that Cdc42 opens the configuration of Pak1 through its interaction with the regulatory domain. A more direct demonstration of this mechanism was obtained as follows. We screened for and identified two single-base-pair mutants of the regulatory domain of Pak1 that failed to bind Cdc42 yet still were capable of full-strength binding to the catalytic domain, as judged by two-hybrid interactions. The mutations, S148A and H155A, were each independently introduced into the full-length Pak1. We then tested if Cdc42^{V12,C189S} could induce the open configuration of either Pak1^{S14A} or Pak1^{H155A}. It could not, indicating that the opening of Pak1 is the consequence of the direct binding of Cdc42 to the regulatory domain.

DISCUSSION

Previous studies showed that the intramolecular interaction between Byr2 regulatory and kinase catalytic domains keeps that kinase in a closed configuration and establishes autoinhibition (31). In this report, we first describe a similar potential for intramolecular interaction within Pak1, the fission yeast homolog of PAK. Expression of segment fusions indicated that the highly conserved region of the regulatory domain of Pak1 (Pak1-Reg), to which Cdc42 also binds, was capable of binding to the catalytic domain. This mapping was later confirmed by point mutation analysis.

Since this potential Pak1 intramolecular interaction resembles that found in Byr2, we incorporated the insights gained from Byr2 to guide us in further studies. In particular, we next demonstrated that Pak1 can exist in the wild-type closed configuration and a mutant open configuration, which differ in their ability to bind a free regulatory domain. Mutants with the open configuration have mutations in the conserved regulatory domain, and these mutant domains are unable to bind separated catalytic domains. These studies strongly support the existence of intramolecular interaction between the regulatory and catalytic domains of wild-type Pak1.

In the case of Byr2, the intramolecular interaction causes autoinhibition, and its release is associated with kinase activation. The same appears to be true for Pak1. First, the expression of the smallest regulatory region of Pak1 capable of binding the catalytic region, a region that does not bind to Cdc42, inhibits the toxicity resulting from expression of the free catalytic domain. Second, the majority of Pak1^{open} mutants are more active than wild-type Pak1, and some of them behaved similarly to the activated Pak1 lacking its regulatory domain. Third, Cdc42, a known activator of Pak1, both in vivo and in vitro, induces the open configuration, as discussed below.

Our genetic results indicate that not all Pak1^{open} mutants are equally activated, and none are as active as the construct which lacks the entire regulatory region. There are many possible explanations for this. First, these proteins may be expressed at different levels. Second, although we cannot detect intramolecular interaction in the mutants by two-hybrid analysis, the mutants may nevertheless have a closed configuration in vivo. Third, there may be other features of the regulatory domain that are inhibitory for full biological activity. Indeed, other proteins that bind to the regulatory domain of Pak1 have recently been identified (9). Our studies are not designed to resolve these questions.

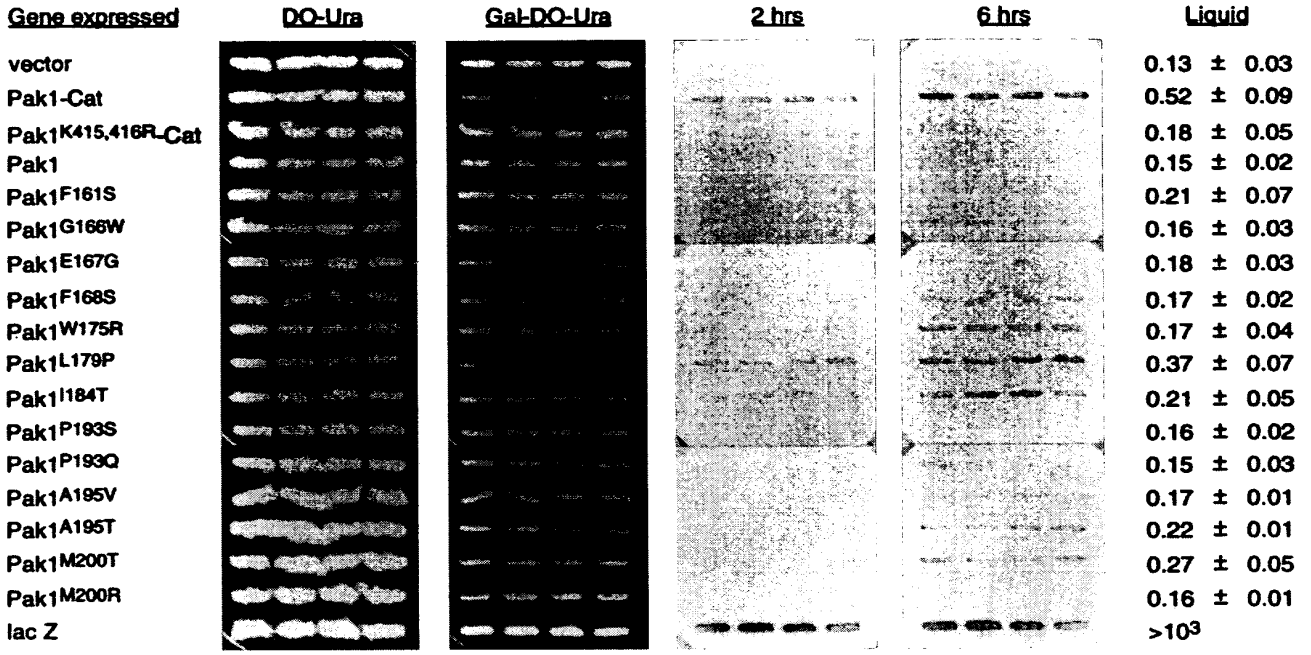

FIG. 8. Activity of the Pak1^{open} mutants in the *FUS1-lacZ* induction assay. AN43-5A was transformed with either pYX113 (the empty vector with the GAL1 promoter), pYX113-Pak1-Cat, pYX113-Pak1^{K415,416R}-Cat, pYX113-Pak1, 13 of the pYX113-Pak1^{open} mutants, or pYX113-*lacZ*. Transformants were subjected to a 20-h galactose induction before being assayed for β-galactosidase production from the *FUS1* promoter. Overlay filters were incubated with X-Gal for 2 to 6 h, and results of quadruplicate transformants are shown. Cultures were also harvested for β-galactosidase liquid assays, performed on four independent transformants. The assay results, ± standard deviations, are shown at right.

In our previous studies, we found that activated Pak1 could induce the open configuration of Byr2. We suspected that Cdc42 might do the same to Pak1. First, it was known that Cdc42 was an activator. Second, Cdc42 and the catalytic domain bind to overlapping regions of the regulatory domain. Third, we could not observe a stable trimeric complex among Cdc42, Pak1-Reg, and Pak1-Cat. We thus tested if Cdc42 could open Pak1. We used three different molecular probes for the open configuration of Pak1: GAD-Pak1-Reg, GAD-Pak1$^{149-210}$, and GAD-Pak1$^{157-210}$. None are able to bind full-length Pak1, all three are able to bind the isolated catalytic domain, and only the first is also able to bind Cdc42. Indeed, when Cdc42 was overexpressed, the release of the kinase catalytic domain of full-length Pak1 to bind GAD-Pak1$^{149-210}$ and GAD-Pak1$^{157-210}$ was clear. Moreover, opening by Cdc42 could not be observed on mutant Pak1 proteins that do not bind Cdc42.

Although Cdc42 does activate Pak1, binds to Pak1, and opens its conformation and the open-conformation mutants are more active than wild type, these experiments do not rule out additional functions for Cdc42 in the activation of Pak1. For example, Cdc42 may facilitate the localization of Pak1 or the binding of other activating proteins.

It may be useful to draw a parallel between the interactions of Cdc42 and those of Ras1 with their respective protein kinase targets. Many of the same relations are retained: Ras1 is an in vivo regulator of Byr2, it binds directly to Byr2, and its domain of interaction overlaps with the site where the catalytic subunit also binds (22, 31, 32). Yet we were unable to demonstrate the opening of Byr2 by Ras1. In fact, no direct in vitro activation of Byr2 by Ras1 (or of Raf by H-ras) has been observed, and we have observed a stable complex between Ras1 and the Byr2 catalytic domain bridged by a mutant regulatory domain of Byr2 with enhanced affinity for the catalytic domain (30a). Thus, the mechanisms of action of these two very similar GTPases on two similar protein kinases are likely to be very different.

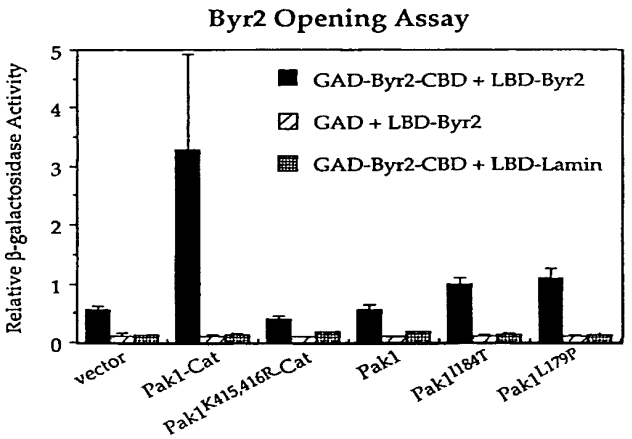

FIG. 9. Induction of the open configuration of Byr2 by the overexpression of Pak1^{open} mutants. L40 was transformed with either pGAD-Byr2-CBD or pGAD; either pLBD-Byr2 or pLBD-Lamin; and either pLS104-Pak1-Cat, pLS104-Pak1^{K415,416R}-Cat, pLS104-Pak1^{wt}, pLS104-Pak1^{I184T}, pLS104-Pak1^{L179P}, or just the pLS104 vector alone. Transformants were tested quantitatively for β-galactosidase production. Values shown are relative levels. Standard deviations from at least four independent transformants are shown by error bars.

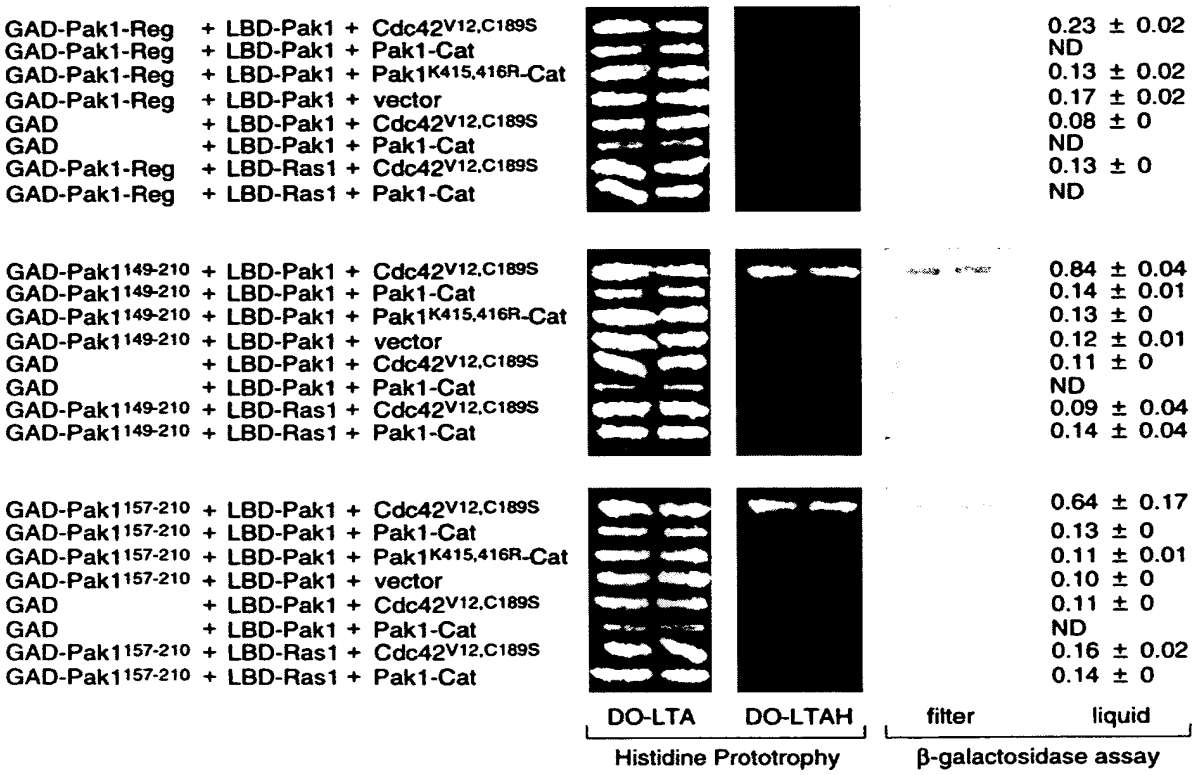

FIG. 10. Induction of the open configuration of Pak1 by the overexpression of Cdc42. L40 was transformed with either pGAD-Pak1-Reg, pGAD-Pak1$^{149-210}$, pGAD-Pak1$^{157-210}$, or pGAD vector alone; either pLBD-Pak1 or pLBD-Ras1; and either pLS104-Cdc42^{V12,C189S}, pLS104-Pak1-Cat, pLS104-Pak1^{K415,416R}-Cat, or pLS104 vector alone. Transformants were tested for growth on the medium lacking histidine (DO-LTAH) and assayed for β-galactosidase production. DO-LTA is the medium lacking leucine, tryptophan, and adenine. Values shown are relative levels (means ± standard deviations). ND, not determined.

The region of the Pak1 regulatory domain that can bind to both Cdc42 and the catalytic domain is highly conserved among all members of the PAK family. Hence, this intramolecular interaction is highly likely to be conserved among them as well. Indeed, during the preparation of this paper, Zhao et al. reported the identification of a conserved negative regulatory region in αPAK (39). The authors showed that mutations on residues 101 to 137 of αPAK render that kinase constitutively active. They further provided evidence that αPAK$^{83-149}$, a 67-amino-acid peptide, can block PAK activation by Cdc42 in vitro and suppresses PAK functions in vivo. This conserved negative regulatory region on αPAK corresponds to the Pak1 autoinhibitory region reported here. Our results are exactly complementary.

It may be proper to think of four kinases comprising the prototypic MAPK module: MAPK, MEK, MEKK, and PAK. MAPKs and MEKs have limited regions outside of the kinase catalytic domain and need to be phosphorylated at conserved residues in the catalytic domain to gain maximum kinase activities (34) (reviewed in reference 19). Thus, MEKs and MAPKs are predominantly regulated by dynamic phosphorylation and dephosphorylation and perhaps do not display autoregulation. MEKKs, such as Mekks, STE11, Byr2, and Raf, have long regulatory domains, which may bind and mask the kinase catalytic domains, and thus are kept in inactive form. MEKK autoregulation can be antagonized by PAK phosphorylation. PAKs, like MEKKs, also utilize regulatory and catalytic interaction to exert kinase autoregulation. Both PAKs and MEKKs can be regulated by p21 GTPases. However, while PAK regulation by Rho-family GTPases may be caused in part by direct release from autoinhibition, the regulation of MEKKs by GTPases may be more indirect (15, 30).

ACKNOWLEDGMENTS

We thank Ken Chang, Doug Johnson, and Aaron Neiman for providing DNA and yeast strains; Mike Riggs for DNA sequencing; Terry Vale, Hong Ma, Peter Gergen, and Marion Carlson for helpful discussion; the Cold Spring Harbor Laboratory Art Department for artwork; and Patricia Bird for secretarial assistance.

This work was supported by grants from the American Cancer Society and the National Cancer Institute (NIH) to M.W. M.W. is an American Cancer Society Professor.

REFERENCES

1. **Bagrodia, S., B. Derijard, R. J. Davis, and R. A. Cerione.** 1995. Cdc42 and PAK-mediated signaling leads to JNK and p38 mitogen-activated protein kinase activation. J. Biol. Chem. 270:1–4.
2. **Barr, M. M., H. Tu, L. Van Aelst, and M. Wigler.** 1996. Identification of Ste4 as a potential regulator of Byr2 in the sexual response pathway of *Schizosaccharomyces pombe*. Mol. Cell. Biol. 16:5597–5603.
3. **Brown, J., L. Stowers, M. Baer, A. Trejo, S. Coughlin, and J. Chant.** 1996. Human STE20 homologue hPAK1 links GTPases to the JNK MAP kinase pathway. Curr. Biol. 6:598–605.
4. **Burbelo, P. D., D. Drechsel, and A. Hall.** 1995. A conserved binding motif defines numerous candidate target proteins for both Cdc42 and Rac GTPases. J. Biol. Chem. 270:29071–29074.
5. **Chang, E. C., M. Barr, Y. Wang, V. Jung, H.-P. Xu, and M. Wigler.** 1994. Cooperative interaction of *S. pombe* proteins required for mating and morphogenesis. Cell 79:131–141.

6. **Coso, O. A., M. Chiariello, J. C. Yu, H. Teramoto, P. Crespo, N. Xu, T. Miki, and J. S. Gutkind.** 1995. The small GTP-binding proteins Rac1 and Cdc42 regulate the activity of the JNK/SAPK signaling pathway. Cell **81**:1137–1146.
7. **Cvrckova, F., C. De Virgilio, E. Manser, J. Pringle, and K. Nasmyth.** 1995. Ste20-like protein kinases are required for normal localization of cell growth and for cytokinesis in budding yeasts. Genes Dev. **6**:1817–1830.
8. **Fields, S., and O.-K. Song.** 1989. A novel genetic system to detect protein-protein interactions. Nature **340**:245–246.
9. **Gilbreth, M., P. Yang, D. Wang, J. Frost, A. Polverino, M. H. Cobb, and S. Marcus.** 1998. The highly conserved skb1 gene encodes a protein that interacts with SHK1, a fission yeast Ste20/PAK homolog. Proc. Natl. Acad. Sci. USA **93**:13802–13807.
10. **Hagen, D., G. McCaffrey, and G. Sprague.** 1991. Pheromone response elements are necessary and sufficient for basal and pheromone-induced transcription of the *FUS1* gene of *Saccharomyces cerevisiae*. Mol. Cell. Biol. **11**: 2952–2961.
11. **Hill, C. S., J. Wynne, and R. Treisman.** 1995. The Rho family GTPases RhoA. Rac1, and CDC42Hs regulate transcriptional activation by SRF. Cell **81**:1159–1170.
12. **Ito, H., Y. Fukuda, K. Murata, and A. Kimura.** 1983. Transformation of intact yeast cells treated with alkali cations. J. Bacteriol. **153**:163–168.
13. **Leberer, E., D. Dignar, D. Harcus, D. Thomas, and M. Whiteway.** 1992. The protein kinase homologue Ste20p is required to link the yeast pheromone response G-protein β subunits to downstream signalling components. EMBO J. **11**:4815–4824.
14. **Leberer, E., D. Dignard, L. Hougan, D. Y. Thomas, and M. Whiteway.** 1992. Dominant-negative mutants of yeast G-protein β subunit identify two functional regions involved in pheromone signaling. EMBO J. **11**:4805–4813.
15. **Leevers, S. J., H. F. Paterson, and C. J. Marshall.** 1994. Requirement for Ras in Raf activation is overcome by targeting Raf to the plasma membrane. Nature **369**:411–418.
16. **Manser, E., T. Leung, H. Salihuddin, Z. S. Zhao, and L. Lim.** 1994. A brain serine/threonine protein kinase activated by Cdc42 and Rac1. Nature **367**: 40–46.
17. **Marcus, S., A. Polverino, E. Chang, D. Robbins, M. H. Cobb, and M. Wigler.** 1995. Shk1. a homolog of the *Saccharomyces cerevisiae* Ste20 and mammalian p65pak protein kinases, is a component of a Ras/Cdc42 signaling module in the fission yeast, *Schizosaccharomyces pombe*. Proc. Natl. Acad. Sci. USA **92**: 6180–6184.
18. **Marcus, S., A. Polverino, M. Barr, and M. Wigler.** 1994. Complexes between STE5 and components of the yeast pheromone-responsive MAP kinase module. Proc. Natl. Acad. Sci. USA **91**:7762–7766.
19. **Marshall, C.** 1994. MAP kinase kinase kinase, MAP kinase kinase, and MAP kinase. Curr. Opin. Genet. Dev. **4**:82–89.
20. **Martin, H., A. Mendoza, J. M. Rodriguez-Pachon, M. Molina, and C. Nombela.** 1997. Characterization of SKM1, a *Saccharomyces cerevisiae* gene encoding a novel Ste20/PAK-like protein kinase. Mol. Microbiol. **23**:431–444.
21. **Maser, E., C. Chong, Z. S. Zhao, T. Leung, G. Michael, C. Hall, and L. Lim.** 1998. Molecular cloning of a new member of the p21-Cdc42/Rac-activated kinase (PAK) family. J. Biol. Chem. **2740**:25070–25078.
22. **Masuda, T., K.-C. Kariya, M. Shinkai, T. Okada, and T. Kataoka.** 1995. Protein kinase Byr2 is a target of Ras1 in the fission yeast *Schizosaccharomyces pombe*. J. Biol. Chem. **270**:1979–1982.
23. **Minden, A., A. Lin, F. X. Claret, A. Abo, and M. Karin.** 1995. Selective activation of the JNK signaling cascade and c-Jun transcriptional activity by the small GTPases Rac and Cdc42Hs. Cell **81**:1147–1157.
24. **Mullis, K. B., and F. A. Faloona.** 1987. Specific synthesis of DNA in vitro via a polymerase-catalyzed chain reaction. Methods Enzymol. **155**:335–350.
25. **Neiman, A., and I. Herskowitz.** 1994. Reconstitution of a yeast protein kinase cascade in vitro: activation of the yeast MEKK homologue STE7 by STE11. Proc. Natl. Acad. Sci. USA **91**:3398–3402.
26. **Ottilie, S., P. J. Miller, D. I. Johnson, C. L. Creasy, M. A. Sells, S. Bagrodia, S. L. Forsburg, and J. Chernoff.** 1995. Fission yeast *pak1*+ encodes a protein kinase that interacts with Cdc42p and is involved in the control of cell polarity and mating. EMBO J. **14**:5908–5919.
27. **Polverino, A., J. Frost, P. Yang, M. Hutchison, A. Neiman, M. Cobb, and S. Marcus.** 1995. Activation of mitogen-activated protein kinase cascade by p21-activated protein kinase in cell-free extracts of Xenopus oocytes. J. Biol. Chem. **270**:26067–26070.
28. **Ramer, S. W., and R. W. Davis.** 1993. A dominant truncation allele identifies a gene, STE20, that encodes a putative protein kinase necessary for mating in *Saccharomyces cerevisiae*. Proc. Natl. Acad. Sci. USA **90**:452–456.
29. **Soderling, T. R.** 1990. Protein kinases. J. Biol. Chem. **265**:1823–1826.
30. **Stokoe, D., S. G. MacDonald, K. Caddwallader, M. Symons, and J. F. Hancock.** 1994. Activation of Raf as a result of recruitment to the plasma membrane. Science **264**:1463–1467.

30a. **Tu, H.** Unpublished findings.

31. **Tu, H., M. Barr, D. L. Dong, and M. Wigler.** 1997. Multiple regulatory domains on the Byr2 protein kinase. Mol. Cell. Biol. **17**:5876–5887.
32. **Van Aelst, L., M. Barr, S. Marcus, A. Polverino, and M. Wigler.** 1993. Complex formation between RAS and RAF and other protein kinases. Proc. Natl. Acad. Sci. USA **90**:6213–6217.
33. **Vojtek, A., S. M. Hollenberg, and J. A. Cooper.** 1993. Mammalian Ras interacts directly with the serine/threonine kinase Raf. Cell **74**:205–214.
34. **Ward, Y., S. Gupta, P. Jensen, M. Wartmann, R. J. Davis, and K. Kelly.** 1994. Control of MAP kinase activation by the mitogen-induced threonine/tyrosine phosphatase PAC1. Nature **367**:651–654.
35. **White, M., C. Nicolette, A. Minden, A. Polverino, L. Van Aelst, M. Karin, and M. Wigler.** 1995. Multiple RAS functions can contribute to mammalian cell transformation. Cell **80**:533–541.
36. **Wu, C., M. Whiteway, D. Y. Thomas, and E. Leberer.** 1995. Molecular characterization of Ste20p, a potential mitogen-activated protein or extracellular signal-regulated kinase kinase (MEK) kinase kinase from *Saccharomyces cerevisiae*. J. Biol. Chem. **270**:15984–15992.
37. **Yang, P., S. Kansra, R. A. Pimental, M. Gibreth, and S. Marcus.** 1998. Cloning and characterization of shk2, a gene encoding a novel p21-activated protein kinase from fission yeast. J. Biol. Chem. **273**:18481–18489.
38. **Zhang, S., J. Han, M. Sells, J. Chernoff, U. G. Knaus, R. J. Ulevitch, and G. M. Bokoch.** 1995. Rho family GTPases regulate p38 mitogen-activated protein kinase through the downstream mediator Pak1. J. Biol. Chem. **270**: 23934–23936.
39. **Zhao, Z. S., E. Manser, X. Q. Chen, C. Chong, T. Leung, and L. Lim.** 1998. A conserved negative regulatory region in αPAK: inhibition of PAK kinases reveals their morphological roles downstream of Cdc42 and Rac1. Mol. Cell. Biol. **18**:2153–2163.
40. **Zhou, Y., X. Zhang, and R. H. Ebright.** 1991. Random mutagenesis of gene-sized DNA molecules by use of PCR with TAQ DNA polymerase. Nucleic Acids Res. **19**:6052.

J. Membrane Biol. 188, 55–71 (2002)
DOI: 10.1007/s00232-001-0174-2

The Journal of
Membrane
Biology

CFTR is a Monomer: Biochemical and Functional Evidence

J.-H. Chen, X.-B. Chang, A.A. Aleksandrov, J.R. Riordan
Mayo Foundation and Mayo Clinic Scottsdale, S. C. Johnson Medical Research Center, 13400 E. Shea Blvd., Scottsdale, AZ 85259, USA

Received: 28 December 2001/Revised: 18 March 2002

Abstract. Although the CFTR protein alone is sufficient to generate a regulated chloride channel, it is unknown how many of the polypeptides form the channel. Using biochemical and functional assays, we demonstrate that the CFTR polypeptide is a monomer. CFTR sediments as a monomer in a linear, continuous sucrose gradient. Cells co-expressing different epitope-tagged CFTR provide no evidence of co-assembly in immunoprecipitation and nickel affinity binding experiments. Co-expressed wild-type and ΔF508 CFTR are without influence on each other in their ability to progress through the secretory pathway, suggesting they do not associate in the endoplasmic reticulum. No hybrid conducting single channels are seen in planar lipid bilayers with which membrane vesicles from cells co-expressing similar amounts of two different CFTR conduction species have been fused.

Key words: ABC protein — CFTR — Chloride channel — Cystic fibrosis — Quaternary structure — CFTR monomer

Introduction

Adenine nucleotide binding cassette (ABC) proteins are products of a very large gene family, primarily membrane proteins that mediate translocation of solutes across lipid bilayers (Higgins, 1992). Each of these transporter units contains two membrane-integrated domains and two nucleotide-binding domains either in a single polypeptide or two or four associating polypeptides (Doige & Ames, 1993; Higgins, 1992; Dean, Rzhetsky & Allikmets, 2001). In the cases of the single large polypeptides their active oligomeric structures have generally not yet been determined. The P-glycoprotein multidrug transporter has been most studied from this perspective (Boscoboinik et al., 1990; Naito & Tsuruo, 1992; Poruchynsky & Ling, 1994; Loo & Clarke, 1996; Jette, Potier & Beliveau, 1997; Juvvadi et al., 1997; Rosenberg et al., 1997; Taylor et al., 2001). Although there is some evidence that it may form dimers (Boscoboinik et al., 1990; Naito & Tsuruo, 1992; Poruchynsky & Ling, 1994; Jette et al., 1997; Juvvadi et al., 1997) several recent studies, including low-resolution 3-D structure, indicate that it exists and functions as a monomer (Loo & Clarke, 1996; Rosenberg et al., 1997; Taylor et al., 2001). The only convincing example of an oligomeric functional ABC protein is the SUR1 subunit within the K_{ATP} channel (Aguilar-Bryan et al., 1998). This channel is constituted by four Kir6.2 inwardly rectifying potassium channel polypeptides, each associated with one SUR1, resulting in an octamer (Clement et al., 1997; Inagaki, Gonoi & Seino, 1997; Shyng & Nichols, 1997). However, this assembly essentially reflects the typical tetrameric structure of potassium channels (MacKinnon, 1991; Liman, Tytgat & Hess, 1992; Yang, Jan & Jan, 1995; Corey et al., 1998); there is no evidence of interactions between the four SUR1 subunits.

The CFTR polypeptide alone without additional proteins is sufficient to generate a regulated low-conductance chloride channel (Bear et al., 1992; Ramjeesingh et al., 1997). However, it is unknown how many CFTR polypeptides constitute the channel. As briefly outlined above, the bias from the ABC protein perspective might point in the direction of a monomer. In contrast, since nearly all known ion channels are homo- or hetero-oligomers (Hille, 2001), the possibility that CFTR may possess a quaternary structure also has to be considered.

In an initial assessment of whether CFTR polypeptides self-associate, Marshall et al. (1994) co-expressed full-length and C-terminally-truncated forms

Correspondence to: J.R. Riordan; email: riordan@mayo.edu

of CFTR and immunoprecipitated with an antibody that recognized an epitope at the extreme C-terminus and hence absent from the truncated species. The latter was not co-immunoprecipitated with the full-length protein, implying that self-association did not occur or was not maintained in the solubilizing detergent. However, more recently-detected binding of the CFTR C-terminus to multivalent PDZ-domain proteins (Hall et al., 1998; Wang et al., 1998; Short et al., 1998; Sun et al., 2000; Wang et al., 2000) could not have occurred with the truncated form. Therefore these original experiments could not have detected possible associations mediated by PDZ-domain proteins.

A second evaluation of CFTR quaternary structure came from an estimation of the cross-sectional area of freeze-fracture particles observed in membranes of *Xenopus* oocytes expressing CFTR (Eskandari et al., 1998). When compared with several other integral membrane proteins with known numbers of bilayer-spanning helices, the CFTR particle area corresponded more closely to 24 than 12 packed helices and hence it was concluded the CFTR may be dimeric in the membrane. There are several possible caveats to this interpretation, including the unknown helix packing arrangement and the possibility that all membrane-spanning sequences contributing to the particle area may not be from CFTR. In a third approach, the possibility that a homodimeric assembly forms the CFTR chloride channel was tested by expression of concatemers of two wild-type sequences or a wild type linked to an R-domain-deleted form (Zerhusen et al., 1999). Intermediate regulatory properties of the latter were interpreted as evidence of a chimeric channel formed by one wild-type and one mutant polypeptide. These regulatory properties were not very precisely defined, however, and there was no compelling evidence that the pore was formed by contributions from the two different CFTR sequences.

The issue of mediated rather than direct interactions between two CFTR polypeptides was raised by the finding that CFTR, like several other membrane receptors, transporters and channels (Fanning & Anderson, 1999; Garner, Nash & Huganir, 2000; Sheng & Sala, 2001) bound via its C-terminus to proteins containing multiple PDZ-domains (Hall et al., 1998; Short et al., 1998; Wang et al., 1998; Sun et al., 2000; Wang et al., 2000). Although physical complexes of more than one CFTR protein together with a PDZ-domain protein such as EBP-50 (ezrin binding protein 50) have not been directly demonstrated, stoichiometric titrations with bivalent forms of EBP-50 (Raghuram, Mak & Foskett, 2001) or another PDZ-domain protein, CAP70 (CFTR-associated protein 70 or PDZK1, (Kocher et al., 1999; Wang et al., 2000), were reported to increase the open probability of CFTR in membrane patches. These experiments have been interpreted as indicating that promotion of dimer formation increases channel activity.

Most recently Ramjeesingh et al. (2001) detected forms of CFTR of approximately monomeric and dimeric sizes in electrophoretic gels and gel filtration columns under partially dissociating conditions. In their experiments, the two forms did not exhibit significantly different protein kinase A-stimulated chloride flux, single-channel or ATPase activities and the significance of the larger species interpreted as containing two CFTR polypeptides was not elaborated upon.

We have now evaluated CFTR quaternary structure from endogenously and heterologously expressing cells by both biochemical and functional means and find no evidence of self-association of individual CFTR polypeptides to form homo-oligomeric structures.

Materials and Methods

Tissue Culture

BHK-21 (baby hamster kidney) cells were cultured as previously described (Loo et al., 1998). HEK293 cells were grown in DMEM (GIBCO-BRL) supplemented with 10% FBS, 1 mM glutamine, MEM nonessential amino acids, 1 mM sodium pyruvate, and 1% penicillin-streptomycin. Calu3 cells were grown in MEM (GIBCO-BRL), 10% FBS, 1 mM glutamine, 1 mM sodium pyruvate, and 1% penicillin-streptomycin. Clonal BHK-21 cells stably expressing wild type or ΔF508 C-terminally-tagged with HSV were generated by transfection by calcium phosphate (Sambrook & Russell, 2001), followed by growth and selection in DMEM-F12, 5% FBS, 1% penicillin-streptomycin, and 500 μM methotrexate. For transient transfection, cells at 70% confluence were transfected by calcium phosphate and harvested 48 hr post-transfection. All cells were grown at 37°C in 5% CO_2.

Velocity Gradient Centrifugation

Microsomal membranes from Calu3 and BHK cells stably expressing CFTR were isolated according to published protocols (Aleksandrov & Riordan, 1998). Membranes were solubilized in 1 ml of 0.09% NP-40, 0.2% Triton X-100, or RIPA (1% Triton X-100, 1% deoxycholic acid, and 0.1% SDS) in 150 mM NaCl and 50 mM Tris, pH 7.4 and layered on top of an 11-ml linear, continuous 10–36% sucrose gradient containing the respective detergent buffer. The sucrose gradient was formed by a gradient former (BioRad) and layered from the bottom to the top with a peristaltic pump (Buchler Instruments). Following centrifugation at 260,000 × *g* for 12 hr in an SW41Ti swing-out rotor (Beckman), twentyfour 500-μl fractions were collected from the top. Odd-numbered fractions were diluted with equal volume of RIPA buffer and immunoprecipitated with the CFTR monoclonal antibody M3A7 (1:250) (Kartner & Riordan, 1998) followed by protein G agarose beads (GIBCO-BRL), and blotted with the rabbit antibody 155 (1:1250). Molecular-weight markers IgM (950 kDa), thyroglobulin (660 kDa), urease (trimer, 272 kDa), catalase (240 kDa), and alkaline phosphatase (90 kDa) were diluted in 1 ml of 0.09% NP-40, 0.2% Triton X-100, or RIPA detergent buffer and sedimented as de-

scribed above. Peak migration of each species was determined by Coomassie staining of all fractions. The sucrose content of each fraction following centrifugation was measured by a handheld 0° to 10° Brix refractometer (Fisher) after a 1:3 sample dilution.

In Vitro Mutagenesis

The Flag M2 and HSV epitopes were introduced to either the C or N terminus of CFTR by PCR using primers encoding DYKDDDDK and QPELAPEDPED, respectively (single-letter amino acid) and cloned into full-length CFTR in pcDNA3 (Invitrogen) and pNUT vectors. To facilitate cloning, a NotI site was introduced immediately following the STOP codon for the C-terminal tags; a KpnI site was placed upstream of the Kozak sequence for the N-terminal tags. PCR primers for generating C-terminal M2 and HSV epitopes were 5′-GAA GAG ATG CAA GAT ACA AGG CTT GAC TAC AAG GAT GAC GAT GAC AAG TAG CGG CCG CAT-3′ and 5′-GAA GAG ATG CAA GAT ACA AGG CTT CAG CCT GAA CTC GCT CCA GAG GAT CCG GAA GAT TAG CGG CCG CAT-3′, respectively. PCR primers for generating N-terminal M2 and HSV epitopes (inserted between residues 1 and 2 of CFTR) were 5′-CTT GGT ACC CGA GAG ACC ATG GAC TAC AAG GAT GAC GAT GAC AAG CAG AGG TCG CCT CTG GAA AAGG-3′ and 5′-CTT GGT ACC CGA GAG ACC ATG CAG CCT GAA CTC GCT CCA GAG GAT CCG GAA GAT CAG AGG TCG CCT CTG GAA AAGG-3′, respectively. The ΔF508 mutation was cloned from pNUT-ΔF508 into C-terminally tagged CFTR by swapping the AflII-HpaI fragments. Missense mutations S341A and R347D were generated by site-directed mutagenesis (Stratagene) and cloned into CFTR-M2 by replacing the AflII-HpaI fragment, and into M2-CFTR by replacing the XbaI-HpaI fragment. The AflII-HpaI fragment containing TT338,339AA mutations (Linsdell et al., 1997) was substituted into CFTR-HSV in pcDNA3. The cloning description of the HA-tagged EPP-50 can be obtained from Chen and Riordan. Cloning was verified by restriction-enzyme digestion and sequencing by the Mayo Molecular Biology Core Facility.

Immunoprecipitation and Nickel-Affinity Binding

Cells transiently co-expressing M2- and HSV-tagged CFTR at either the C or N terminus were harvested with lysis buffer consisting of (in mM): 150 NaCl, 50 Tris, 10 $NaMoO_4$, and 0.09% NP-40, pH 7.4 supplemented with protease inhibitors E64 (3.5 μg/ml), benzamidine (157 μg/ml), aprotinin (2 μg/ml), leupeptin (1 μg/ml), and Pefabloc (480 μg/ml). Post-nuclear supernatant was immunoprecipitated with either M3A7 (1:250), anti-M2 (1:100, stock antiserum diluted with glycerol to 2 mg/ml, Sigma), anti-HSV (1:250 for C-terminal CFTR-HSV or 1:125 for N-terminal HSV-CFTR, Novagen), or the irrelevant anti-c-myc antibody 9E10 (1:250) overnight followed by 30 μl of packed protein G agarose beads for 2 hr at 4°C. Immune complexes were washed extensively with lysis buffer and eluted from protein G agarose beads with electrophoresis sample buffer. Immune precipitates were separated by SDS-PAGE and blotted with M3A7 (1:2500), anti-M2 (1:1000), anti-HSV (1:5000), or the anti-calnexin antibody K-9 (1:1000, kind gift from Dr. David Williams). BHK cells transiently co-expressing M2-CFTR, HSV-CFTR, and HA-EBP-50 were lysed in 0.09% NP-40 and analyzed as described above. EBP-50 signals were detected by Western blotting with 3F10 (1:2500). Immunoprecipitation experiments were also performed with other buffers containing 150 mM NaCl, 50 mM Tris, pH 7.4 and one of the following detergents: 1% *n*-octyl-β-D-glucopyranoside (OG, Calbiochem), 1% *n*-dodecyl-β-D-maltoside (DDM, Calbiochem), 0.1% $C_{12}E_8$ (Calbiochem), 0.2% $C_{10}E_6$ (Calbiochem), 0.2% Triton X-100, 1% digitonin, 1.5% 3-[(3-cholamidopropyl)dimethylammonio]-1-propanesulfonate (CHAPS), 0.2% lauryldimethyladmine oxide (LDAO, Calbiochem), and 0.15% zwittergent 3–14 (Calbiochem).

BHK cells stably expressing C-terminal polyhistidine-tagged CFTR were transiently transfected with either CFTR-M2 or CFTR-HSV and solubilized in lysis buffer consisting of 150 mM NaCl, 50 mM Tris, 25 mM imidazole, 0.09% NP-40, pH 8.0 and protease inhibitors. Post-nuclear supernatant was either immunoprecipitated with anti-M2 (1:100) or anti-HSV (1:250) followed by protein G agarose, or incubated with 30 μl packed Ni-NTA agarose beads (Qiagen) for 4 hr at 4°C. Ni-NTA beads were washed 6 times with solubilization buffer and eluted with lysis buffer containing 500 mM imidazole, pH 7.2 for 2 hr at 4°C. Residual proteins on Ni-NTA beads were washed off with electrophoresis sample buffer.

Cell Surface Labeling

BHK cells stably expressing CFTR-HSV were transfected with ΔF508-M2 and grown for 2 days at 37°C. Cells were incubated with 1 mg/ml EZ-link sulfo-NHS-LC-biotin (Pierce) in PBS, pH 8.0 supplemented with 0.1 mM $CaCl_2$ and 1.0 mM $MgCl_2$ for 30 min at 4°C. The reaction was quenched with glycine, BSA, and NH_4Cl for 30 min at 4°C. Cells were rinsed 6 times with PBS and lysed in 0.09% NP-40 buffer with protease inhibitors. Equal volume of post-nuclear supernatant was immunoprecipitated with either anti-M2 (1:100) or anti-HSV (1:250) followed by protein G agarose beads, or incubated with 50 μl packed immobilized streptavidin beads (Pierce) overnight. Bound complexes were eluted with electrophoresis sample buffer, fractionated by SDS-PAGE, and blotted with anti-M2 (1:1000) or anti-HSV (1:5000).

Single-Channel Measurements in Planar Lipid Bilayers

Single-channel recordings in planar lipid bilayers were performed according to published protocols (Gunderson & Kopito, 1995; Aleksandrov & Riordan, 1998). Briefly, microsomes from BHK-21 cells transiently expressing CFTR were pelleted and phosphorylated with 100 units/ml PKA (Promega) and 2 mM Na_2ATP (Sigma) at room temperature for 30 min in 10 mM HEPES, 5 mM $MgCl_2$, and 250 mM sucrose, pH 7.2. Membranes were added to the cis compartment of a Teflon cup separating the cis and trans compartments by a 0.2-mm aperture. Single channels were observed after the fusion of vesicles with a planar lipid bilayer consisting of 2:1 (wt:wt) 1-palmitoyl-2-oleoyl-*sn*-glycero-3-phosphoethanolamine: 1-palmitoyl-2-oleoyl-*sn*-glycero-3-phosphoserine (Avanti Polar Lipids) in *n*-decane painted onto the aperture. Channel measurements were made at 30°C in symmetric solutions containing (in mM): 300 Tris-HCl, 6 $MgCl_2$, and 1 EGTA, pH 7.2. To maximize channel openings, 5 mM Na_2ATP and 67 u/ml PKA were added to the cis compartment. Voltage potential is the difference between cis and trans (ground) compartments. Current measurements were performed under voltage-clamp conditions and filtered with an 8-pole Bessel low-pass filter with a corner frequency of 50 Hz and digitized at 500 Hz. pCLAMP 6.0 (Axon Instruments) and Origin 4.1 (Microcal) softwares were used for data analysis and fitting current-amplitude histograms.

To obtain approximately equal expression of different epitope-tagged CFTR-conduction variants, BHK cells were transiently cotransfected with cDNA in the following ratios: 6:1, S341A-M2:WT-HSV;7:5,R347D-M2:WT-HSV;1:1,S341A-M2:TT338,339AA-HSV;3:11,R347D-M2:TT338,339AA-HSV;6:1,M2-S341A:HSV-WT; and 1:1,M2-R347D:HSV-WT. To determine the relative expression of each conduction species, equal volume of membrane

was solubilized in electrophoresis sample buffer and blotted with either anti-M2 or anti-HSV. To determine relative expression of each species, anti-HSV and anti-M2 signal intensities were normalized to M3A7 signal intensities for each conjugated CFTR species. The normalizing factor of anti-M2:anti-HSV for C-terminally-tagged CFTR was 0.33 obtained from the ratio CFTR-$M2_{anti\text{-}M2}$/CFTR-$M2_{M3A7}$*CFTR-HSV_{M3A7}/CFTR-$HSV_{anti\text{-}HSV}$ with respective values (in OD·mm) 0.98, 0.34, 0.28, and 2.48. Similarly, for N-terminally-tagged CFTR, the normalizing factor of anti-M2:anti-HSV was 1.36, obtained from the ratio M2-$CFTR_{anti\text{-}M2}$/M2-$CFTR_{M3A7}$*HSV-$CFTR_{M3A7}$/HSV-$CFTR_{anti\text{-}HSV}$, with respective values (in OD·mm) 2.10, 1.96, 1.19, and 0.94. Gel scanning and image analysis were performed with Quantity One (PDI).

Results

Velocity-Gradient Centrifugation of Detergent-Solubilized CFTR

As one means of estimating the molecule's size and thereby its oligomeric state, the protein solubilized from membranes of BHK cells in which it was heterologously expressed (Loo et al., 1998), was subjected to velocity sedimentation in linear, continuous sucrose gradients. Mild conditions were employed to minimize disruption of protein-protein interactions. The non-ionic NP-40 at a low concentration was previously found to be suitable for this purpose, as it maintained the delicate association between nascent CFTR and the molecular chaperone, Hsp90 (Loo et al., 1998). Under these conditions, mature CFTR migrated as a sharp peak in 3 of 12 fractions examined (Fig. 1*A*, left panel). The center of this peak at fraction 6 corresponds to an M_r of approximately 130 kDa relative to the migration of standards (Fig. 1*C*, left panel). When another non-ionic detergent was employed at a relatively low concentration (0.2% Triton X-100), there was migration to a slightly higher sucrose density corresponding to an M_r in the 200 kDa range, possibly reflecting the binding of more of this detergent. Significantly, however, migration was not substantially altered under the much stronger dissociating conditions of RIPA buffer (Fig. 1*A*, right panel) and 1% SDS (*data not shown*). From the size estimates obtained by interpolation from the standard curves, these observations indicate that the bulk of CFTR in the BHK cell membranes is monomeric. It is abundantly clear from these blots and even at much longer exposures that no larger species representing oligomers or aggregates are detected at higher fraction numbers. This is also true when CFTR was heterologously co-expressed with EBP-50 (*data not shown*).

Although the reports interpreting CFTR as dimeric also employed heterologous expression systems (Eskandari et al., 1998; Zerhusen et al., 1999; Wang et al., 2000), it is possible that conditions or factors required for self-association were not ideal in BHK cells. Therefore the same types of experiment were performed employing membranes from Calu-3 epithelial cells in which CFTR is endogenously expressed and functions as a secretory chloride channel (Haws et al., 1994; Shen et al., 1994). Figure 1*B* shows that the sedimentation is nearly identical under all three solubilizing conditions as it was in the case of the recombinant protein. Hence, even in the assumed native state where all requirements of normal CFTR function are fulfilled, including the presence of such things as PDZ-domain proteins that might tether C-termini of two CFTRs together, the bulk species present would appear to be a monomer.

The observations do not exclude the possibility that multiple CFTR glycoproteins might assemble by interactions that are disrupted even by mild solubilizing conditions. In that case, such interactions might be expected to be captured by chemical cross-linking and this approach is addressed in a separate study (Chen and Riordan, unpublished data).

Co-Expression of Differentially Epitope-Tagged CFTR Species

Our initial co-immunoprecipitation experiments were conceptually analogous to those of Marshall et al. (1994) in that the co-expressed species had different C-termini. In their case, a segment of the C-terminus was simply absent from one of the species, whereas we attached different epitope tags to the C-terminus of full-length CFTR. This modification did not alter either the processing or function of the molecule. Both of these strategies, however, preclude the association of the two CFTRs by a bivalent PDZ-domain protein and perhaps not surprisingly, no association was detected. This is apparent from the immunoprecipitation experiment depicted in Fig. 2. When expressed separately, the M2- and HSV-tagged species were detected only by the antibody recognizing its epitope (Fig. 2*A*) and this remained true when the two were co-expressed (Fig. 2*B*). This finding demonstrates the lack of strong interactions between parts of the protein other than the C-terminus. As an internal test for a co-immunoprecipitation, calnexin, an ER-membrane chaperone that binds nascent CFTR molecules (Pind, Riordan & Williams, 1994) is detected in these immunoprecipitates at ratios approximating that of immunoprecipitated CFTR (Fig. 2*B*, *compare* M3A7 and anti-CNX blots). This was further confirmed by the finding that neither of the C-terminally epitope-tagged species were present in the Ni-NTA-bound fraction together with a polyhistidine-tailed CFTR when they were co-expressed with it (Fig. 2*C*).

To determine if associations might occur when the C-termini were free to participate, similar experiments were performed but with the epitopes fused at the N-termini rather than the C-termini (Fig. 2*D*).

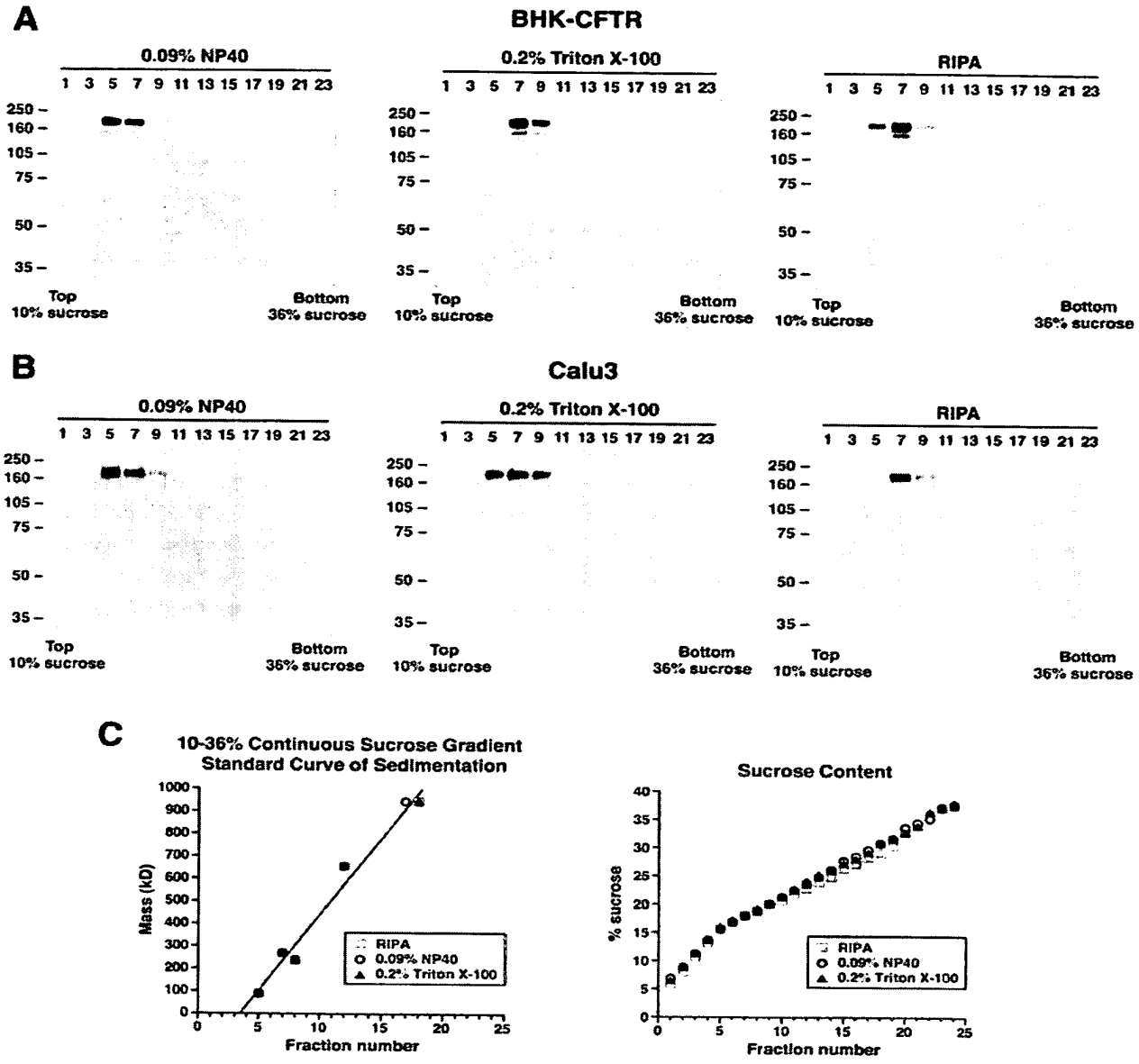

Fig. 1. CFTR sediments as a monomer in 10–36% linear, continuous sucrose gradients. Microsomal membranes from (*A*) BHK cells heterologously expressing CFTR and from (*B*) Calu3 cells endogenously expressing CFTR were solubilized in 1 ml of 0.09% NP-40, 0.2% Triton X-100, or RIPA (0.7 to 1.0 mg/ml protein) and layered on top of an 11-ml linear, continuous 10–36% sucrose gradient containing the respective detergent buffer. Following centrifugation at 260,000 × *g* for 12 hr, twentyfour 500-μl fractions were collected from the top. CFTR in odd-numbered fractions was immunoprecipitated with M3A7 (1:250) and blotted with antibody 155 (1:1250). Following centrifugation, the linearity of the sucrose gradient was confirmed by quantifying sucrose content by refraction. In all conditions, CFTR sediments between fractions 5–9. (*C*) Standard curve derived from the sedimentation of molecular weight standards in 10–36% linear, continuous sucrose gradient containing 0.09% NP-40, 0.2% Triton X-100, or RIPA: IgM (950 kDa), thyroglobulin (660 kDa), urease (trimer, 272 kDa), catalase (240 kDa), and alkaline phosphatase (90 kDa).

However, as shown in Fig. 2*E*, the two species differentially tagged at the N-termini did not co-immunoprecipitate either. This was also seen when the two N-terminally tagged species were co-expressed with EBP-50 (Fig. 2*F*). Despite possessing a strong in vitro binding interaction, an association between CFTR and the PDZ-domain protein was detected only when excess amounts of immunoprecipitating antibodies were used, indicating that their association may be compartmentalized or dynamically

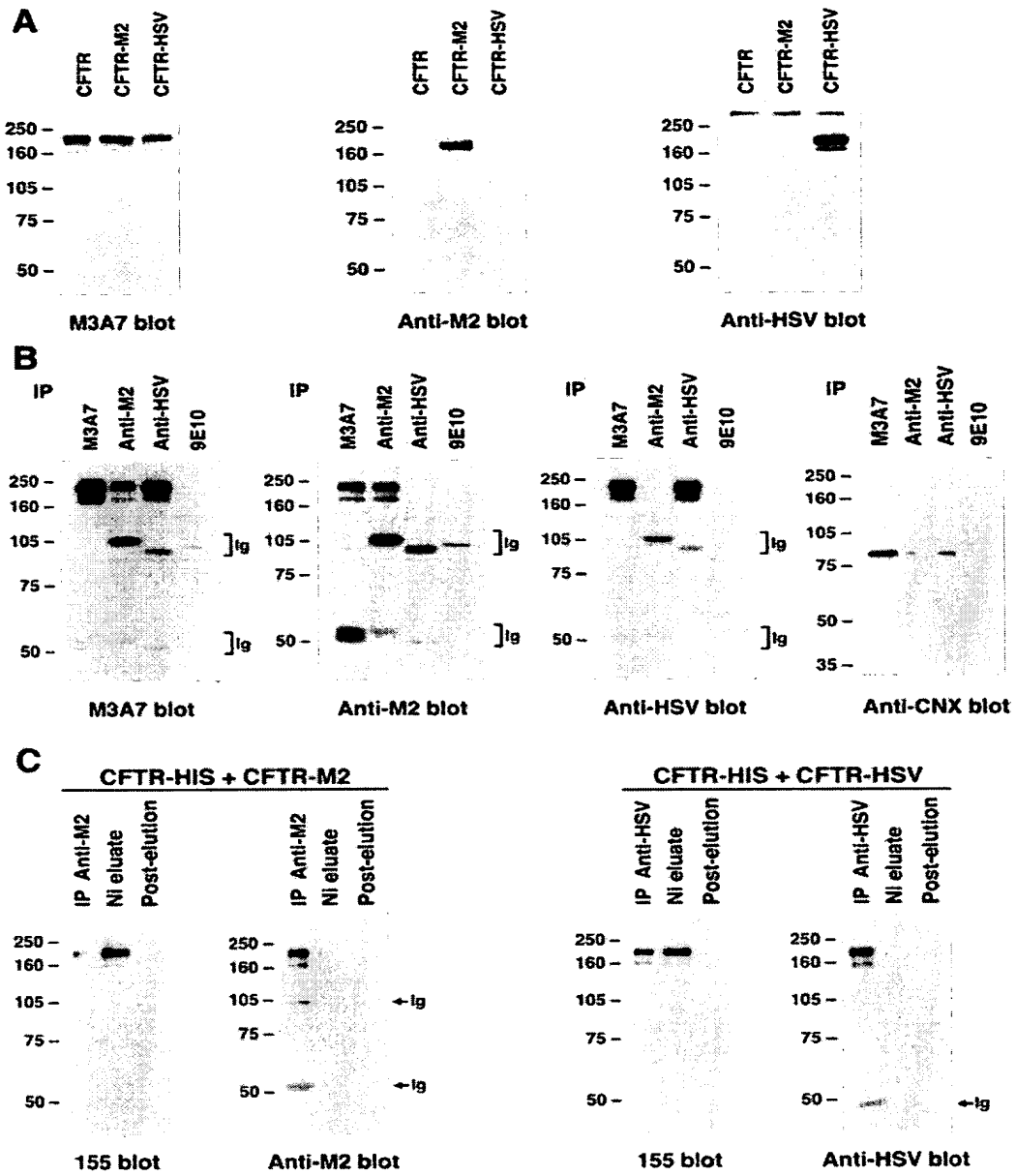

Fig. 2. No detectable association between different epitope-tagged CFTR species by immunoprecipitation and nickel affinity binding. (*A*) Lysates of BHK cells expressing wild-type and C-terminally M2 and HSV epitope-tagged CFTR (CFTR, CFTR-M2, and CFTR-HSV, respectively). Cell lysates (45 μg per lane) were blotted with M3A7 (1:2500), anti-M2 (1:1000), or anti-HSV (1:5000). The tagged constructs are recognized specifically by their corresponding antibody. (*B*) BHK cells transiently co-expressing CFTR-M2 and CFTR-HSV were solubilized in 0.09% NP-40 and immunoprecipitated with M3A7 (1:250), anti-M2 (1:100), anti-HSV (1:250), or the irrelevant antibody 9E10 (1:250). No co-immunoprecipitation of CFTR-M2 and CFTR-HSV is seen (lane *3*, anti-M2 blot and lane *2*, anti-HSV blot). As an internal control for a co-immunoprecipitation, calnexin is detected in these immunoprecipitates. (*C*) BHK cells stably expressing polyhistidine-tagged CFTR were transiently transfected with CFTR-M2 or CFTR-HSV and solubilized in 0.09% NP-40. Postnuclear supernatant was either immunoprecipitated with anti-M2 (1:100) or anti-HSV (1:250), or incubated with Ni-NTA agarose beads. Bound CFTR was eluted with 500 mM imidazole. Residual CFTR was washed off with sample buffer. No detectable association between CFTR-M2 and CFTR-HSV with polyhistidine-tagged CFTR is evident (lane *2*, anti-M2 and anti-HSV blots).

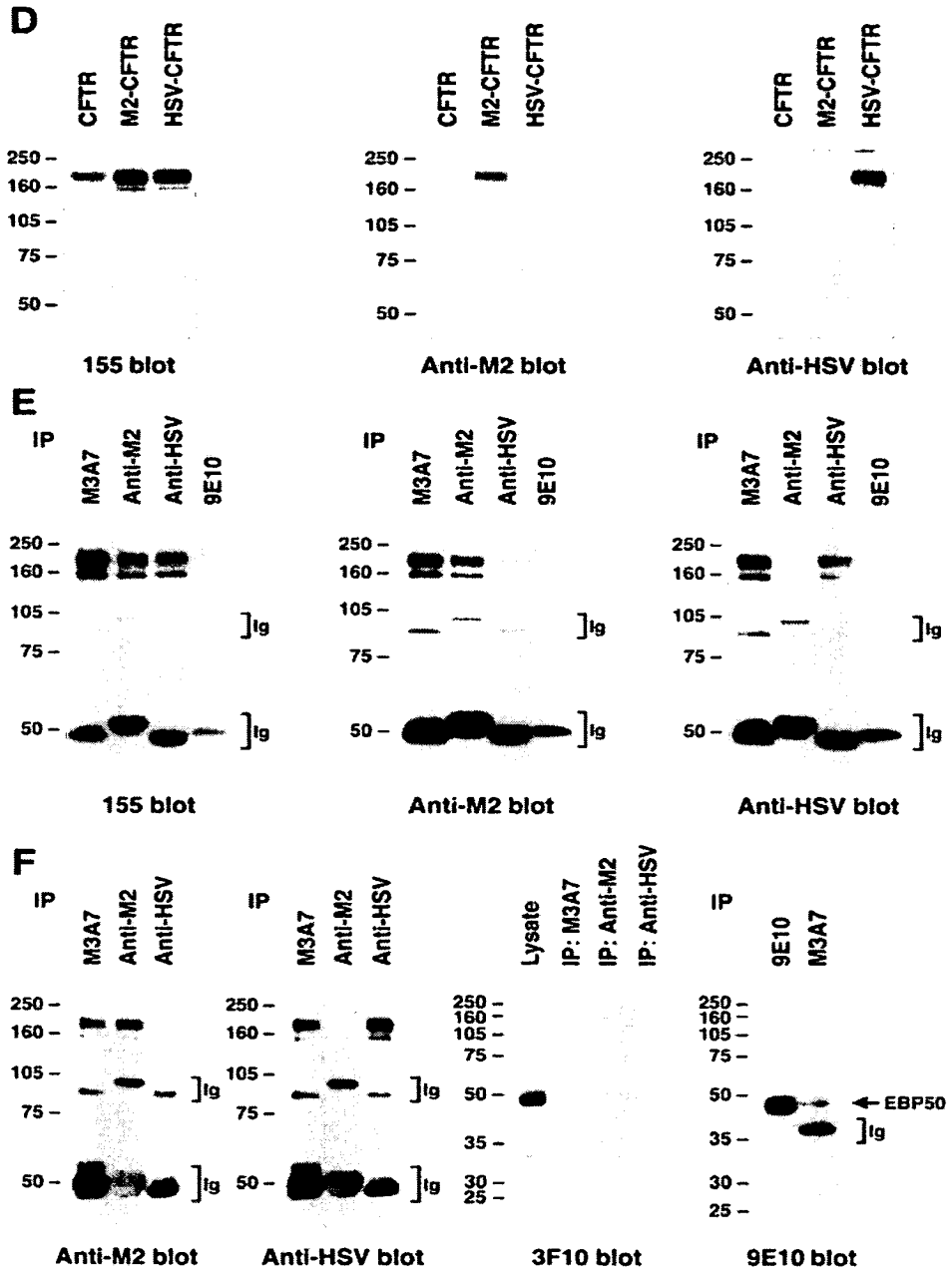

Fig. 2. (*Continued*). (*D*) Lysates of BHK cells expressing wild-type and N-terminally M2 and HSV epitope-tagged CFTR (CFTR, M2-CFTR, and HSV-CFTR, respectively). Cell lysates (45 μg per lane) were blotted with M3A7 (1:2500), anti-M2 (1:1000), or anti-HSV (1:5000). The tagged constructs are recognized specifically by their corresponding antibody. (*E*) BHK cells transiently co-expressing M2-CFTR and HSV-CFTR were lysed in 0.09% NP-40 and immunoprecipitated with M3A7 (1:250), anti-M2 (1:100), anti-HSV (1:125), or the irrelevant antibody 9E10 (1:250). No co-immunoprecipitation of M2-CFTR and HSV-CFTR is seen (lane *3*, anti-M2 blot and lane *2*, anti-HSV blot). (*F*) M2-CFTR and HSV-CFTR co-expressed with HA-tagged EBP-50 in BHK cells were lysed in 0.09% NP-40 and immunoprecipitated with M3A7 (1:250), anti-M2 (1:100), and anti-HSV (1:100). Immunoprecipitates were blotted with anti-M2 (1:1000), anti-HSV (1:5000), and 3F10 (1:2500). Lane *1* of the 3F10 blot contains 10 μg of cell lysate. To demonstrate an association between CFTR and EBP-50, BHK cells co-expressing CFTR and EBP-50 C-terminally tagged with c-myc were lysed in 0.09% NP-40 and immunoprecipitated with M3A7 (1:67) and 9E10 (1:67). EBP-50 signal was detected by Western blotting with 9E10 (1:2500). The M3A7 immunoprecipitates were loaded at eight times the volume of 9E10 immunoprecipitates.

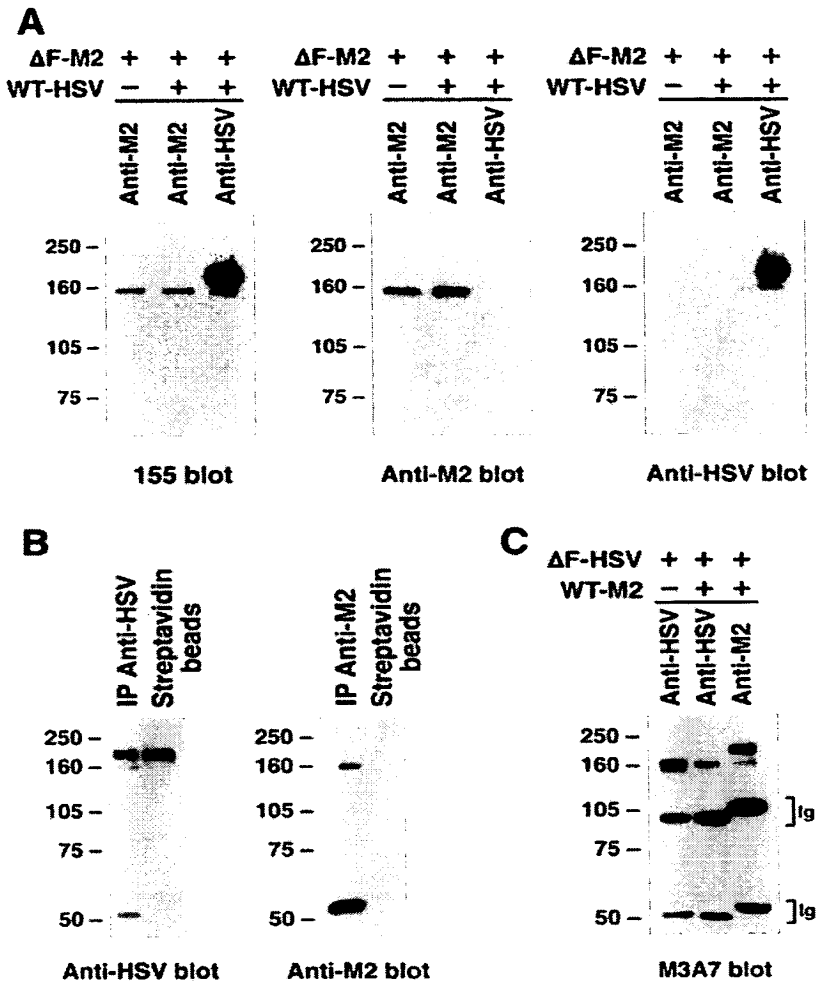

Fig. 3. Co-exressed epitope-tagged wild-type and ΔF508 CFTR do not co-assemble or influence each other's maturation (*A*) Parental BHK cells and BHK cells stably expressing WT-HSV were transiently transfected with ΔF508-M2 and grown for 48 hours at 37°C. Cells were lysed in 0.09% NP-40 and immunoprecipitated with anti-M2 (1:100) and anti-HSV (1:250). ΔF508-M2 does not acquire complex glycosylation in the presence or absence of wild-type CFTR (lanes *1* and *2*, 155 blot). In addition, ΔF508-M2 and WT-HSV do not co-immunoprecipitate (lane *3*, anti-M2 blot and lane *2*, anti-HSV blot). (*B*) Cells co-expressing ΔF508-M2 and WT-HSV as in (*A*) were surface-biotinylated and lysed in 0.09% NP-40. Postnuclear supernatant was either immunoprecipitated with anti-M2 (1:100) or anti-HSV (1:250), or incubated with immobilized streptavidin beads. Whereas the mature WT-HSV is surface-labeled (lane *2*, anti-HSV blot), neither ΔF508-M2 nor immature WT-HSV are labeled (lane *2*, anti-M2 blot and lane *2*, anti-HSV blot). (*C*) BHK cells stably expressing ΔF508-HSV were lysed in 0.09% NP-40 and immunoprecipitated with anti-HSV (1:250). ΔF508-HSV is core-glycosylated (lane *1*) with an additional smaller CFTR species due either to an alternative translation initiation site or a proteolytic cleavage of a small N-terminal fragment. ΔF508-HSV-expressing cells were transiently transfected with WT-M2 and grown for two days at 37°C. Cells were solubilized in 0.09% NP-40 and immunoprecipitated with anti-HSV (1:250) or anti-M2 (1:100). Neither the retention of WT-M2, as evident by the normal ratio of mature and immature CFTR signal intensities (lane *3*), nor maturation of ΔF508-HSV (lane *2*) are seen.

regulated (Fig. 2*F*). This may account for an undetectable amount of PDZ-mediated associating CFTR molecules, as had also been reported by Wang et al. (2000). Hence, as in the velocity gradient sedimentation experiments, individual CFTR polypeptides solubilized from membranes in mild detergent show no propensity to associate with each other.

The lack of association between the two immunologically-different CFTR species was also evident in other experimental conditions (*data not shown*), including co-expression in HEK293 cells, complete immunoprecipitation of CFTR using excess amounts of anti-M2 and anti-HSV antibodies, and solubilization of CFTR in other mild nonionic and zwitterionic detergent buffers including 0.1% $C_{12}E_8$, 0.2% $C_{10}E_6$, 0.2% Triton X-100, 1% OG, 1% DDM, 1% digitonin, 0.15% zwittergent 3-14, 0.2% LDAO, and 1.5% CHAPS. To test the possibility that CFTR may associate to form transient complexes when activated (Wang et al., 2000; Schillers et al., 2001), we treated BHK cells co-expressing C- or N-terminally-tagged CFTR with forskolin prior to solubilization; no association was evident by immunoprecipitation following CFTR stimulation (*data not shown*).

Co-Assembly of Wild-type and ΔF508 CFTR is not Detected

CFTR is a glycoprotein that is biosynthetically processed through the secretory pathway. At the endoplasmic reticulum (ER), CFTR is core-glycosylated at two asparagine residues in the fourth extracellular loop (Chang et al., 1994; Cheng et al., 1990; Gregory et al., 1990; Hämmerle et al., 2000). Following conformational maturation at the ER (Lukacs et al., 1994), CFTR is transported to the Golgi apparatus where its oligosaccharide chains undergo mannose trimming and complex glycosylation. These different glycosylation states provide facile assessment of the state of CFTR processing and trafficking by western

blotting (Fig. 3). The biosynthesis of CFTR at the ER is stringently regulated as ~20–30% of newly synthesized wild-type CFTR proteins acquire a mature conformation (Lukacs et al., 1994). Since subunit assembly at the ER is a component in the biosynthetic maturation of oligomeric proteins (Hurtley & Helenius, 1989; von Heijne, 1997), we assayed for CFTR structure by co-expressing two CFTR molecules with different maturation capabilities. In a report indicating that P-gp oligomerizes, its assembly occurred at the ER (Poruchynsky & Ling, 1994).

We monitored the biosynthetic processing of wild-type and the CF mutant ΔF508 CFTR in co-expression studies to test for possible CFTR assembly at the ER. Virtually all ΔF508 proteins are retained at the ER where it is cotranslationally poly-ubiquitinated and degraded (Jensen et al., 1995; Ward, Omura & Kopito, 1995; Sato, Ward & Kopito, 1998). If CFTR were oligomeric, wild-type CFTR might "rescue" the ΔF508 protein to the cell surface by assembly at the ER; equally likely, CFTR oligomers containing ΔF508 and wild-type CFTR might be retained at the ER. Wild-type and ΔF508 molecules were epitope-tagged at their C termini to differentiate each species. To study whether wild-type CFTR can promote ΔF508 expression at the plasma membrane, BHK cells stably expressing WT-HSV were transiently transfected with ΔF508-M2 and grown for two days at 37°C prior to solubilization and immunoprecipitation with anti-M2 and anti-HSV antibodies. When co-expressed with WT-HSV, ΔF508-M2 did not acquire complex glycosylation or associate with WT-HSV by immunoprecipitation (Fig. 3*A*). Addressing the possibility that ΔF508 can reach the plasma membrane in the absence of complex glycosylation, surface biotinylation on cells co-expressing WT-HSV and ΔF508-M2 labeled the mature form of wild type, but not ΔF508 (Fig. 3*B*). As an internal control, the immature ER-resident form of WT-HSV was not biotinylated. To assess the influence of ΔF508 on the biosynthesis of wild-type CFTR, WT-M2 was transiently expressed in BHK cells stably expressing ΔF508-HSV for two days at 37°C. Neither the retention of the wild-type protein, as evident by the normal ratio of complex and core-glycosylated CFTR band intensities, nor the acquisition of complex glycosylation by ΔF508 were seen (Fig. 3*C*). While the possibility that wild-type and ΔF508 CFTR nascent chains associate in the ER is not excluded by these observations, they do show that if this does occur it is without influence on the ability of either to progress through the secretory pathway.

Co-Expression of CFTR Variants with Different Unitary Conductances

The sixth transmembrane helix of CFTR has a profound influence on chloride conductance (Dawson, Smith & Mansoura, 1999). Mutations S341A and R347D (single-letter amino acid) dramatically lower chloride conductance (Tabcharani et al., 1993; McDonough et al., 1994) while the double mutation TT338, 339AA enhances chloride conduction (Linsdell et al., 1997). Because most oligomeric pore-forming proteins organize their subunits around the pore (Song et al., 1996; Chang et al., 1998; Doyle et al., 1998; Koronakis et al., 2000), we tested whether CFTR is monomeric or oligomeric by analyzing the population of channel conductances from cells co-expressing two conduction variants. An oligomeric channel comprised of different subunits each with a different channel conductance should exhibit a hybrid conductance that is intermediate to those of the two constituents (Cooper, Couturier & Ballivet, 1991). In contrast, two co-existing monomers should simply reveal two discrete conductance populations.

To monitor the expression of each species in co-expression experiments, we coupled the M2 and HSV epitopes to either the C or N terminus of CFTR. These epitope tags have negligible effects on CFTR conductance as all channels displayed slight outward rectification measuring ~14 pS and ~10 pS at negative and positive potentials, respectively (Fig. 4*A*, 4*B*, 5*A*, and 5*B*). In these bilayer experiments only those CFTR channels whose NBDs face the cis compartment containing MgATP are active. Thus, positive currents are outwardly directed currents. Although we did not extensively characterize the single-channel kinetics of these epitope-tagged CFTR proteins, they were indistinguishable from unmodified CFTR channels (Aleksandrov & Riordan, 1998). From 3-minute continuous single-channel recordings with 5 mM MgATP at 30°C, mean open and closed times were: τ_o = 176 msec τ_c = 174 msec with the N-terminal M2 epitope and τ_o = 177 msec, τ_c = 160 msec with the HSV epitope. This is different from the report by Chan et al. (2000) whose M2-tagged CFTR channels possessed a slower opening rate and lower open channel probability. Factors contributing to these differences may include different experimental conditions (for example a temperature of 30°C in our experiments versus 21–23°C in theirs) and the substitution of the residue immediately following the M2 epitope (second residue of wild-type CFTR) from glutamine to leucine by Chan et al. Also our measurements were made in planar lipid bilayers where conditions are not identical to those in *Xenopus* oocyte membranes where theirs were made.

To the C-terminal ends of CFTR, we attached the M2 epitope to S341A and R347D and the HSV epitope to wild type and TT338, 339AA (S341A-M2, R347D-M2, WT-HSV, and TT338, 339AA-HSV, respectively). Single-channel chord conductances for S341A-M2, R347D-M2, WT-HSV, and TT338, 339AA-HSV at −100 mV were (in pS): 2.2, 5.1, 14.3, and 15.6, respectively (Figs. 4*C* and 4*D*). The relative conductance

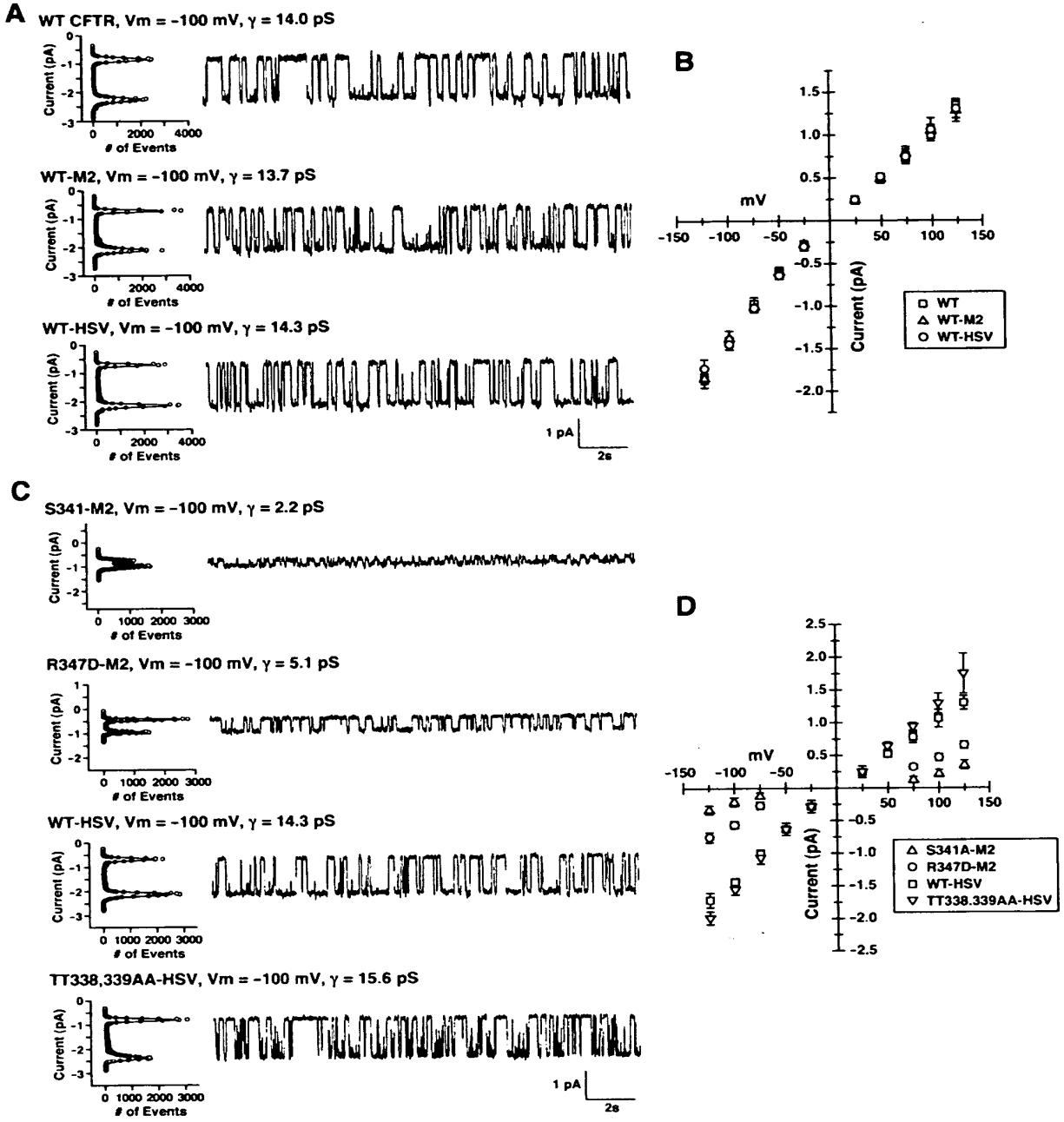

Fig. 4. No detectable hybrid conducting channel from microsomal vesicles containing two C-terminally-tagged CFTR pore variants. Single-channel measurements of microsomes from BHK cells transiently expressing CFTR are described in Materials and Methods. CFTR-containing membranes were phosphorylated with the catalytic subunit of PKA. All channel measurements were performed under voltage-clamp conditions at 30°C in symmetric buffer containing (in mM): 300 Tris-HCl, 6 $MgCl_2$, 1 EGTA, pH 7.2; 5 mM Na_2ATP and 67 u/ml PKA were added to the cis compartment to maximize channel activity. Current is measured with the trans compartment grounded. (*A*) Amplitude histograms and single-channel recordings of unmodified and C-terminally M2- and HSV-tagged CFTR (WT, WT-M2, and WT-HSV, respectively). All channels display similar single-channel kinetics and open-channel probabilities. CFTR channels possess a conductance of ~ 14pS at −100 mV. (*B*) Single-channel current-voltage relationships of WT, WT-M2, WT-HSV. All channels display a slight outward rectification of current. (*C*) Amplitude histograms and single-channel recordings of low-conduction mutants S341A and R347D C-terminally tagged with M2 (S341A-M2 and R347D-M2, respectively), and high-conduction variants WT and TT338, 339AA C-terminally tagged with HSV (WT-HSV and TT338, 339AA-HSV, respectively). At a holding potential of −100 mV, single-channel conductances are 2.2, 5.1 14.3, and 15.6 pS, respectively. (*D*) Single-channel current-voltage relationships of S341A-M2, R347D-M2, WT-HSV, and TT338,339A-HSV.

E **Co-Expression of S341A-M2 and WT-HSV**

	Number of Channels		Number of Channels	Total # of Channels
2 pS	70	14 pS	87	165
		9.5 pS	5	95% CI = 0 - 2.2%
		7.5 pS	3	
	70		95	
	42.4%		57.6%	
	S341A-M2		WT-HSV	
	0.351 OD x mm		1.065 OD x mm	
	50.2%		49.8%	

Co-Expression of R347D-M2 and WT-HSV

	Number of Channels		Number of Channels	Total # of Channels
5 pS	70	14 pS	85	163
		9.5 pS	3	95% CI = 0 - 2.2%
		7.5 pS	5	
	70		93	
	42.9%		57.1%	
	R347D-M2		WT-HSV	
	0.368 OD x mm		1.133 OD x mm	
	49.8%		50.2%	

Co-Expression of S341A-M2 and TT338,339AA-HSV

	Number of Channels		Number of Channels	Total # of Channels
2 pS	107	16 pS	56	170
		8 pS	7	95% CI = 0 - 2.2%
	107		63	
	62.9%		37.1%	
	S341A-M2		TT338,339AA-HSV	
	0.722 OD x mm		1.314 OD x mm	
	62.7%		37.3%	

Co-Expression of R347D-M2 and TT338,339AA-HSV

	Number of Channels		Number of Channels	Total # of Channels
5 pS	84	16 pS	61	154
2 pS	1	12 pS	4	95% CI = 0 - 2.4%
		8 pS	4	
	85		69	
	55.2%		44.8%	
	R347D-M2		TT338,339AA-HSV	
	0.499 OD x mm		1.506 OD x mm	
	50.3%		49.7%	

Fig. 4. (*Continued*). (*E*) Tabulation of single-channel conductances from microsomes containing a low-conducting (S341A.M2 or R347D-M2) and a high-conducting species (WT-HSV or TT338,339AA-HSV). Holding potential was −100 mV. The relative expression of each co-expressed species was determined by densitometry as described in Materials and Methods. No hybrid-conducting channel is detected (95% CI ≤ 2.4% in all combinations).

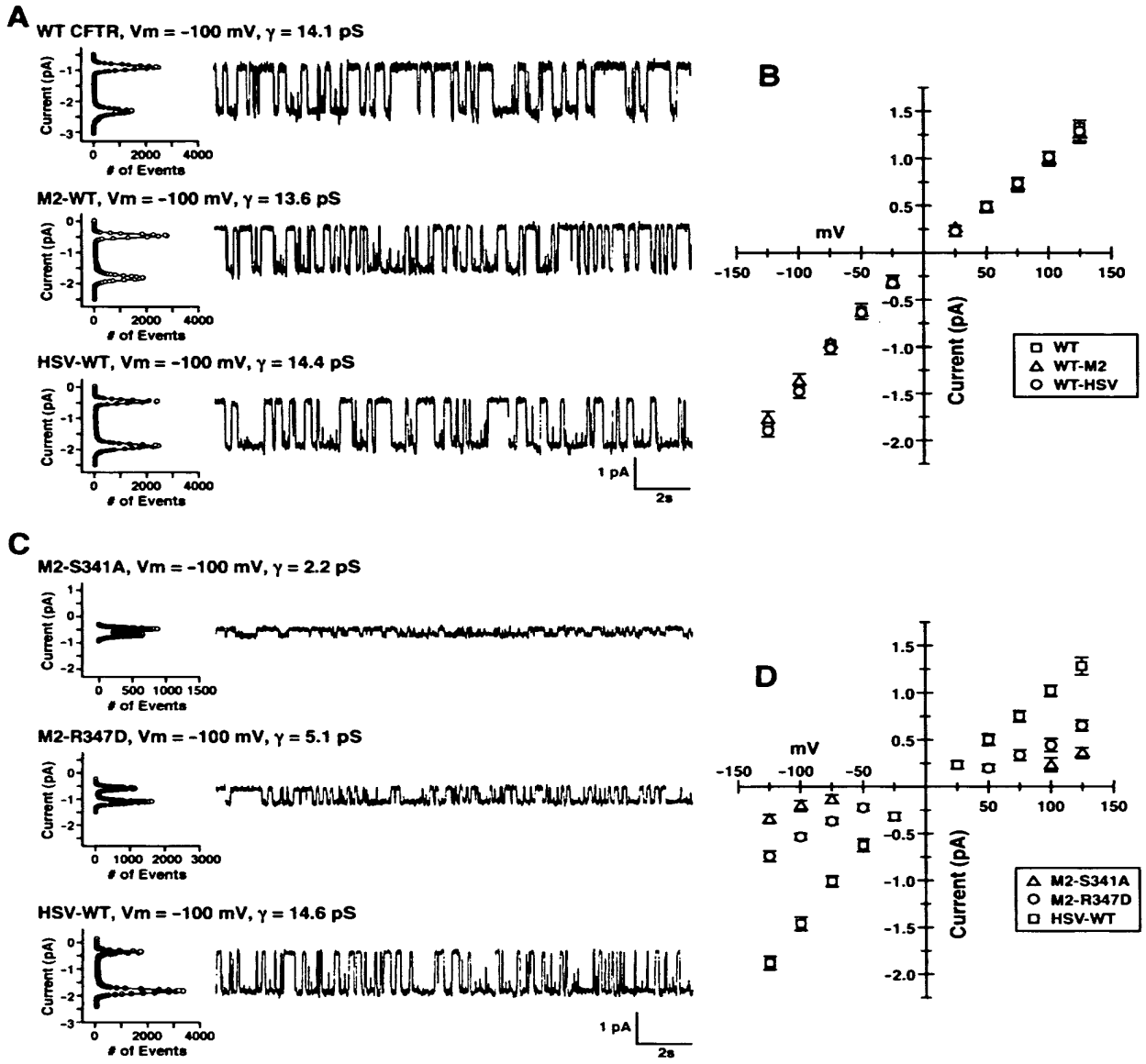

Fig. 5. No detectable hybrid conducting channel from microsomal vesicles containing two N-terminally-tagged CFTR pore variants. Single-channel measurements of microsomes from BHK cells transiently expressing CFTR as described in Fig. 4. (*A*) Amplitude histograms and single-channel recordings of unmodified and N-terminally M2- and HSV-tagged CFTR (WT, M2-WT, and HSV-WT, respectively). All channels display similar single-channel kinetics and open-channel probabilities. CFTR channels possess a conductance of ~14pS at −100 mV. (*B*) Single-channel current-voltage relationships of WT, M2-WT, and HSV-WT. All channels display a slight outward rectification of current. (*C*) Amplitude histograms and single-channel recordings of S341A and R347D N-terminally tagged with M2 (M2-S341A and M2-R347D, respectively), and WT N-terminally tagged with HSV (HSV-WT). Single-channel conductances at −100 mV are 2.2, 5.1, and 14.6 pS, respectively. (*D*) Single-channel current-voltage relationships of M2-S341A, M2-R347D, and HSV-WT.

of each to HSV-WT is in close agreement with reported values (Tabcharani et al., 1993; McDonough et al., 1994; Linsdell et al., 1997). To assess CFTR stoichiometry, we co-expressed approximately equal amounts of a low-(S341A-M2 or R347D-M2) and a high-conduction species (WT-HSV or TT338,339AA-HSV) for single-channel analysis (Fig. 4*E*). To maximize channel kinetics, all recordings were made in the presence of 5 mM MgATP and PKA at 30°C. In all combinations, the majority of observed conduc-

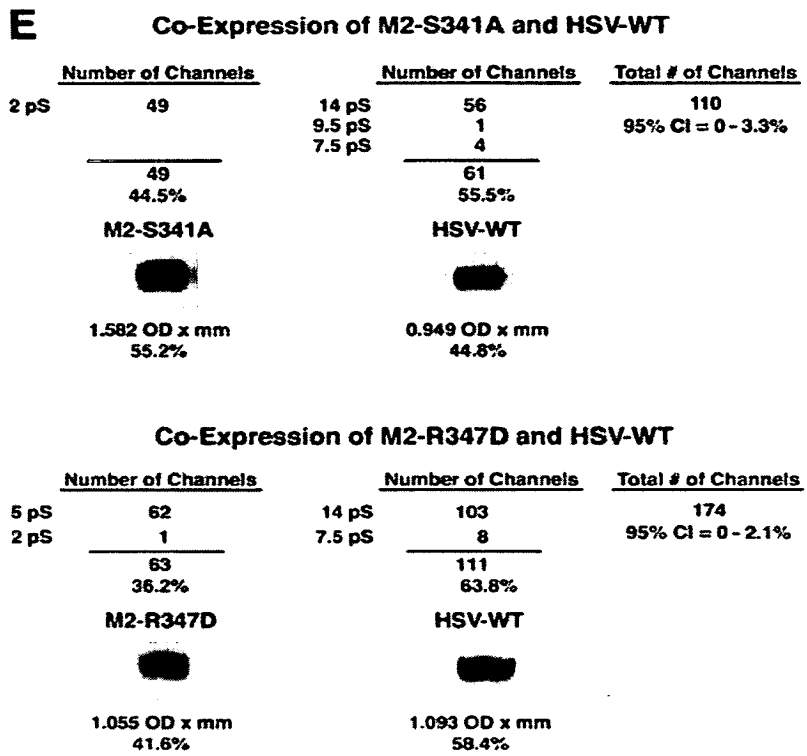

Fig. 5. (*Continued*). (*E*) Tabulation of single-channel conductances from microsomes containing HSV-WT and either M2-S341A or M2-R347D. Holding potential was −100 mV. The relative expression of each co-expressed species was determined by densitometry as described in Material and Methods. Co-expressed CFTR proteins do not form a hybrid channel (95% CI ≤ 3.3% for M2-S341A and HSV-WT, and ≤ 2.1% for M2-R347D and HSV-WT).

tances was comprised of each co-expressed conduction species. Intermediate conducting channels were infrequently observed; membrane vesicles containing WT-HSV plus S341A-M2 or R347D-M2 produced 9.5 pS and 7.5 pS channels, and vesicles containing TT338,339AA-HSV plus S341A-M2 or R347D-M2 yielded 12 pS, 8 pS, and 2 pS channels. These channels were most likely subconductances of WT-HSV (9.5 pS and 7.5 pS channels), TT338,339AA-HSV (12 pS and 8 pS), and R347D-M2 (2 pS) since they were seen with microsomes containing each of these species alone. Moreover, the same subconductance states of WT-HSV and TT338,339AA-HSV were seen when each was co-expressed with a different low-conduction species. The 7.5 pS (WT-HSV) and 8 pS (TT338, 339AA-HSV) conductances possessed very fast channel kinetics and interconverted with the main conductance state. The 95% confidence interval (CI) that the intermediate conducting channels were the products of co-assembled pore variants was ≤ 2.4% in all cases. The low frequency of intermediate conducting channels favored a binomial distribution of monomeric, but not oligomeric CFTR channels, given random assembly of subunits. In each experiment, the relative appearance of each co-expressed species closely approximated its relative expression level (*see* Materials and Methods).

Similar results were seen when these pore variants were epitope-tagged at their N termini. The chord conductances of M2-S341A, M2-R347D, and HSV-WT at −100 mV (in pS) were 2.2, 5.1, and 14.6, respectively (Fig. 5*C* and 5*D*). When co-expressed, microsomes containing HSV-WT and either M2-S341A or M2-R347D produced conductances that were predominantly channels of each constituent in their main conductance states and infrequently their subconductance states (Fig. 5*E*). The possibility that these intermediate conductances resulted from a hybrid assembly of multiple CFTR molecules was ≤ 3.3% and ≤ 2.1% for HSV-WT plus M2-S341A and M2-R347D, respectively. Similarly, the low frequency of intermediate-conducting channels favored a monomeric CFTR structure, with relative appearance of each co-expressed channel species closely matching its relative expression level. Similar results were seen when these pore variants in the absence of epitope-tagging were co-expressed, although their relative expression levels could not be quantified (*data not shown*).

Hence we conclude that two CFTR polypeptides do not assemble to form a single pore. These single-channel data per se, however, do not preclude assembly of two polypeptides where each constitutes a separate pore such as occurs with concatamers of two different ClC family members (Weinreich & Jentsch, 2001). However, in that case, in contrast to the situation with CFTR, there is good biochemical and genetic evidence that these are dimeric

proteins (Steinmeyer et al., 1994; Jentsch et al., 1999).

Discussion

Knowledge of a protein's quaternary structure is essential to an understanding of its mechanism of action. Homo- or hetero-oligomeric structures are common, especially in prokaryotes where the mean length of individual polypeptides is relatively short compared with larger multi-domain proteins that are more common in eukaryotes (Doolittle, 1995). This paradigm is indeed well illustrated by ABC proteins where in many prokaryotic transporters each of the nucleotide-binding and membrane-integrated domains are products of separate polycistronic transcripts, whereas in eukaryotic versions these are fused into single or at most two mRNAs (Higgins, 1992). As mentioned in the Introduction, it is still less clear whether more than one four-domain unit is required for function. The only well-established examples of hetero-oligomeric structures involving ABC proteins are the K_{ATP} channels where a sulfonylurea receptor of the ABCC subfamily associates with an inwardly rectifying potassium channel subunit (Aguilar-Bryan et al., 1998). Since these latter subunits form homotetramers as in other potassium channels, K_{ATP} channels are octameric (Clement et al., 1997; Inagaki et al., 1997; Shyng & Nichols, 1997).

Other potassium channels that are either voltage or ligand gated have similar homo-tetrameric pores (MacKinnon, 1991, 1995; Yang et al., 1995; Doyle et al., 1998). Other cation channels involved in membrane excitability, such as sodium and calcium channels, have repeat units in longer single polypeptides rather than separate pore-forming subunits that assemble (Catterall, 1988). However, while these large repeat-containing α subunits are usually capable of basic channel activity, they often associate with smaller regulatory subunits (Walker & De Waard, 1998; Catterall, 2000). The large family of ligand-gated channels typified by the nicotinic acetylcholine receptor are heteroligomeric (Cooper et al., 1991; Unger et al., 1999) as are in fact the majority of other known channels (Hille, 2001).

Interestingly, compared with the channels alluded to above that are cation channels, the major class of anion channels, members of the large ClC family (Jentsch et al., 1999; Maduke, Miller & Mindell, 2000), are double-barreled homodimers with each large polypeptide chain containing multiple membrane-spanning helices (Fahlke et al., 1997; Mindell et al., 2001; Weinreich & Jentsch, 2001; Dutzler et al., 2002). Consistent with their structures as homodimers, ClC mutations, including those causing several different diseases, are dominant (Koch et al., 1992; Steinmeyer et al., 1994).

Of the approximately 1000 disease-associated mutations identified in the CFTR gene, none exhibit dominant behaviors and hence there is no genetic evidence indicating that the CFTR chloride channel may be other than monomeric. It is of course possible that any potential dominant negative effect of one mutant subunit in a CFTR oligomer might be incomplete as only a small number of active molecules may be sufficient for physiological function (Johnson et al., 1992). The results we obtained with the co-expression of wild-type and ΔF508 CFTR corroborate the in vivo evidence that this mutant has no detectable dominant negative action. We have also directly tested whether more than one CFTR polypeptide contributes to the chloride ion pore by co-expressing forms with different amino acids at positions within TM6 known to strongly influence unitary conductance (Tabcharani et al., 1993; McDonough et al., 1994; Linsdell et al., 1997). Although the two forms were expressed in approximately equal amounts as judged by detection of different epitope tags attached to each, channels of conductances other than those of the two co-expressed were not detected at frequencies higher than when these species were expressed separately. Given the strong evidence that residues within TM6 contribute directly to pore formation (Dawson et al., 1999; Smith et al., 2001), TM6s from each form expressed should have influenced pore properties if two CFTR polypeptides are required for its formation.

Supportive of these electrophysiological findings were the observations that CFTR polypeptides were not found to be self-associated when solubilized under mild conditions from membranes of cells expressing the protein heterologously or endogenously. In both cases, the protein sedimented as a single uniform species of size approximating that of a monomer with bound detergent. No larger species representing either oligomers or non-specific aggregates were detected.

As an additional very sensitive means of detecting associations between individual CFTR polypeptides, they were distinctly tagged with different epitopes at either the N- or C-termini and co-expressed. Although each was readily immunoprecipitated with antibody to the epitope it contained, none of the form containing the other epitope was coprecipitated. Conditions that activate CFTR channels, such as forskolin treatment of cells, did not alter these distributions. While it might be argued that such a result might be expected with the PDZ-domain-binding C-termini blocked by the fused epitopes or absent in the case of the similar experiments of Marshall et al. (1994), the N-terminally tagged forms would not be compromised in this way. Even overexpression of EBP-50 did not lead to any detectible associations. This would indicate that if the stimulatory effects of increasing amounts of EBP-50

(Raghuram et al., 2001) or CAP-70 (Wang et al., 2000) are due to mediated crosslinking of two CFTRs via their C-termini, the proportion of the bulk CFTR population so affected must be very small. This would of course not mean that it is functionally unimportant.

To conclude, it may be worth considering the difference between the possibility of the CFTR channel possessing a true quaternary structure, in which contributions from more than one CFTR polypeptide chain are essential to pore formation and the tethering together of two or more chains, which might modulate the activity of either. Neither our present study nor any of those previously published (Zerhusen et al., 1999; Wang et al., 2000; Raghuram et al., 2001; Ramjeesingh et al., 2001) provides any evidence that a higher structure than a monomer is essential for channel function. Zerhusen et al. (1999) showed that a forced dimer had somewhat different properties from the native state, i.e., with low-level heterologous expression of a non-concatamerized construct or endogenous expression. These investigators did not show that a monomeric species was inactive. Similarly the studies of Wang et al. (2000) and Raghuram et al. (2001) showed only that bivalent PDZ-domain protein addition modulated CFTR-channel activity. The latter authors interpreted this as evidence of a stable dimer, whereas the former group acknowledged alternative explanations. The more recent report of Ramjeesingh et al. (2001) unequivocally states that a CFTR monomer is sufficient for both channel and ATPase activity, although larger dimeric species were also detected. In agreement with these observations we have found in extensive chemical crosslinking studies (Chen and Riordan, *unpublished data*) that heterologously overexpressed CFTR can be crosslinked to large molecular complexes containing more than one CFTR species and other proteins.

Final proof of CFTR quaternary structure awaits determination of the 3-dimensional structure of the active purified protein. The two mammalian ABC proteins for which low-resolution 3-D structures have been determined have yielded two different results. P-glycoprotein appears monomeric in 2-dimensional crystals (Rosenberg et al., 1997), while multidrug resistance protein 1 appears dimeric (Rosenberg et al., 2001). Interestingly, the diameters of P-gp freeze-fracture particles in the membrane (~10 nm; Sehested et al., 1989; Arsenault, Ling & Kartner, 1988), and of 2-D crystalline arrays of the purified protein (10–12 nm; Rosenberg et al., 1997) are very similar. Furthermore, although interpreted by the authors as dimeric, the CFTR freeze-fracture particles in *Xenopus* oocyte membranes had virtually identical dimensions (~9 nm; Eskandari et al., 1998). The MsbA lipid A transporter of *E. coli* (Chang & Roth, 2001) when crystallized consists of two fused nucleotide-binding and membrane-integrated polypeptides or is monomeric in the terminology of the single-chain eukaryotic family members such as CFTR as is the BtuCD vitamin B12 importer (Locher et al. 2000).

This work was supported by the NIDDK of the NIH (DK51619) and the Cystic Fibrosis Foundation. J.-H. C. is a recipient of the Howard B. Burchell Scholarship from the American Heart Association. We thank Dr. Joseph Bryan for technical advice concerning velocity gradient centrifugation, and Sharon Fleck and Marv Ruona for assistance with preparation of the manuscript and the figures, respectively.

References

Aguilar-Bryan, L., Clement, J.P., Gonzalez, G., Kunjilwar, K., Babenko, A., Bryan, J. 1998. Toward understanding the assembly and structure of KATP channels, *Physiol. Rev.* **78**:227–245

Aleksandrov, A.A., Riordan, J.R. 1998. Regulation of CFTR ion channel gating by MgATP. *FEBS Lett.* **431**:97–101

Arsenault, A.L., Ling, V., Kartner, N. 1988. Altered plasma membrane ultrastructure in multidrug-resistant cells. *Biochim. Biophys. Acta* **938**:315–321

Bear, C.E., Li, C.H., Kartner, N., Bridges, R.J., Jensen, T.J., Ramjeesingh, M, Riordan, J.R. 1992. Purification and functional reconstitution of the cystic fibrosis transmembrane conductance regulator (CFTR). *Cell* **68**:809–818

Boscoboinik, D., Debanne, M.T., Stafford, A.R., Jung, C.Y., Gupta, R.S., Epand, R.M. 1990. Dimerization of the P-glycoprotein in membranes. *Biochim. Biophys. Acta* **1027**:225–228

Catterall, W.A. 1988. Structure and function of voltage-sensitive ion channels. *Science* **242**:50–61

Catterall, W.A. 2000. From ionic currents to molecular mechanisms: the structure and function of voltage-gated sodium channels. *Neuron* **26**:13–25

Chan, K.W., Csanady, L., Seto-Young, D., Nairn, A.C., Gadsby, D.C. 2000. Severed molecules functionally define the boundaries of the cystic fibrosis transmembrane conductance regulator's NH(2)-terminal nucleotide binding domain. *J. Gen. Physiol.* **116**:163-180

Chang, X.B., Hou, Y.X., Jensen, T.J., Riordan, J.R. 1994. Mapping of cystic fibrosis transmembrane conductance regulator membrane topology by glycosylation site insertion. *J Biol. Chem.* **269**:18572-5

Chang, G., Roth, C.B. 2001. Structure of MsbA from *E. coli*: a homolog of the multidrug resistance ATP binding cassette (ABC) transporters. *Science* **293**:1793–1800

Chang, G., Spencer, R.H., Lee, A.T., Barclay, M.T., Rees, B.C. 1998. Structure of the MscL homolog from Mycobacterium tuberculosis: a gated mechanosensitive ion channel. *Science* **282**:2220–2226

Cheng, S.H., Gregory, R.J., Marshall, J., Paul, S., Souza, D.W., White, G.A., O'Riordan, C.R., Smith, A.E. 1990. Defective intracellular transport and processing of CFTR is the molecular basis of most cystic fibrosis. *Cell* **63**:827-34

Clement, J.P.t., Kunjilwar, K., Gonzalez, G., Schwanstecher, M., Panten, U., Aguilar-Bryan, L., Bryan, J. 1997. Association and stoichiometry of K(ATP) channel subunits. *Neuron* **18**:827–838

Cooper, E., Couturier, S., Ballivet, M. 1991. Pentameric structure and subunit stoichiometry of a neuronal nicotinic acetylcholine receptor. *Nature* **350**:235–238

Corey, S., Krapivinsky, G., Krapivinsky, L., Clapham, D.E. 1998. Number and stoichiometry of subunits in the native atrial G-protein-gated K^+ channel, IKACh. *J. Biol. Chem.* **273**:5271–5278

Dawson, D.C., Smith, S.S., Mansoura, M.K. 1999. CFTR: mechanism of anion conduction. *Physiol. Rev.* **79**:S47–S75

Dean, M., Rzhetsky, A., Allikmets, R. 2001. The human ATP-binding cassette (ABC) transporter superfamily. *Genome Res.* **11**:1156–1166

Doige, C.A., Ames, G.F. 1993. ATP-dependent transport systems in bacteria and humans: relevance to cystic fibrosis and multidrug resistance. *Annu. Rev. Microbiol.* **47**:291–319

Doolittle, R.F. 1995. The multiplicity of domains in proteins. *Annu. Rev. Biochem.* **64**:287–314

Doyle, D.A., Morais Cabral, J., Pfuetzner, R.A., Kuo, A., Gulbis, J.M., Cohen, S.L., Chait, B.T., MacKinnon, R. 1998. The structure of the potassium channel: molecular basis of K^+ conduction and selectivity. *Science* **280**:69–77

Dutzler, R., Campbell, E.B., Cadene, M., Chait, B.T., MacKinnon, R. 2002. X-ray structure of a CIC chloride channel at 3.0 A reveals the molecular basis of anion selectivity. *Nature* **415**:287-94

Eskandari, S., Wright, E.M., Kreman, M., Starace, D.M., Zampighi, G.A. 1998. Structural analysis of cloned plasma membrane proteins by freeze-fracture electron microscopy. *Proc. Natl. Acad. Sci. USA* **95**:11235–11240

Fahlke, C., Knittle, T., Gurnett, C.A., Campbell, K.P., George Jr., A.L., 1997. Subunit stoichiometry of human muscle chloride channels. *J. Gen. Physiol.* **109**:93–104

Fanning, A.S., Anderson, J.M. 1999. PDZ domains: fundamental building blocks in the organization of protein complexes at the plasma membrane. *J. Clin. Invest.* **103**:767–772

Garner, C.C., Nash, J., Huganir, R.L. 2000. PDZ domains in synapse assembly and signalling. *Trends Cell Biol.* **10**:274–280

Gregory, R.J., Cheng, S.H., Rich, D.P., Marshall, J., Paul, S., Hehir, K., Ostedgaard, L., Klinger, K.W., Welsh, M.J., Smith, A.E. 1990. Expression and characterization of the cystic fibrosis transmembrane conductance regulator. *Nature* **347**:382-6

Gunderson, K.L., Kopito, R.R. 1995. Conformational states of CFTR associated with channel gating: the role ATP binding and hydrolysis. *Cell* **82**:231–239

Hall, R.A., Ostedgaard, L.S., Premont, R.T., Blitzer, J.T., Rahman, N., Welsh, M.J., Lefkowitz, R.J. 1998. A C-terminal motif found in the beta2-adrenergic receptor, P2Y1 receptor and cystic fibrosis transmembrane conductance regulator determines binding to the Na^+H^+ exchanger regulatory factor family of PDZ proteins. *Proc. Natl. Acad. Sci. USA* **95**:8496–8501

Hämmerle, M.M., Aleksandrov, A.A., Chang, X., Riordan, J.R. 2000. A novel CFTR disease-associated mutation causes addition of an extra N-linked oligosaccharide. *Glycoconj J* **17**: 807-13

Haws, C., Finkbeiner, W.E., Widdicombe, J.H., Wine, JJ. 1994. CFTR in Calu-3 human airway cells: channel properties and role in cAMP-activated Cl-conductance. *Am. J. Physiol.* **266**:L502–L512

Higgins, C.F. 1992. ABC transporters: from microorganisms to man. *Annu. Rev. Cell Biol.* **8**:67–113

Hille, B. 2001. Ion channels of excitable membranes. Sinauer, Sunderland, Mass.

Hurtley, S.M., Helenius, A. 1989. Protein oligomerization in the endoplasmic reticulum. *Annu. Rev. Cell. Biol.* **5**:227–307

Inagaki, N., Gonoi, T., Seino, S. 1997. Subunit stoichiometry of the pancreatic beta-cell ATP-sensitive K^+ channel. *FEBS Lett.* **409**:232–236

Jensen, T.J., Loo, M.A., Pind, S., Williams, D.B., Goldberg, A.L., Riordan, J.R. 1995. Multiple proteolytic systems, including the proteasome, contribute to CFTR processing. *Cell* **83**:129–135

Jentsch, T.J., Friedrich, T., Schriever, A., Yamada, H. 1999. The CLC chloride channel family. *Pfluegers Arch.* **437**:783–795

Jette, L., Potier, M., Beliveau, R. 1997. P-glycoprotein is a dimer in the kidney and brain capillary membranes: effect of cyclosporin A and SDZ-PSC 833. *Biochemistry* **36**:13929–13937

Johnson, L.G., Olsen, J.C., Sarkadi, B., Moore, K.L., Swanstrom, R., Boucher, R.C. 1992. Efficiency of gene transfer for restoration of normal airway epithelial function in cystic fibrosis. *Nat. Genet.* **2**:21–25

Juvvadi, S.R., Glavy, J.S., Horwitz, S.B., Orr, G.A. 1997. Domain organization of murine mdrlb P-glycoprotein: the cytoplasmic linker region is a potential dimerization domain. *Biochem. Biophys. Res. Comm.* **230**:442–447

Kartner, N., Riordan, J.R. 1998. Characterization of polyclonal and monoclonal antibodies to cystic fibrosis transmembrane conductance regulator. *Methods Enzymol.* **292**:629–652

Koch, M.C., Steinmeyer, K., Lorenz, C., Ricker, K., Wolf, F., Otto, M., Zoll, B., Lehmann-Horn, F., Grzeschik, K.H., Jentsch, TJ. 1992. The skeletal muscle chloride channel in dominant and recessive human myotonia. *Science* **257**:797–800

Kocher, O., Cornelia, N., Gilchrist, A., Pal, R., Tognazzi, K., Brown, L.F., Knoll, J.H. 1999. PDZK1, a novel PDZ domain-containing protein up-regulated in carcinomas and mapped to chromosome Iq21, interacts with cMOAT (MRP2), the multidrug resistance-associated protein. *Lab. Invest.* **79**:1161–1170

Koronakis, V., Sharff, A., Koronakis, E., Luisi, B., Hughes, C. 2000. Crystal structure of the bacterial membrane protein TolC central to multidrug efflux and protein export. *Nature* **405**:914–919

Liman, E.R., Tytgat, J., Hess, P. 1992. Subunit stoichiometry of a mammalian K^+ channel determined by construction of multimeric cDNAs. *Neuron* **9**:861–871

Linsdell, P., Tabcharani, J.A., Rommens, J.M., Hou, Y.X., Chang, X.B., Tsui, L.C., Riordan, J.R., Hanrahan, J.W. 1997. Permeability of wild-type and mutant cystic fibrosis transmembrane conductance regulator chloride channels to polyatomic anions. *J. Gen. Physiol.* **110**:355–364

Locher, K.P., Lee, A.T., Rees, D.C. 2002. The E. coli BtuCD structure: a framework for ABC transporter architecture and mechanism. *Science* **296**:1091-8

Loo, M.A., Jensen, T.J., Cui, L., Hou, Y., Chang, X.B., Riordan, J.R. 1998. Perturbation of Hsp90 interaction with nascent CFTR prevents its maturation and accelerates its degradation by the proteasome. *Embo J.* **17**:6879–6887

Loo, T.W., Clarke, D.M. 1996. The minimum functional unit of human P-glycoprotein appears to be a monomer. *J. Biol. Chem.* **271**:27488–27492

Lukacs, G.L., Mohamed, A., Kartner, N., Chang, X.B., Riordan, J.R., Grinstein, S. 1994. Conformational maturation of CFTR but not its mutant counterpart (delta F508) occurs in the endoplasmic reticulum and requires ATP. *Embo J.* **13**:6076–6086

MacKinnon, R. 1991. Determination of the subunit stoichiometry of a voltage-activated potassium channel. *Nature* **350**:232–235

MacKinnon, R. 1995. Pore loops: an emerging theme in ion channel structure. *Neuron* **14**:889–892

Maduke, M., Miller, C., Mindell, J.A. 2000. A decade of CLC chloride channels: structure, mechanism, and many unsettled questions. *Annu. Rev. Biophys. Biomol. Struct.* **29**:411–438

Marshall, J., Fang, S., Ostedgaard, L.S., O'Riordan, C.R., Ferrara, D., Amara, J.F., Hoppe, H.T., Scheule, R.K., Welsh, M.J., Smith, A.E., et al. 1994. Stoichiometry of recombinant cystic fibrosis transmembrane conductance regulator in epithelial cells and its functional reconstitution into cells in vitro. *J. Biol. Chem.* **269**:2987–2995

McDonough, S., Davidson, N., Lester, H.A., McCarty, N.A. 1994. Novel pore-lining residues in CFTR that govern permeation and open-channel block. *Neuron* **13**:623–634

Mindell, J.A., Maduke, M., Miller, C., Grigorieff, N. 2001. Projection structure of a ClC-type chloride channel at 6.5 A resolution. *Nature* **409**:219–223

Naito, M., Tsuruo, T. 1992. Functionally active homodimer of P-glycoprotein in multidrug-resistant tumor cells. *Biochem. Biophys. Res. Comm.* **185**:284–290

Pind, S., Riordan, J.R., Williams, D.B. 1994. Participation of the endoplasmic reticulum chaperone calnexin (p88, IP90) in the biogenesis of the cystic fibrosis transmembrane conductance regulator. *J. Biol. Chem.* **269**:12784–12788

Poruchynsky, M.S., Ling, V. 1994. Detection of oligomeric and monomeric forms of P-glycoprotein in multidrug resistant cells. *Biochemistry* **33**:4163–4174

Raghuram, V., Mak, D.D., Foskett, J.K. 2001. Regulation of cystic fibrosis transmembrane conductance regulator single-channel gating by bivalent PDZ-domain-mediated interaction. *Proc. Natl. Acad. Sci. USA* **98**:1300–1305

Ramjeesingh, M., Li, C., Garami, E., Huan, L.J., Hewryk, M., Wang, Y., Galley, K., Bear, C.E. 1997. A novel procedure for the efficient purification of the cystic fibrosis transmembrane conductance regulator (CFTR). *Biochem. J.* **327**:17–21

Ramjeesingh, M., Li, C., Kogan, L, Wang, Y., Huan, L.J., Bear, C.E. 2001. A monomer is the minimum functional unit required for channel and ATP activity of the cystic fibrosis transmembrane conductance regulator. *Biochemistry* **40**:10700–10706

Rosenberg, M.R, Callaghan, R., Ford, R.C., Higgins, C.F. 1997. Structure of the multidrug resistance P-glycoprotein to 2.5 nm resolution determined by electron microscopy and image analysis. *J. Biol. Chem.* **272**:10685–10694

Rosenberg, M.F., Mao, Q., Holzenburg, A., Ford, R.C., Deeley, R.G., Cole, S.P. 2001. The structure of the multidrug resistance protein 1 (MRP1/ABCC1). Crystallization and single-particle analysis. *J. Biol. Chem.* **276**:16076–16082

Sambrook, J., Russell, D.W. 2001. Molecular cloning: a laboratory manual. Cold Spring Harbor Laboratory Press, Cold Spring Harbor, NY

Sato, S., Ward, C.L., Kopito, R.R. 1998. Cotranslational ubiquitination of cystic fibrosis transmembrane conductance regulator in vitro. *J. Biol. Chem.* **273**:7189–7192

Schillers, H., Danker, T., Madeja, M., Oberleithner, H. 2001. Plasma membrane protein clusters appear in CFTR-expressing *Xenopus laevis* oocytes after cAMP stimulation. *J. Membrane Biol.* **180**:205–212

Sehested, M., Simpson, D., Skovsgaard, T., Buhl-Jensen, P. 1989. Freeze-fracture study of plasma membranes in wild type and daunorubicin-resistant Ehrlich ascites tumor and P388 leukemia cells. *Virchows Arch. B Cell Pathol. Incl. Mol. Pathol.* **56**:327–335

Shen, B.Q., Finkbeiner, W.E., Wine, J.J., Mrsny, R.J., Widdicombe, J.H. 1994. Calu-3: a human airway epithelial cell line that shows cAMP-dependent Cl-secretion. *Am. J. Physiol.* **266**:L493–L501

Sheng, M., Sala, C. 2001. PDZ domains and the organization of supramolecular complexes. *Annu. Rev. Neurosci.* **24**:1–29

Short, D.B., Trotter, K.W., Reczek, D., Kreda, S.M., Bretscher, A., Boucher, R.C., Stutts, M.J., Milgram, S.L. 1998. An apical PDZ protein anchors the cystic fibrosis transmembrane conductance regulator to the cytoskeleton. *J. Biol. Chem.* **273**:19797–19801

Shyng, S., Nichols, C.G. 1997. Octameric stoichiometry of the KATP channel complex. *J. Gen. Physiol.* **110**:655–664

Smith, S.S., Liu, X., Zhang, Z.R., Sun, F., Kriewall, T.E., McCarty, N.A., Dawson, B.C. 2001. CFTR. Covalent and noncovalent modification suggests a role for fixed charges in anion conduction. *J. Gen. Physiol.* **118**:407–432

Song, L., Hobaugh, M.R., Shustak, C., Cheley, S., Bayley, H., Gouaux, J.E. 1996. Structure of staphylococcal alpha-hemolysin, a heptameric transmembrane pore. *Science* **274**:1859–1866

Steinmeyer, K., Lorenz, C., Pusch, M., Koch, M.C., Jentsch, T.J. 1994. Multimeric structure of ClC-1 chloride channel revealed by mutations in dominant myotonia congenita (Thomsen). *Embo J.* **13**:737–743

Sun, F., Hug, M.J., Lewarchik, C.M., Yun, C., Bradbury, N.A., Frizzell, R.A. 2000. E3KARP mediates the association of ezrin and protein kinase A with the cystic fibrosis transmembrane conductance regulator in airway cells. *J. Biol. Chem.* **275**:29539–29546

Tabcharani, J.A., Rommens, J.M., Hou, Y.X., Chang, X.B., Tsui, L.C., Riordan, J.R., Hanrahan, J.W. 1993. Multi-ion pore behaviour in the CFTR chloride channel. *Nature* **366**:79–82

Taylor, J.C., Horvath, A.R., Higgins, C.F., Begley, G.S. 2001. The multidrug resistance p-glycoprotein oligomeric state and intramolecular interactions. *J. Biol. Chem.* **276**:36075–36078

Unger, V.M., Kumar, N.M., Gilula, N.B., Yeager, M. 1999. Three-dimensional structure of a recombinant gap junction membrane channel. *Science* **283**:1176–1180

von Heijne, G. 1997. Membrane protein assembly. Chapman & Hall, New York

Walker, D., De Waard, M. 1998. Subunit interaction sites in voltage-dependent Ca^{2+}-channels: role in channel function. *Trends Neurosci.* **21**:148–154

Wang, S., Raab, R.W., Schatz, P.J., Guggino, W.B., Li, M. 1998. Peptide binding consensus of the NHE-RF-PDZ1 domain matches the C-terminal sequence of cystic fibrosis transmembrane conductance regulator (CFTR). *FEBS Lett.* **427**:103–108

Wang, S., Yue, H., Derin, R.B., Guggino, W.B., Li, M. 2000. Accessory protein facilitated CFTR-CFTR interaction, a molecular mechanism to potentiate the chloride channel activity. *Cell* **103**:169–179

Ward, C.L., Omura, S., Kopito, R.R. 1995. Degradation of CFTR by the ubiquitin-proteasome pathway. *Cell* **83**:121–127

Weinreich, F., Jentsch, T.J. 2001. Pores formed by single subunits in mixed dimers of different CLC chloride channels. *J. Biol. Chem.* **276**:2347–2553

Yang, J., Jan, Y.N., Jan, L.Y. 1995. Determination of the subunit stoichiometry of an inwardly rectifying potassium channel. *Neuron* **15**:1441–1447

Zerhusen, B., Zhao, J., Xie, J., Davis, P.B., Ma, J. 1999. A single conductance pore for chloride ions formed by two cystic fibrosis transmembrane conductance regulator molecules. *J. Biol. Chem.* **274**:7627–7630

A Monomer Is the Minimum Functional Unit Required for Channel and ATPase Activity of the Cystic Fibrosis Transmembrane Conductance Regulator†

Mohabir Ramjeesingh,‡ Canhui Li,‡ Ilana Kogan,§ Yanchun Wang,‡ Ling-Jun Huan,‡ and Christine E. Bear*,‡,§

Research Institute, Hospital for Sick Children, and Physiology Department, University of Toronto, Toronto, Ontario M5G 1X8, Canada

Received April 23, 2001; Revised Manuscript Received June 11, 2001

ABSTRACT: The cystic fibrosis transmembrane conductance regulator (CFTR) normally functions as a phosphorylation-regulated chloride channel on the apical surface of epithelial cells, and lack of this function is the primary cause for the fatal disease cystic fibrosis (CF). Previous studies showed that purified, reconstituted CFTR can function as a chloride channel and, further, that its intrinsic ATPase activity is required to regulate opening and closing of the channel gate. However, these previous studies did not identify the quaternary structure required to mediate conduction and catalysis. Our present studies show that CFTR molecules may self-associate in CHO and Sf9 membranes, as complexes close to the predicted size of CFTR dimers can be captured by chemical cross-linking reagents and detected using nondissociative PAGE. However, CFTR function does not require a multimeric complex for function as we determined that purified, reconstituted CFTR monomers are sufficient to mediate regulated chloride conduction and ATPase activity.

An understanding of the structural basis for the chloride channel and ATPase activities of the cystic fibrosis transmembrane conductance regulator (CFTR)[1] has fundamental basic importance as well as relevance to our understanding of the molecular mechanisms underlying the disease cystic fibrosis. To date, we know that several of the predicted transmembrane helices in CFTR are important in providing a pore for chloride electrodiffusion through CFTR including TM6 and TM12 (*1*−*3*). The two predicted nucleotide binding folds can bind ATP, and at least one, if not both, is capable of hydrolyzing ATP (*4*−*8*). Furthermore, we know that the putative regulatory (R) domain is phosphorylated at multiple sites by protein kinase A and that the structure of the isolated R domain is altered by phosphorylation (*9*−*11*). The amino and carboxy termini of CFTR are involved in interactions with other proteins, and these interactions may be important for the regulation of CFTR itself or its partner proteins (*12*, *13*). However, many important questions remain, and in this paper we address one in particular which has received considerable attention and stimulated a recent debate (*14*): namely, what is the number of molecules of CFTR required to form a regulated chloride channel?

Originally, Marshall et al. (*15*) concluded that CFTR existed primarily as a monomer in membranes, as differentially tagged versions of the protein could not be co-immunoprecipitated. However, more recently, Zerhusen et al. (*14*) showed that concatemers of two tethered CFTR molecules form a single pore with a unitary conductance of 9 pS, the conductance usually attributed to a native single CFTR channel. Cleaving the link between the concatamers with thrombin altered gating kinetics but did not result in the appearance of two channels. Furthermore, a concatemer of a normal protein tethered to a mutant protein known to exhibit altered channel gating led to the appearance of a channel with "hybrid" gating kinetics. These observations prompted the authors to suggest that two CFTR molecules are required to form a single conductance pore.

In the present paper, we report that chemical cross-linking experiments and studies using nondissociative gel electrophoresis show that CFTR exists as monomers and multimers in biological membranes. Further, purified, reconstituted CFTR also exists as monomers and multimers in proteoliposomes. To determine the minimal functional unit of CFTR, purified and reconstituted CFTR monomers and dimers were separated by gel filtration chromatography, and the fractions containing each CFTR structure were reconstituted separately for functional analyses. We found that both monomeric and dimeric CFTR could mediate chloride electrodiffusion and ATPase activity. Hence, our data support the notion that CFTR monomers are fully active. The functional significance of the existence of CFTR dimers in biological membranes remains to be determined.

† These studies were supported by an operating grant from the Canadian Cystic Fibrosis Foundation (CCFF) to C.E.B. I.K. is a CCFF Studentship awardee.

* Address correspondence to this author at the Hospital for Sick Children. Telephone: 416-813-5981. Fax: 416-813-5028. E-mail: bear@sickkids.on.ca.

‡ Hospital for Sick Children.

§ University of Toronto.

[1] Abbreviations: CF, cystic fibrosis; CFTR, cystic fibrosis transmembrane conductance regulator; NBDs, nucleotide binding domains; ABC, ATP binding cassette; PFO, pentadecafluorooctanoic acid; PE, phosphatidylethanolamine; PS, phosphatidylserine; PC, phosphatidylcholine; POPC, 1-palmitoyl-2-oleoylacyl-*sn*-glycero-3-phosphocholine; PKA, protein kinase A; PEI, poly(ethylenimine); sulfo-EGS, ethylene glycol bis(sulfosuccinimidyl succinate); DMS, dimethyl suberimidate hydrochloride; PBS, phosphate-buffered saline; AE1, band 3 protein.

10.1021/bi0108195 CCC: $20.00
Published on Web 08/08/2001

EXPERIMENTAL PROCEDURES

Materials. Phosphatidylethanolamine (PE), phosphatidylcholine (PC), phosphatidylserine (PS), and 1-palmitoyl-2-oleoylacyl-*sn*-glycero-3-phosphocholine (POPC) were obtained from Avanti Polar Lipids (Alabaster, AL). Pentadecafluorooctanoic acid (PFO) manufactured by Fluorochem (U.K.) was obtained from Oakwood Products Inc. (West Colombia, SC). Immobilized Ni−NTA agarose resin was obtained from Qiagen (Mississauga, ON).

Chemical Cross-Linking of CFTR in Intact Sf9 Cells. The Sf9 baculovirus expression system was used for large-scale production of wild-type or mutant CFTR proteins as described in our previous publications (*16*). Sf9 cells expressing CFTR were harvested from a 75 cm^2 flask, sedimented to form a pellet, and washed using PBS containing the protease inhibitor benzamidine. An aliquot containing $(2-3) \times 10^6$ cells was incubated with 10 mM dimethyl suberimidate hydrochloride (DMS) in PBS at pH 8.5 or 10 mM sulfo-EGS [ethylene glycol bis(sulfosuccinimidyl succinate)] in PBS at pH 8.0. Samples were nutated for 1 h at room temperature, and the cells were pelleted and resuspended with 100 mM Tris, pH 7.5, for 15 min at room temperature before being lysed in 2% SDS.

Purification of CFTR. Most of the procedures describing the purification of CFTR-His proteins have been published previously (*17*). Briefly, Sf9 cells harvested from 1 L of suspension culture were lysed in a French press (Spectronic Inst., Rochester, NY), the nuclei and other particles were pelleted, and the supernatant was centrifuged at 100000*g* for 90 min to sediment a crude membrane pellet. Peripheral proteins were extracted from this membrane pellet using 25 volumes of ice-cold 10 mM sodium hydroxide and 0.5 mM EDTA. The "stripped" membranes were sedimented by centrifugation at 100000*g* for 2 h. CFTR was solubilized from this membrane preparation by spinning overnight at room temperature in a solution containing 8% PFO and 25 mM phosphate at pH 8.0. Then, solubilized CFTR protein was purified by virtue of its 10× His tag using nickel affinity chromatography closely following the procedures previously described (*16*). A pH gradient (pH 8.0−6.0) was applied using an FPLC in order to elute CFTR from the column. Fractions possessing CFTR (identified by dot blot) were eluted at approximately pH 6.8 and concentrated at room temperature in Amicon YM100 concentrators (no. 4212, Millipore Corp., Bedford, MA) to a final volume of about 100 μL. Concentrated samples in 4% PFO (w/v), 25 mM phosphate, and 100 mM NaCl were diluted 1:10 in buffer containing 8 mM Hepes and 0.5 mM EGTA, pH 7.2, and further concentrated to a final volume of 100 μL to reduce the PFO concentration to 0.4%. Three microliters from each concentrated fraction was subjected to 6% SDS−PAGE gels (Novex, Carlsbad, CA) and analyzed for the quantity and purity of CFTR proteins by Western blot and silver-stained protein gel, as described previously (*18*, *19*). For immunoblotting, the protein was transferred to a nitrocellulose membrane and probed with an anti-CFTR polyclonal antibody generated against a fusion protein corresponding to the predicted NBD2 and C-terminus of CFTR, amino acids N1197−L1480. Immunopositive bands were visualized by enhanced chemiluminescence (Amersham, Oakville, ON).

CFTR Reconstitution into Liposomes. Procedures describing liposome preparation are reported elsewhere (*17*). Concentrated fractions containing purified CFTR-His in 0.4% PFO (approximately 100 μL) were mixed with an excess (1 mg) of a sonicated liposome preparation containing phosphatidylethanolamine (PE):phosphatidylserine (PS):phosphatidylcholine (PC):ergosterol (5:2:1:1 by weight; phospholipids from Avanti Polar Lipids Inc., Birmingham, AL). A lipid control was generated by diluting 1 mg of the liposome mixture containing PE:PS:PC:ergosterol into 100 μL of a buffer containing 8 mM Hepes and 0.5 mM EGTA, pH 7.2. The concentrated CFTR fractions and lipid control were dialyzed in a Spectra/Por dialysis membrane (Spectrum Laboratories Inc., Rancho Dominguez, CA; molecular mass cutoff 50 kDa) overnight at 4 °C against 4 L of a buffer containing 8 mM Hepes and 0.5 mM EGTA, pH 7.2.

Separation of CFTR Monomers and Dimers by Gel Filtration Chromatography. Proteoliposomes containing purified CFTR were collapsed by addition of detergent 4% PFO in a buffer solution also containing 25 mM phosphate, 0.5 mM EDTA, and 1 mM DTT at pH 7.5. A 500 μL aliquot containing 10 μg of CFTR protein was applied to a Superose 6 column (120 × 1 cm), and fractions were eluted with 25 mM phosphate, 100 mM NaCl, 4% PFO, 0.5 mM EDTA, and 1 mM DTT at pH 7.5 at flow rate of 0.2 mL/min. Immediately, 100 μL aliquots of each fraction were supplemented with 0.5 mg of lipid [containing PE:PS:PC:ergosterol (5:2:1:1)], passed through an Extractigel column (Pierce, Rockford, IL), and eluted with a buffer containing 8 mM Hepes at pH 7.2. Larger volume samples were first concentrated in a Microcon concentrator (Millipore Corp., Bedford, MA; 50 kDa cutoff) to about 50 μL, diluted 10 times with Hepes buffer, and concentrated again to 50 μL before application to the Extractigel column. The oligomeric status of the CFTR protein in each reconstituted fraction was assessed by PFO−PAGE, as previously described (*20*).

Assay of the Catalytic Activity of CFTR Protein. The catalytic activity was measured as the production of [α-^{32}P]-ADP from [α-^{32}P]ATP by purified, reconstituted, and PKA-phosphorylated CFTR, as described previously (*7*, *17*). Radiolabeled ADP and ATP were separated by poly(ethylenimine) (PEI) chromatography. Correction for spontaneous hydrolysis of ATP in reactions containing proteoliposomes was done by subtracting the [α-^{32}P]ADP/[α-^{32}P]ATP ratio of control liposomes. The ATPase assay was carried out in a reaction mixture containing 30 μL of freshly dialyzed proteoliposomes or liposomes, 1 mM nonradioactive ATP, 20 mM Tris, 40 mM NaCl, 4 mM $MgCl_2$, pH 7.5, and 2 μCi of [α-^{32}P]ATP (10 μCi/μL; Amersham, Oakville, ON).

ATPase reaction mixtures were incubated at 33 °C for 2 h and then stopped by the addition of 14 μL of 10% SDS and 88% formic acid (v/v). One microliter samples from the ATPase reaction were spotted onto PEI−cellulose plates (VWR, Mississauga, ON) and developed in 1 M formic acid and 0.5 M LiCl, as described previously (*20*). A STORM 840 Molecular Dynamics PhosphorImager was used to visualize ADP production by phosphorylated and nonphosphorylated CFTR samples. The quantity of ATP hydrolyzed was determined using the ImageQuant software package (Molecular Dynamics, Sunnyvale, CA).

Assays of CFTR Chloride Channel Activity. Concentrative Tracer Uptake Assay. We used a concentrative tracer uptake

assay developed by Garty et al. (*21*) and modified by Goldberg and Miller (*22*) to characterize the chloride conductance properties of reconstituted, PKA-phosphorylated CFTR. Proteoliposomes were preloaded with 150 mM KCl and centrifuged through Sephadex G-50 columns equilibrated with glutamate-containing salts, potassium glutamate (125 mM), sodium glutamate (25 mM), glutamic acid (10 mM), and Tris−glutamate (20 mM) at pH 7.6, to replace external chloride. Uptake was initiated and quantified by addition of 1.0 μCi mL^{-1} or 1.5 mM ^{36}Cl. Intraliposomal ^{36}Cl was assayed at various time points following separation of liposomes from the external media using a mini anion-exchange column (AG 1-X8 resin; Bio-Rad, Mississauga, ON).

Planar Bilayer Studies of Purified CFTR. As in our previous studies, proteoliposome fusion with planar lipid bilayers was facilitated and detected by the introduction of nystatin (120 μg mL^{-1}), a technique originally described by Woodbury and Miller (*23*). Planar lipid bilayers were formed by painting a 10 mg mL^{-1} solution of phospholipid (PE:PS:POPC in the ratio 4:4:2) in *n*-decane over a 200 μm aperture in a bilayer chamber. Typically, the cis compartment of the bilayer chamber, defined as that compartment to which liposomes were added, contains 300 mM KCl, and the trans compartment, connected to ground, contains 50 mM KCl. Single channel currents were detected after the addition of the purified catalytic subunit of PKA (220 nM; Promega Corp., Madison, WI) and 1 mM MgATP with a bilayer amplifier (custom made by M. Shen, Physics Laboratory, University of Alabama). Data were recorded and analyzed using pCLAMP 6.0.2 software (Axon Instruments Inc., Foster City, CA). Prior to analysis of dwell times, single channel data were digitally filtered at 100 Hz. Transitions to 50% of the current level (or greater) for a single open pore were considered as a channel opening.

Statistics. Statistical analyses of electrogenic flux and ATPase measurements were performed using the unpaired Student's *t* test. Differences between two groups were considered significant with p values <0.05.

RESULTS

CFTR Exists as a Multimeric Complex in Biological Membranes. The oligomeric structure of CFTR stably expressed in CHO cells and transiently transfected in Sf9 cells was assessed by nondissociative gel electrophoresis and using chemical cross-linkers. PFO−PAGE is a novel gel electrophoresis method which permits the assessment of the quaternary structure of cytosolic and membrane proteins (*20*). Analysis of CHO membranes expressing CFTR by PFO−PAGE revealed both a major and minor band (Figure 1a, i). The minor band migrated as a 170 kDa protein, consistent with the molecular mass reported for complex glycosylated CFTR protein. The major band migrated as a larger protein, possibly a homodimer or heterodimer containing CFTR (indicated by an asterisk in Figure 1a, i). Similarly, PFO−PAGE analysis of Sf9 membranes revealed major and minor bands consistent with the expected mass of CFTR homodimers and monomers, respectively. To determine the contribution of heterogeneous peripheral proteins to the higher molecular mass complex, we assessed the effect of pretreating CHO membranes bearing CFTR with urea (4 M),

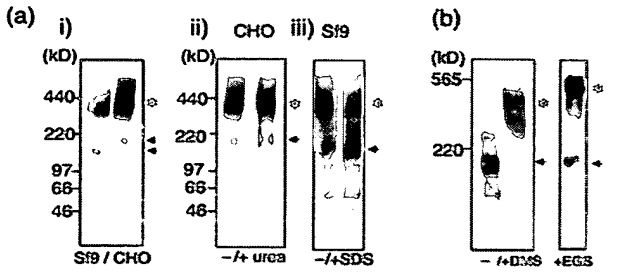

FIGURE 1: CFTR exists as oligomers in vivo. (a, i) Membranes were prepared from Sf9 and CHO cells expressing CFTR, solubilized in 4% PFO, and subjected to PFO−PAGE and Western analysis (polyclonal antibody was used; see Experimental Procedures). The predominant band (*) corresponds to a CFTR multimer. Monomeric CFTR (indicated by arrow) migrates as 170 kDa protein for CHO membrane preparation and as a 140 kDa protein for Sf9 membranes. (a, ii) Treatment of CHO membranes with urea (4 M) does not alter migration of CFTR on PFO−PAGE. (a, iii) Treatment of Sf9 membranes with 2% SDS increases the relative abundance of CFTR in monomeric form (arrow). (b) Intact Sf9 cells untreated (−) or treated (+) with cross-linkers DMS (10 mM) or EGS (10 mM). Membrane preparations were subsequently analyzed by SDS−PAGE.

a treatment which dissociates peripheral proteins (*24*). As this treatment did not affect the migration of the CFTR-containing complex, we suggest that the complex may not represent association of CFTR with accessory cytosolic proteins (Figure 1a, ii). Furthermore, as the higher molecular weight complex could be dissociated by treatment of PFO-solubilized membranes with SDS (2%), we suggest that this higher molecular weight band is unlikely to represent a PFO−detergent-induced protein aggregate (Figure 1a, iii).

Chemical Cross-Linkers. DMS, with a spacer arm of 11 Å, and sulfo-EGS, a cross-linker with a spacer arm of 14 Å, were applied to the exofacial surface of intact Sf9 cells to assess the quaternary structure of CFTR. Following cell lysis, analysis by SDS−PAGE, and Western blotting, we found that immunoreactive CFTR isolated from cells treated with either DMS or sulfo-EGS migrated primarily as a major band with a mass greater than that predicted for a monomer (Figure 1b). DMS can permeate cell membranes; hence, it could be capturing interactions of CFTR with itself, with other transmembrane proteins, or with intracellular, peripheral membrane proteins (*25*). The mass of the complex cross-linked by DMS appeared closer to that expected for a dimer than that detected in sulfo-EGS-treated cells. The larger apparent mass of the sulfo-EGS cross-linked complex suggests that the cross-linker with the longer spacer arm may be capturing a larger complex of proteins. Sulfo-EGS cannot permeate the membrane; therefore, this cross-linker must be capturing interactions of CFTR with itself or other membrane spanning proteins.

Purified CFTR Is Reconstituted as Monomers and Multimers. To determine directly whether CFTR self-associates to form an oligomeric complex, we assessed the quaternary structure of purified CFTR protein. CFTR expressed in Sf9 membranes was solubilized in pentafluorooctanoic acid (8% PFO) and purified by metal affinity by virtue of its polyhistidine tag (Figure 2a), as previously described (*17*). Analysis by PFO−PAGE revealed that purified, detergent-solubilized CFTR existed primarily as a monomer (Figure 2b, left panel). However, following reconstitution into phospholipid liposomes, a broader band corresponding to

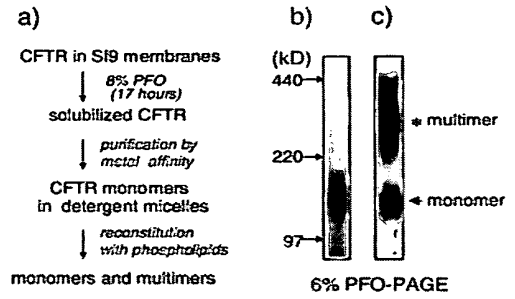

FIGURE 2: Purified, reconstituted CFTR exists as oligomers after reconstitution. (a) Flow chart shows that CFTR monomers are purified in the presence of 8% PFO but reconstitution of purified CFTR in phospholipid liposomes promotes formation of multimers. (b) CFTR purified in PFO exists primarily as a monomer as assessed by PFO–PAGE. (c) Purified CFTR reconstituted in phospholipids exists in oligomeric (probably dimeric) and monomeric forms as assessed by PFO–PAGE.

multimeric CFTR could be detected in addition to CFTR monomers by PFO–PAGE (Figure 2c). These findings suggest that this higher order structure can be generated during transition from a partially folded to a fully folded protein.

CFTR Monomers and Dimers Exhibit Chloride Channel Function and ATPase Activity. We showed in our previous studies that purified CFTR protein mediates PKA phosphorylation-stimulated ATPase activity and phosphorylation-regulated chloride channel activity (*7*, *16*, *26*, *27*). To determine whether CFTR monomers or dimers conferred these activities, we separated each structure in the mixture by gel filtration chromatography. Separation by gel filtration first required that the proteoliposomes be disrupted while preserving the quaternary structure of CFTR. This was achieved by adding PFO (4%) to CFTR-containing proteoliposomes prior to separation. Then, 10 μg of purified CFTR protein in a 100 μL volume containing mixed detergent–phospholipid micelles was added to a long narrow Superose 6 column, previously calibrated with the intrinsic membrane protein AE1 (monomers and dimers) and the ryanodine receptor (RyR2) monomer in the same detergent. This particular column was essential to provide the resolution necessary to effectively separate CFTR monomers and dimers. The fractions containing CFTR protein were assessed by dot blot, and pixel intensity was analyzed using NIH Image software to provide an estimate of the relative quantities of CFTR in each fraction. Two prominent and distinctive peaks (A and B) were evident from the elution profile (Figure 3). The protein in peak A elutes between those fractions containing dimeric AE1 protein (200 kDa) and the ryanodine receptor (565 kDa). Hence the mass of the protein eluted in peak A is close to that predicted for a CFTR dimer (CFTR 2′mer, approximately 330 kDa). The protein in peak B is well separated from peak A and elutes in fractions between those containing dimeric (200 kDa) and monomeric (100 kDa) AE1 protein; hence, its mass is consistent with that predicted for monomeric CFTR (CFTR 1′mer, 160–165 kDa). The results of this gel filtration experiment are consistent with the interpretation that purified CFTR protein in lipid–detergent micelles exists as a heterogeneous mixture of monomers and dimers.

To reconstitute each structure separately and with the highest level of fidelity, we rapidly extracted detergent from

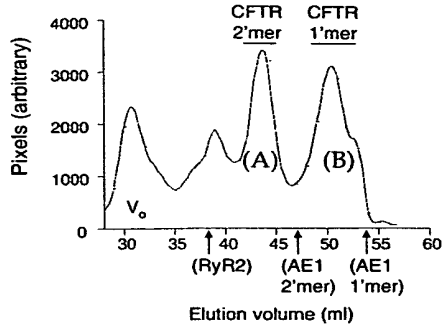

FIGURE 3: Monomers and dimers of CFTR are separated by gel filtration on a Superose 6 column. Proteoliposomes containing purified, reconstituted CFTR were collapsed using detergent (4% PFO) containing buffer as described in Experimental Procedures and applied to a Superose 6 column (120 × 1 cm) calibrated using AE1 monomers and dimers and the ryanodine receptor (RyR2). This elution profile was generated by dot blotting and pixel analysis by NIH Image software. Arrows correspond to volumes in which AE1 monomers (AE1 1′mer, 100 kDa), AE1 dimers (2′mer, 200 kDa), and RyR2 (1′mer, 565 kDa) elute. V_0 indicates where the void volume is eluted. Peaks correspond to the molecular mass predicted for CFTR monomers (CFTR 1′mer, B) and CFTR dimers (CFTR 2′mer, A).

multiple CFTR-containing fractions simultaneously by hydrophobic interaction chromatography (*28*) in the presence of excess phospholipid (the same composition as in the previous reconstitution). Detergent extraction and reconstitution into phospholipid were completed within 5–10 min. Excess phospholipid was added during reconstitution to ensure an extremely low protein to lipid ratio. For monomeric CFTR, 150 ng of CFTR was reconstituted in 0.5 mg of lipid, and for dimeric CFTR, 163 ng of protein was reconstituted in 0.5 mg of lipid. The reconstituted protein was analyzed immediately by nondissociative PFO–PAGE, and as shown in Figure 4a, CFTR monomers were effectively separated from dimers by gel filtration and these structures were maintained during reconstitution. Reconstituted monomers and dimers remain remarkably stable as evident in Figure 4b. Even after storage of liposomes for approximately 2–3 months at −80 °C and following thawing, PFO–PAGE analysis revealed that monomeric CFTR had not dimerized.

The relative PKA- and MgATP-dependent chloride channel function of CFTR monomers and dimers was determined immediately after reconstitution into phospholipid liposomes by measuring cumulative ^{36}Cl flux, an assay developed by Garty et al. for the study of populations of ion channel proteins (*21*). We compared the chloride flux mediated by empty liposomes (with no reconstituted CFTR) and liposomes bearing CFTR protein from fraction 50 (monomeric CFTR, as shown in Figure 4a) with flux mediated by liposomes bearing CFTR protein from fraction 44 (dimeric CFTR, Figure 4a). In all cases, liposomes were pretreated with PKA plus MgATP in order to activate channel function. Empty liposomes mediated less ^{36}Cl uptake than liposomes bearing monomeric CFTR protein ($p = 0.013$). The extent of cumulative flux mediated by protein reconstituted from fraction 50 [monomeric CFTR, 66.1 ± 23.7 (SD) nmol (μg of protein)$^{-1}$ h^{-1}] was not statistically different from that mediated by protein in fraction 44 [dimeric CFTR, 42.4 ± 17.5 (SD) nmol (μg of protein)$^{-1}$ h^{-1}, $p = 0.25$, Figure 4c].

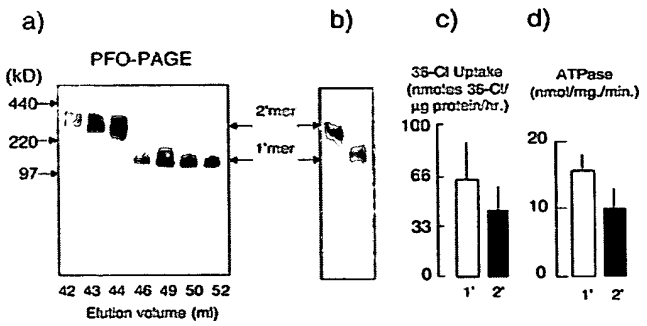

FIGURE 4: CFTR monomers and dimers can mediate chloride electrodiffusion and ATPase activity. (a) CFTR protein in each fraction eluted from the gel filtration column was reconstituted into phospholipid liposomes as described in Experimental Procedures and analyzed by PFO−PAGE and immunoblotting using a CFTR polyclonal antibody. This immunoblot shows that CFTR monomers have been effectively separated from CFTR dimers. (b) Reconstituted monomeric CFTR protein and dimeric CFTR were analyzed by PFO−PAGE 2−3 months after storage at −80 °C and thawing. (c) There is no significant difference between electrogenic ^{36}Cl uptake mediated by proteoliposomes bearing monomeric or dimeric CFTR protein; $p = 0.25$. Bars indicate mean ± SD for triplicate measurements. (d) ATPase activity by purified, phosphorylated CFTR protein reconstituted from fraction 49 (monomeric, empty bar; mean of triplicate measurements ± SD) and by phosphorylated CFTR protein from fraction 44 (dimeric, dark bar; mean of triplicate measurements ± SD) are not significantly different; $p = 0.22$.

Hence, both monomeric and dimeric CFTR structures are capable of mediating chloride flux.

The relative ATPase activity of monomeric and dimeric CFTR was also determined after reconstitution and PKA phosphorylation (Figure 4d). Empty liposomes (Ct) exhibit low levels of activity relative to proteoliposomes bearing monomeric CFTR protein ($p = 0.02$). On the other hand, proteoliposomes containing monomeric CFTR [15.3 ± 1.8 (SD) nmol mg^{-1} min^{-1}] and proteoliposomes bearing dimeric CFTR [10.8 ± 3.0 (SD) nmol mg^{-1} min^{-1}] exhibit comparable ATPase activities (Figure 4d, $p = 0.22$). Two other preparations of purified and reconstituted CFTR were fractionated and similar relative activities measured for fractions containing monomeric and dimeric CFTR.

To study the detailed properties of channel gating by CFTR monomers and dimers, proteoliposomes derived from fraction 50 or 44, respectively, were fused with planar lipid bilayers for single channel analyses. As in our previous studies (*7*, *16*, *26*, *27*), all proteoliposomes were rendered equally fusogenic by the addition of nystatin and ergosterol. We found that fusion of proteoliposomes containing monomeric CFTR (Figure 5a, top panel) conferred single channel activity that was similar to that previously described for CFTR channel function in biological membranes (*29*). As reported for CFTR function in membranes, channel activity by monomeric CFTR required phosphorylation by PKA (200 nM) as well as the presence of MgATP (1 mM). Furthermore, channel activity by monomeric CFTR exhibited selectivity for anions over cations (10:1; data not shown) and a low unitary conductance of approximately 11−12 pS (in the presence of asymmetrical solutions, as described in the legend for Figure 5). These findings suggest that a CFTR monomer is capable of forming a regulated chloride channel with properties similar to those described for the native channel.

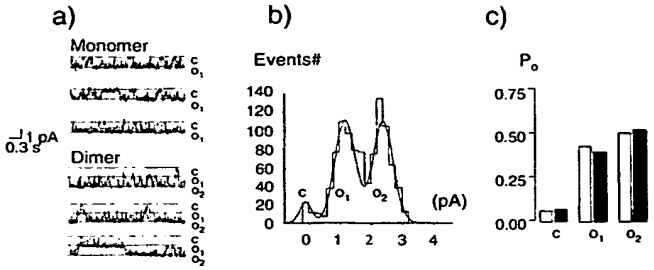

FIGURE 5: CFTR monomers can mediate low-conductance single channel activity. (a) Upper panel: Fusion of proteoliposomes containing monomeric CFTR in the presence of PKA (200 nM) and MgATP (1 mM) with planar lipid bilayers leads to the appearance of channel activity with a unitary conductance of 11−12 pS when bilayer compartments contain asymmetric solutions (300 vs 50 mM KCl; cis vs trans compartments, respectively). Eight bilayer experiments were performed (i.e., fresh liposomes added to a naïve bilayer). Lower panel: Fusion of proteoliposomes bearing dimeric CFTR leads commonly to the appearance of multiple conductance steps, each with a unitary conductance of 11−12 pS channels. (b) Amplitude histogram shows three major conductance levels in channel records of dimeric CFTR channel function, corresponding to the closed conductance level and openings of one or two channels. The area under each peak provides a measure of the relative probability of each conductance level during recordings totaling 3 min in duration. (c) The bar graph in the lower panel compares the relative probability of each conductance level (c = both conductance pores closed, o_1 = one conductance pore open, o_2 = two conductance pores open) determined from the above amplitude histogram (empty bar; pCLAMP 6.01, Axon Instruments Inc., Foster City, CA) with that predicted if openings of each channel occur independently, i.e., assuming a binomial distribution (dark bar). The following set of equations was used to determine the predicted probabilities of the three current levels (*30*): $P_0 = f_{o1}/2 + f_{o2}$; $f_0 = (1 - P_0)^2$; $f_1 = 2P_0(1 - P_0)$; $f_2 = P_0^2$.

Fusion of proteoliposomes bearing CFTR dimers typically led to the appearance of multiple anion-selective channels similar to those described for monomeric CFTR, with PKA- and MgATP-dependent gating and a unitary conductance of 11−12 pS (Figure 5a, bottom panel). Amplitude histograms of recordings totaling 3 min were fitted by the sum of three Gaussian distributions with equidistant peaks (c, o1, and o2). The relative areas covered by the three Gaussian components yield the probabilities of the closed and of the two open levels, respectively (Figure 5b). The values of the probabilities (empty bars) are similar to the predictions from a simple binomial superposition of two independently gating channels (dark bars, Figure 5c). These data suggest that there is no cooperativity between multiple pores observed following CFTR dimer reconstitution.

DISCUSSION

Our studies provide direct evidence supporting the hypothesis that the minimal functional unit of CFTR required for regulated channel function and ATPase activity is a monomer. Our findings also suggest that CFTR can exist as a complex, both in biological membranes and in our reconstitution system for purified protein. However, the biological significance for self-assembly of CFTR in membranes remains unclear, as, at least in our reconstitution system of purified protein, coassembly does not appear to regulate intrinsic function.

Our evidence supporting the function of monomeric CFTR rests in large part on our ability to separate purified

monomeric CFTR from purified dimeric CFTR and to study the function of each structure individually after reconstitution into phospholipid liposomes. The fractionation of monomeric CFTR from dimeric CFTR appeared successful on the basis of PFO−PAGE analyses and immunoblotting (Figure 3). However, the possibility exists that each fractionated form could be contaminated by an infinitesimal quantity (i.e., undetectable by immunoblotting) of CFTR protein in a different quaternary structure. It is difficult to rule out the contribution of such contamination in planar lipid bilayer studies of single molecules. However, our macroscopic studies of populations of proteoliposomes containing either monomeric or dimeric CFTR report the cumulative function of all protein in each fraction. As evident in Figure 4, there was no difference in the relative channel and catalytic activity by populations of reconstituted monomers or dimers, providing direct evidence that CFTR monomers are functional and, further, that there is unlikely to be any intrinsic cooperativity between CFTR molecules in a homodimeric complex.

Our findings seemingly contradict a recent report by Zerhusen et al. suggesting that a single conductance pore of CFTR requires assembly of two molecules as a dimeric complex. Their interpretation was based on electrophysiological recordings from concatemers of two CFTR molecules tethered in a head to tail orientation (*14*). In these studies, a single channel pore was observed with hybrid gating when one wild-type (Wt) CFTR molecule was tethered to a mutant CFTR protein known to have altered gating properties (i.e., CFTRΔR). However, as suggested by the authors themselves, although these observations could support a model wherein two CFTR molecules comprise a single pore, alternatively, the appearance of a single pore may reflect an inhibitory effect of the artificial tether on one of the CFTR molecules.

While our data suggest that monomeric CFTR is the minimal channel- and ATPase-forming unit of this protein, we also report evidence that supports the possibility that CFTR can exist in complexes, possibly dimeric complexes, in biological membranes. Specifically, we found that CFTR complexes could be preserved in PFO-solubilized CHO and Sf9 cell membranes and when analyzed by the relatively nondissociative PFO−PAGE method (*20*). Although it is possible that the PFO detergent we employed in these studies may have artificially induced the formation of aggregates, we think that this latter possibility is unlikely as treatment of PFO-solubilized membranes with SDS could effectively dissociate the complex to form monomeric CFTR. In addition, we have shown previously that PFO−PAGE accurately reports the tetrameric structure of inwardly rectifying potassium channels and aquaporin as well as the dimeric structure of AE1 transporters (*17*). Furthermore, two different cross-linking agents applied to the exofacial surface of Sf9 cells could capture CFTR-containing complexes with the approximate mass of a CFTR dimer and higher. Together, our data obtained using membranes and whole cells argue that CFTR associates with itself and possibly other proteins. Our findings, however, contrast with previous studies by Marshall et al. showing that the tagged versions of CFTR could not co-immunoprecipitate with other CFTR molecules with distinctive tags (*15*). These authors suggested that CFTR molecules could not coassemble, at least not through strong, detergent-resistant interactions. Conceivably, the PFO detergent used in the present studies may have the capacity to protect associations between membrane proteins. Further, our findings support the electron microscopic studies of the CFTR quaternary structure in *Xenopus* oocyte membranes which previously revealed a dimeric structure of CFTR in this expression system (*30*).

We also show that purified CFTR protein can assemble as dimers during reconstitution into phospholipid liposomes and that the protein in this structure is functional in assays of ATPase activity and electrogenic chloride flux. Planar lipid bilayer studies revealed that the two channels conferred by fusion of proteoliposomes bearing dimeric CFTR gated independently. Unlike the double barrel channel signature of the ClC family of chloride channels, there is no evidence of a common gate acting to regulate a pair of CFTR conductance pores (*31*, *32*). Hence, in our reconstitution system there is no indication that the formation of a dimeric complex significantly alters the function of individual CFTR pores. On the other hand, in vivo studies point to the possible significance of this dimeric structure in biological membranes. For example, Wang et al. recently published the description of an accessory protein (CAP70), which contains multiple PDZ binding domains, that may tether the carboxy termini of two CFTR molecules (*13*). In fact, these authors suggest that any bifunctional molecule may be capable of tethering two CFTR molecules by their carboxy termini to cause, like CAP70, an increase channel open probability. Hence, dimer formation may lead to changes in function in native membranes because interactions with accessory proteins are enhanced. In our future studies we plan to assess this hypothesis by determining directly whether certain accessory proteins may bind preferentially with purified dimeric rather than monomeric CFTR.

ACKNOWLEDGMENT

The authors express their gratitude to Dr. G. Lukacs (HSC, Toronto) for providing CHO cells stably transfected with CFTR and to Dr. D. H. MacLennan (University of Toronto) for providing HEK-293 cells transfected with ryanodine receptor (RyR2) with a specific antibody directed against this protein.

REFERENCES

1. McDonough, S., Davidson, N., Lester, H. A., and McCarty, N. A. (1994) *Neuron. 13*, 623−634.
2. Tabcharani, J. A., Linsdell, P., and Hanrahan, J. W. (1997) *J. Gen. Physiol. 110*, 341−354.
3. Sheppard, D. N., Rich, D. P., Ostedgaard, L. S., Gregory, R. J., Smith, A. E., and Welsh, M. J. (1993) *Nature 362*, 160−164.
4. Anderson, M. P., Berger, H. A., Rich, D. P., Gregory, R. J., Smith, A. E., and Welsh, M. J. (1991) *Cell 67*, 775−784.
5. Ko, Y. H., and Pedersen, P. L. (1995) *J. Biol. Chem. 270*, 22093−22096.
6. Carson, M. R., Travis, S. M., and Welsh, M. J. (1995) *J. Biol. Chem. 270*, 1711−1717.
7. Li, C., Ramjeesingh, M., Wang, W., Garami, E., Hewryk, M., Lee, D., Rommens, J. M., Galley, K., and Bear, C. B. (1996) *J. Biol. Chem. 271*, 28463−28468.
8. Szabo, K., Szakacs, G., Hegeds, T., and Sarkadi, B. (1999) *J. Biol. Chem. 274*, 12209−12212.
9. Picciotto, M. R., Cohn, J. A., Bertuzzi, G., Greengard, P., and Nairn, A. C. (1992) *J. Biol. Chem. 267*, 12742−12752.

10. Chang, X. B., Tabcharani, J. A., Hou, Y. X., Jensen, T. J., Kartner, N., Alon, N., and Hanrahan, J. W. (1993) *J. Biol. Chem. 268*, 11304−11311.
11. Dulhanty, A. M., and Riordan, J. R. (1994) *Biochemistry 33*, 4072−4079.
12. Naren, A. Q. M., Collawn, J., and Nelson, D. (1998) *Proc. Natl. Acad. Sci. U.S.A. 95*, 10972−10977.
13. Wang, S., Yue, H., Derin, R. B., Guggino, W. B., and Li, M. (2000) *Cell 103*, 169−179.
14. Zerhusen, B., Zhao, J., Xie, J., Davis, P. B., and Ma, J. (1999) *J. Biol. Chem. 274*, 7627−7630.
15. Marshall, J., Fang, S., Ostedgaard, L. S., O'Riordan, C. R., Ferrara, D., Amara, J. F., Hoppe, H. T., Scheule, R. K., Welsh, M. J., Smith, A. E., et al. (1994) *J. Biol. Chem. 269*, 2987−2995.
16. Ramjeesingh, M., Li, C., Garami, E., Huan, L.-J., Hewryk, M., Wang, Y., Galley, K., and Bear, C. (1997) *Biochem. J. 327*, 17−21.
17. Ramjeesingh, M., Garami, E., Galley, K., Li, C., Wang, Y., and Bear, C. E. (1999) *Methods Enzymol. 294*, 227−246.
18. Laemmli, U. K. (1970) *Nature 227*, 680−685.
19. Kartner, N., Hanrahan, J., Jensen, T., Naismith, L., Sun, S., Ackerley, C., Reyes, E., Tsui, L.-C., Rommens, J. M., Bear, C. E., and Riordan, J. R. (1991) *Cell 64*, 681−691.
20. Ramjeesingh, M., Huan, L.-J., Garami, E., and Bear, C. E. (1999) *Biochem. J. 342*, 119−123.
21. Garty, H., Rudy, B., and Karlish, S. J. (1983) *J. Biol. Chem. 258*, 13094−13099.
22. Goldberg, A. F., and Miller, C. (1991) *J. Membr. Biol. 124*, 199−206.
23. Woodbury, D. J., and Miller, C. (1990) *Biophys. J. 58*, 833−839.
24. Soriano, S., Thomas, S., High, S., Griffiths, G., D'santos, C., Cullen, P., and Banting, G. (1997) *Biochem. J. 324* (Part 2), 579−589.
25. Burt, H. M., and Jackson, J. K. (1990) *J. Rheumatol. 17*, 1359−1363.
26. Bear, C. E., Li, C., Kartner, N., Bridges, R., Jensen, T., Ramjeesingh, M., and Riordan, J. (1992) *Cell 68*, 809−818.
27. Bear, C. E., Li, C., Galley, K., Wang, Y., Garami, E., and Ramjeesingh, M. (1997) *J. Bioenerg. Biomembr. 29*, 465−473.
28. Noel, H., Goswami, T., and Pande, S. V. (1985) *Biochemistry 24*, 4504−4509.
29. Tabcharani, J. A., Chang, X. B., Riordan, J. R., and Hanrahan, J. W. (1991) *Nature 352*, 628−631.
30. Eskandari, S., Wright, E. M., Kreman, M., Starace, D. M., and Zampighi, G. A. (1998) *Proc. Natl. Acad. Sci. U.S.A. 95*, 11235−11240.
31. Ludewig, U., Pusch, M., and Jentsch, T. J. (1996) *Nature 383*, 340−343.
32. Middleton, R. E., Pheasant, D. J., and Miller, C. (1996) *Nature 383*, 337−340.

BI0108195

Am J Physiol Cell Physiol 282: C1170-C1180, 2002. First published January 2, 2002; doi:10.1152/ajpcell.00337.2001
0363-6143/02 $5.00
Vol. 282, Issue 5, C1170-C1180, May 2002

Domain-domain associations in cystic fibrosis transmembrane conductance regulator

Wenlan Wang[1], Zhaoping He[1], Thomas J. O'Shaughnessy[1], John Rux[2], and William W. Reenstra[3]

[1] Alfred I. duPont Hospital for Children, Wilmington, Delaware 19803; [2] Wistar Institute and [3] Institute for Human Gene Therapy, University of Pennsylvania, Philadelphia, Pennsylvania 19104

▶ ABSTRACT

Cystic fibrosis is caused by mutations in the cystic fibrosis transmembrane conductance regulator (CFTR) gene. CFTR is a chloride channel whose activity requires protein kinase A-dependent phosphorylation of an intracellular regulatory domain (R-domain) and ATP hydrolysis at the nucleotide-binding domains (NBDs). To identify potential sites of domain-domain interaction within CFTR, we expressed, purified, and refolded histidine (His)- and glutathione-*S*-transferase (GST)-tagged cytoplasmic domains of CFTR. ATP-binding to his-NBD1 and his-NBD2 was demonstrated by measuring tryptophan fluorescence quenching. Tryptic digestion of in vitro phosphorylated his-NBD1-R and in situ phosphorylated CFTR generated the same phosphopeptides. An interaction between NBD1-R

and NBD2 was assayed by tryptophan fluorescence quenching. Binding among all pairwise combinations of R-domain, NBD1, and NBD2 was demonstrated with an overlay assay. To identify specific sites of interaction between domains of CFTR, an overlay assay was used to probe an overlapping peptide library spanning all intracellular regions of CFTR with his-NBD1, his-NBD2, and GST-R-domain. By mapping peptides from NBD1 and NBD2 that bound to other intracellular domains onto crystal structures for HisP, MalK, and Rad50, probable sites of interaction between NBD1 and NBD2 were identified. Our data support a model where NBDs form dimers with the ATP-binding sites at the domain-domain interface.

tryptophan fluorescence; peptide array; molecular structure; peptide library; phosphorylation

INTRODUCTION

▲ TOP
▲ ABSTRACT
▪ INTRODUCTION
▼ MATERIALS AND METHODS
▼ RESULTS
▼ DISCUSSION
▼ REFERENCES

CYSTIC FIBROSIS (CF) is a genetic disease caused by mutations in the gene encoding the cystic fibrosis transmembrane conductance regulator (CFTR), an epithelial chloride channel (35, 37). CFTR is a member of the ATP-binding cassette (ABC) transporter gene superfamily (14). More than 1,000 ABC transporters are known, and they are found in both prokaryotic and eukaryotic cells where they carry out the unidirectional ATP-dependent transport of a wide variety of molecules. All known ABC transporters have two membrane-spanning domains (MSDs), usually composed of six transmembrane helices, and two nucleotide-binding domains (NBDs) (14). These domains can be expressed in a single subunit, as in CFTR and multidrug resistance protein (MDR), or in multiple subunits, as in the bacterial maltose and histidine transporters. ABC transporters like CFTR and MDR have intracellular NH_2- and COOH-terminals and four intracellular loops, L1 to L4, between transmembrane helices 2 and 3, 4 and 5, 8 and 9, and 10 and 11, respectively. CFTR is unique among ABC family members because it is the only family member to contain an additional intracellular domain, the regulatory or R-domain. CFTR is also the only ABC family member that is known to function as an ion channel (37). The R-domain contains multiple protein kinase A (PKA)-dependent phosphorylation sites that are involved in the regulation of CFTR channel activity (35). The regulation of CFTR channel activity involves a two-step process; phosphorylation of the R-domain, most likely on multiple sites, is required so that ATP hydrolysis by the NBDs can regulate CFTR gating (1, 11, 34, 36, 46). Mutations in the R-domain, most notably at phosphorylation sites, alter ATP-dependent CFTR gating (46). In addition, the CF-causing ΔF508 mutation, located in NBD1, has been shown to alter in situ phosphorylation (18). The fact that alterations in one domain can modulate the function of a second domain indicates that functionally important domain-domain interactions must occur (11). The primary goal of the study was to identify the sites of domain-domain interaction.

A number of studies have suggested that specific domain-domain associations are required for optimal CFTR activity. An in vitro association between NBD1-R and NBD2 constructs has been demonstrated by fluorescence quenching and exclusion chromatography (26). Interactions between the NH_2-and

COOH-terminals with other domains of CFTR have been postulated on the basis of CFTR channel activity (29, 32, 42). However, there is no information on the specific sites of interaction among CFTR domains. In addition, recent electrophysiological and cytochemical studies have suggested that native CFTR may exist as a homodimer (9, 32, 42, 47), but any dimeric form would appear to be relatively unstable because biochemical studies have failed to detect multimeric forms of CFTR (6, 28). Despite the fact that CFTR has been shown by both immunological and yeast two-hybrid studies to interact with a number of membrane-associated proteins (12, 13, 29, 39).

No crystal structures have been generated for any domain of CFTR; however, structures for bacterial NBDs have been reported. These include HisP from the histidine transporter of *Salmonella typhimurium* and MalK from the maltose transporter of *Thermococcus litoralis* (7, 17). In addition, a crystal structure for Rad50, a DNA-binding protein with a similar motif to HisP and MalK, has been reported (15). Comparison of the crystal structures for the NBD monomers suggests that the basic fold is conserved. Recently, two additional crystal structures for NBD monomers have been reported; they have the same structure as the NBDs of HisP and MalK (21, 44). However, crystallographic structures for HisP, MalK, and Rad50 dimers vary considerably. Because the relative orientation of the two NBDs should be conserved among all ABC family members (19), we suggest that no more than one, and possibly none, of the observed dimeric structures are related to the structure in native ABC transporters. Although additional crystal structures may resolve this issue, we have taken a biochemical approach. To this end, individual cytoplasmic domains of CFTR were expressed, purified, and refolded. Sites of domain-domain association were determined by in vitro binding to an overlapping peptide library generated from the intracellular regions of CFTR. Peptides within the NBDs that bound cytoplasmic domains were mapped onto the known NBD structures. Predicted sites of domain-domain interaction were compared with published structures for NBD dimers.

MATERIALS AND METHODS

▲ TOP
▲ ABSTRACT
▲ INTRODUCTION
▪ MATERIALS AND METHODS
▼ RESULTS
▼ DISCUSSION
▼ REFERENCES

Generation of expression constructs. Polymerase chain reaction (PCR) was employed to amplify cDNA fragments of CFTR from a pcDNA vector (Invitrogen) containing CFTR (obtained from Dr. W. Skach, Oregon Health Sciences University). DNA fragments of NBD1 (nucleotides 1249-1899; amino acids 373-589), NBD2 (nucleotides 3583-4560; amino acids 1151-1476), and NBD1-R (nucleotides 1249-2709; amino acids 373-859) were cloned into pProEx HT (Qiagen) with an NH_2-terminal his-x6 tag. Because of its poor expression as a His-tagged protein, R-domain (nucleotides 1891-2709; amino acids 589-830) was cloned into pGEX-5X (Amersham Pharmacia Biotech) with glutathione-*S*-transferase (GST) fused to its NH_2 terminus. The correct recombinants were identified by restriction mapping and sequencing.

Expression, purification, and refolding. CFTR recombinants were expressed in *Escherichia coli* BL21codon-plus (Stratagene). His-tagged CFTR domains were purified from inclusion bodies in 8 M urea by Ni-affinity chromatography according to the manufacturer's instruction (Qiagen). GST-R protein

was purified on glutathione-Sepharose 4B (10). Protein purity was analyzed by SDS-PAGE, and protein concentrations were determined with bicinchoninic acid (40). GST-R domain was renatured by dialyzing overnight against phosphate-buffered saline (PBS, pH 7.2). His-tagged proteins were renatured by diluting 10-fold into binding buffer (50 mM Tris, pH 7.5, 0.15 M NaCl, 1 mM EDTA, 0.5% NP-40, 0.5 mM dithiothreitol, and 0.1 mg/ml BSA) for peptide binding assays or PBS for fluorescence studies.

Fluorescence studies. Fluorescence measurements were performed at room temperature using a Perkin-Elmer LS50B spectrofluorometer. Samples were excited at 295 nm and emission spectra were recorded at 345 nm. Excitation and emission bandwidths were 5.0 nm, and spectra were corrected for background fluorescence. For measurements of ATP-dependent fluorescence quenching, ATP was added to domains in binding buffer and the percent change in fluorescence was calculated at each ATP concentration. For the assay of domain-domain association, separate samples of a single domain and two domains were generated for each experimental condition.

Phosphorylation and two-dimensional peptide mapping. In situ CFTR labeling was performed as previously described (33). Briefly, NIH-3T3 cells stably expressing human CFTR (NIH-CFTR) were incubated with $^{32}P_i$ for 2 h before stimulation with 10 μM forskolin for 2 min. Cells were lysed in 4°C lysis buffer (100 mM NaCl, 50 mM NaF, 0.1% SDS, 1% Na-deoxycholate, 1% Triton X-100, 1 mM EDTA, 1 mM EGTA, 0.1 mM phenylmethylsulfonyl fluoride, 0.1 mg/mL aprotinin, 1 mM orthovanadate, and 50 mM Tris · HCl, pH 7.5) and lysate-cleared by centrifugation. CFTR was immunoprecipitated with a COOH-terminal CFTR antibody (R&D) and protein A beads (Calbiochem) and was then purified by SDS-PAGE. For in vitro labeling, CFTR was immunoprecipitated from NIH-CFTR cells as described, with the exception that cells were not exposed to $^{32}P_i$ or forskolin. Immunoprecipitated CFTR was suspended in 50 μl of kinase buffer (50 mM Tris, 10 mM $MgCl_2$, and 100 μg/ml BSA, pH 7.5) and phosphorylated with 2 units of PKA catalytic subunit (Sigma) and 10 μCi [γ-^{32}P]ATP. CFTR was resolved by SDS-PAGE. For in vitro labeling of NBD1-R, purified protein (1-2 μg) was placed in kinase buffer plus 0.8 M urea and phosphorylated with 2 units of PKA and 10 μCi [γ-^{32}P]ATP. Phosphorylated NBD1-R was separated from the reaction mixture by SDS-PAGE. In all cases, phosphorylated products were visualized with a Storm 860 PhosphorImager.

Two-dimensional phosphopeptide mapping of phosphorylated CFTR and phosphorylated NBD1-R was performed as previously described (2, 45). Phosphorylated CFTR and NBD-R were extracted from the gel and TCA was precipitated. Protein was reacted with trypsin overnight and lyophilized before peptide separation by two-dimensional (2-D) peptide mapping electrophoresis at pH 8.9 and ascending chromatography in butanol-pyridine-acetic acid-water (15:10:3:12 vol:vol:vol:vol). Phosphopeptides were visualized with a Storm 860 PhosphorImager (Molecular Dynamics) and identified by comparison with published (5, 33) and unpublished (Dr. J. Cohn) phosphopeptide maps of CFTR.

Peptide binding assay. Peptide walking was used to identify sites of domain-domain interaction (20). One hundred fifty-seven overlapping 20-mer peptides, spanning all cytoplasmic regions of CFTR, were synthesized by the multipin synthesis method (41) and were purity-analyzed on HPLC (Chiron). Peptides overlapped by 13 residues. All peptides were acetylated at the NH_2 terminus and amidated at

the COOH terminus. Peptides were dissolved in 100% DMSO to a concentration of 2 mM and stored frozen at −70 °C. For binding assays, peptides in DMSO were diluted with distilled water (1:10), and then 10 μg of each peptide were blotted onto polyvinylide difluoride membrane (Bio-Rad). The membranes were air-dried, blocked with 5% milk in PBST (PBS-0.5% Tween), and then incubated with 10 μg/ml of a purified CFTR domain overnight in binding buffer. Bound proteins were detected with monoclonal antibodies against GST or His tags (Upstate Biotechnology) or with a polyclonal antibody against NBD2 (generated against the expressed domain by Covance Research Products). Signals were visualized by enhanced chemiluminescence (Amersham Pharmacia Biotech).

RESULTS

▲ TOP
▲ ABSTRACT
▲ INTRODUCTION
▲ MATERIALS AND METHODS
▪ RESULTS
▼ DISCUSSION
▼ REFERENCES

Expression and characterization of CFTR domains. His-tagged expression vectors for NBD1, NBD2, and the NBD1-R-domain of CFTR were constructed. In addition, we expressed a GST-tagged R-domain because of poor expression of His-tagged R-domain. These proteins, his-NBD1 (amino acids 373-589), his-NBD2 (amino acids 1151-1476), his-NBD1-R (amino acids 373-859), and GST-R (amino acids 589-830), were expressed in *E. coli* and purified by affinity chromatography. As shown in Fig. 1, the purified domains contained >95% of the intended product. His-NBD1, his-NBD2, and GST-R migrated at the expected molecular masses of 24, 36, and 52 kDa, respectively, whereas his-NBD1-R migrated at 60 kDa as opposed to the predicted molecular mass of 53 kDa. In all cases, the identity of the expressed domain was confirmed by Western blotting with the antibodies against individual domains (data not shown).

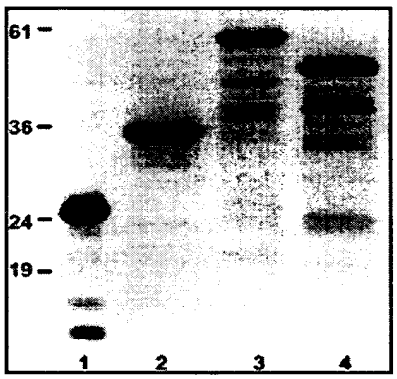

View larger version (97K):
[in this window]
[in a new window]

Fig. 1. Expression and purification of cystic fibrosis transmembrane conductance regulator (CFTR) domains. Purified His-tagged nucleotide-binding domains his-NBD1 (*lane 1*), his-NBD2 (*lane 2*), his-NBD1-R (*lane 3*), and glutathione-*S*-transferase-tagged R-domain GST-R (*lane 4*) were run on SDS-PAGE (10%), and proteins were stained with Coomassie blue. Molecular mass markers are indicated at *left*.

Purified domains were refolded as described in MATERIALS AND METHODS. To establish that the purified domains assumed a "native-like" structure, ATP binding to domains containing an NBD was assayed by measuring ATP-dependent changes in tryptophan fluorescence. All NBD-containing domains

bound ATP. ATP binding was concentration dependent (Fig. 2), and disassociation constants for his-NBD1 and his-NBD2 were calculated to be 660 ± 70 and 65 ± 9 μM, respectively. To assess the structural integrity of his-NBD1-R and GST-R, the refolded proteins were phosphorylated in vitro with PKA and [γ-^{32}P]ATP and digested with trypsin, and phosphopeptides were separated by 2-D peptide mapping. In addition, wild-type CFTR, stably expressed in transfected NIH-3T3 cells, was in situ phosphorylated during stimulation with forskolin and in vitro phosphorylated with PKA and [γ-^{32}P]ATP after immunoprecipitation. Phosphorylated proteins were digested with trypsin and phosphopeptides were separated by 2-D peptide mapping. As shown in Fig. 3, the same phosphopeptides were generated by in vitro phosphorylation of his-NBD1-R and in situ phosphorylation of CFTR (data for GST-R not shown). However, in vitro phosphorylation of CFTR resulted in a different pattern of phosphorylation (note the absence of phosphorylation on serines 737 and 813). Although the precise locations of peptides in the three maps differed, this was largely due to differences in the relative separation in the horizontal (electrophoretic) and vertical (chromatographic) directions. Significantly, all phosphopeptides from NBD1-R corresponded to a phosphopeptide in the map for in situ phosphorylated CFTR, whereas in vitro phosphorylated CFTR that had been dissolved in detergent and then resuspended in a detergent-free buffer before phosphorylation showed a distinct pattern of phosphorylation. This suggests that NBD1-R has a structure more similar to that of CFTR in situ than that of in vitro phosphorylated CFTR.

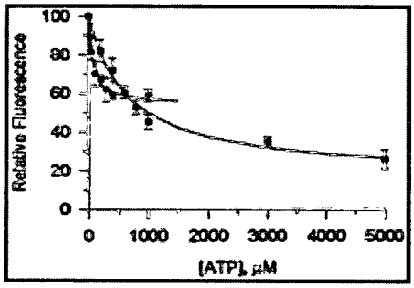

View larger version (15K):
[in this window]
[in a new window]

Fig. 2. ATP-dependent quenching of NBD fluorescence. The tryptophan fluorescence (excitation at 295 nm, emission at 345 nm) of 2.0 μM his-NBD1 (■) or his-NBD2 (●) in PBS plus 0.8 M urea was assayed as a function of ATP concentration. After subtraction of buffer fluorescence, relative fluorescence was calculated as (FNBD + ATP/FNDB) where FNBD + ATP and FNBD are the fluorescences of NBD in the presence and absence of ATP. Data are presented as means ± SE (n = 3). Lines indicate hyperbolic fits to the data.

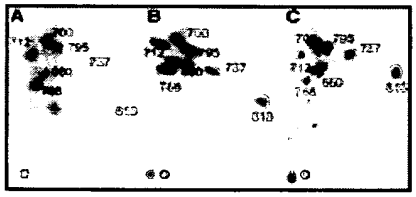

View larger version (40K):
[in this window]
[in a new window]

Fig. 3. Tryptic 2-dimensional phosphopeptide maps of CFTR and his-NBD1-R. In vitro phosphorylated CFTR (*A*), in vitro phosphorylated his-NBD1-R (*B*), and in situ phosphorylated CFTR (*C*) were isolated and digested with trypsin as described in MATERIALS AND METHODS. The resulting peptides were separated by electrophoresis in the horizontal direction and ascending chromatography in the vertical direction. Phosphopeptides were located with a Storm 860 PhosphorImager (Molecular Dynamics). Phosphopeptides were identified (site of phosphorylation) by comparison with published (5, 33) and unpublished (Dr. J. Cohn) phosphopeptide maps of CFTR.

To determine whether expressed domains formed domain-domain associations in vitro, changes in tryptophan fluorescence were monitored when expressed his-NBD1-R and his-NBD2 were mixed together. As shown in Fig. 4*A*, the fluorescence of his-NBD1-R was a linear function of concentration. Based on the assumption that his-NBD2 and his-NBD1-R do not interact, the fluorescence of his-NBD1-R/his-NBD2 mixtures was calculated. These values are indicated by square symbols in Fig. 4*A*. However, as shown by triangle symbols, the observed fluorescence was significantly less than the predicted value. In Fig. 4*A*, *inset*, the percentage decrease in observed fluorescence is plotted as a function of his-NBD1-R concentration. The data were fit to a hyperbolic function with an apparent dissociation constant for his-NBD1-R binding to 1.5 μM his-NBD2 of 0.7 ± 0.3 μM. A weaker association between his-NBD1 and his-NBD2 was also observed (data not shown). Under these experimental conditions, the fluorescence of all expressed domains was linear with respect to concentration, as was the increase in fluorescence from the addition of BSA (data not shown). To determine whether the fluorescence quenching altered ATP binding, we compared the ATP-dependent fluorescence quenching of his-NBD1-R, his NBD2, and a mixture of the two. As shown in Fig. 4*B*, ATP quenched the fluorescence of both of his-NBD1-R and his-NBD2. However, it caused a significant increase in the fluorescence of a mixture of his-NBD1-R and his-NBD2. Although calculation of the amounts of free and associated domains from the data in Fig. 4*A* is not warranted, it is clear that both free and associated domains must exist and, because ATP binding to the free domains decreases tryptophan fluorescence, the increase in fluorescence when ATP binds to the associated domains must be greater than that indicated by the change in total fluorescence. We have also used an overlay assay to demonstrate associations between the expressed domains. As shown in Fig. 5*A*, GST-R, but not GST, bound to his-NBD1 and his-NBD2. An association between his-NBD1 and his-NBD2 was also observed (Fig. 5*B*).

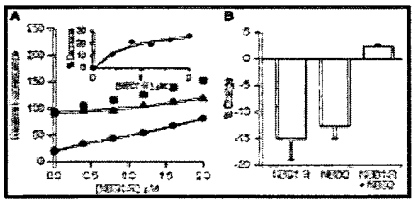

View larger version (16K):
[in this window]
[in a new window]

Fig. 4. Association of his-NBD2 and his-NBD1-R. *A*: the tryptophan fluorescence (excitation at 295 nm, emission at 345 nm) of his-NBD1-R alone (●) and his-NBD1-R in the presence of 1.5 μM his-NBD2 (▲) (F_{obs}) were determined. Also shown is the calculated fluorescence (F_{cal}) of a mixture of 1.5 μM his-NBD1-R and the indicated concentration of his-NBD2 (■) ($F_{NBD1\text{-}R} + F_{NBD2} - F_{BUFFER}$). Data are representative of 3 experiments. *Inset*, the %decrease in fluorescence [$(F_{cal} - F_{obs})/F_{cal}$] is plotted as a function of his-NBD1-R concentration. Line indicates a hyperbolic fit to the data. *B*: the ATP-dependent change in fluorescence for the addition of 5 mM ATP to 2 μM his-NBD1-R, 1.5 μM his-NBD2, and a mixture of 2 μM his-NBD1-R and 1.5 μM his-NBD2 is shown. Data are presented as means ± SE (n = 3).

Fig. 5. Overlay assay of domain-domain binding. *A*: his-NBD1 and his-NBD2 were spotted onto nitrocellulose, overlaid with GST or GST-R and probed with an antibody to

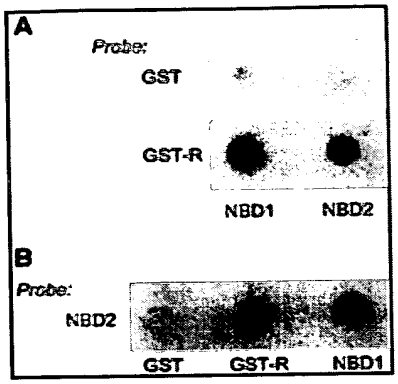

View larger version (56K):
[in this window]
[in a new window]

GST. *B*: GST, GST-R, and his-NBD1 are spotted, overlaid with his-NBD2, and probed with an antibody to NBD2. Controls where his-NBD2 was omitted were negative. For *A* and *B*, bound domains were visualized by chemiluminescence. Data are representative of 2 assays.

Binding of expressed domains to peptides from CFTR. To identify epitopes that are involved in domain-domain interactions, an overlapping peptide library of 20-mers spanning all intracellular amino acids of CFTR was synthesized. Peptides 1-10, 11-17, 18-25, 97-103, and 105-111 spanned the NH_2 terminus and intracellular loops L1-L4, respectively. Peptides 26-96 spanned NBD1 and the R-domain, whereas peptides 112-157 spanned NBD2 and the COOH-terminus. The identity of each peptide is indicated in Fig. 6*A*. As shown in Fig. 6*B*, each peptide was assayed for the ability to bind the expressed domains with an overlay assay. Peptides were spotted onto nitrocellulose membranes and incubated with a domain, and bound domain was probed with antibodies to the domain or the fused tag. To identify false positives, the binding of antibodies, or GST plus anti-GST, in the absence of expressed domains was determined. Our anti-His tag antibody bound to none of our peptides, whereas the anti-NBD2 antibody bound to epitopes on three overlapping peptides (135-137) from NBD2 (data not shown). As shown in Fig. 6*A*, GST was bound by peptides 11, 12, 48, 63, 96, and 106, and more protein was bound to peptide 13. In addition, all three expressed domains bound to peptides 13, 59, 60, 96, and 106, indicated in gray in Fig. 6*A*; these five interactions were considered false positives and not included in the following analysis. In addition, there are undoubtedly peptides that form associations with a domain in the native structure but do not bind the domain in our assay. These false negatives could occur if the association between peptide and domain were to weak, if the peptide were not retained on the membrane, or if spatial restrictions prevented peptide-domain interaction on the membrane. It is likely that some of the more hydrophilic peptides were lost from the membrane because the percentage of bound peptides and Kyte-Dolittle hydrophobicity (24) were correlated ($R^2 = 0.91$; data not shown). Therefore, it is unlikely that we have identified all sites of domain-domain interaction. Because some peptides were likely to be lost from the membrane, comparisons were made only on the basis of the amount of bound domain and not of the relative strength of association. Despite the uncertainty caused by the potential loss of peptides, the specificity of domain binding can be assessed for any peptide that shows differential binding to the tested domains. For example, data with his-NBD2 and GST-R indicate that peptides 135-137 and 144-148 are retained on the membrane. Because there is no evidence for the binding of his-NBD1 to these peptides, these peptides establish a background for nonspecific binding by NBD1.

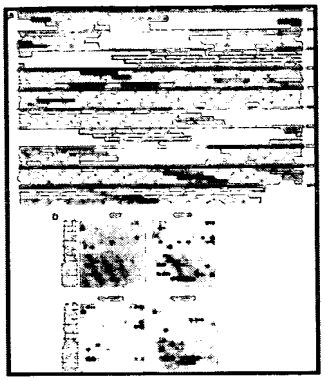

View larger version (47K): [in this window] [in a new window]

Fig. 6. Binding of GST, R-domain, NBD1, and NBD2 to peptides from the cytoplasmic domains of CFTR. *A*: the numbered bars indicate the sequence of each of the 157 overlapping peptides. The sequences contained in NBD1, NBD2, and the R-domain constructs are highlighted in red, blue, and yellow, respectively. Peptides in the 12 transmembrane helices are indicated in red. Peptides that bind to NBD1, NBD2, or the R-domain are colored red, blue, or yellow, respectively, with lighter colors indicating less bound domain. Peptides with 2 colors bound both of the indicated domains. Five peptides that bound all 3 domains are shown in gray. *B*: blots of bound GST, GST-R, his-NBD1, and his-NBD2 are shown. Peptides were blotted onto nitrocellulose membranes, incubated overnight with 1 μg/ml protein, and probed with a polyclonal antibody to the His tag, NBD2, or GST. Bound domains were visualized by chemiluminescence.

As shown in Figure 6*B*, GST-R bound to peptides 1, 2, and 3 in the NH_2 terminus; peptides 14, 16, 105, 109, and 110 in intracellular loops L1 and L4; peptides 46, 48, 49, 53, and 55 in NBD1; and peptides 115, 129, 130, 137, 138, 140, and 144-148 in NBD2 (indicated in yellow in Fig. 6*A*). His-NBD1 and his-NBD2 had distinct patterns of peptide binding, although they also bound to several peptides in common. His-NBD1 bound to peptides 1, 2, 3, and 10 from the NH_2 terminus; peptides 11, 12, and 25 from intracellular loops L1 and L2; peptides 130, 131, 132, 139, and 140 from NBD2; and peptide 48 from NBD1 (indicated in red in Fig. 6*A*). In contrast, his-NBD2 bound to peptide 20 from intracellular loop L2; peptides 44, 45, 46, and 63 in NBD1; and peptides 131, 132, and 145-148 in NBD2 (indicated in blue in Fig. 6*A*). Note that peptide 63, although present in our R-domain construct, has recently been shown to be in NBD1 (3). Associations were observed between his-NBD2 and peptides from all four intracellular loops. Two additional points should be made. Whereas R-domain bound to peptides from NBD1 and NBD2, peptides from the R-domain did not bind to any domain. Associations between NBD1 and peptides from NBD1, as well as NBD2 and peptides in NBD2, may reflect a similarity between the structures of NBD1 and NBD2 or self-associations between the NBDs that are present in a dimeric form of CFTR (9, 32, 42, 47). At present, we have no reason to favor either possibility.

Mapping of binding data to known NBD structures. To better understand the relationship of the binding studies to the structure of the NBD1 and NBD2, we have mapped the binding sites in NBD1 and NBD2 onto crystallographic structures of the HisP and MalK monomers, two bacterial NBDs (7, 17). These proteins are overlaid in Fig. 7*A*. They have sequence identities of only 26%, but comparison of the crystal structures by combinatorial extension (38) gives a root mean square deviation (RMSD) for the α-carbons of 2.7 Å with a Z-score (measure of spatial significance of the fit relative to the alignment of random structures) of 6.7 and a gap size of 18 amino acids. The structure of Rad50, a DNA-binding protein where a structure analogous to that of a HisP monomer is formed from two domains, was also examined (15). An overlay of HisP and Rad50 is shown in Fig. 7*B*. The sequence identity between Rad50 and HisP is 20.2%, but the RMSD for α-carbon atoms is 2.7 Å, with a Z-score of 5.3 and a gap

size of 29 amino acids. A sequence alignment of MalK, HisP, NBD1, NBD2, and Rad50 is shown in Fig. 8, which also shows the alignment of secondary structural elements for MalK, HisP, and Rad50. These results suggest that NBD1 and NBD2, with sequence identities to HisP of 18% and 17% and gap sizes of 32 and 17, respectively, may have similar three-dimensional structures to those of HisP, MalK, and Rad50. Figure 8 also indicates epitopes in NBD1 that bind NBD2 (blue), epitopes in NBD2 that bind NBD1 (red), and epitopes in either NBD that bind to the R-domain (green). Whereas the monomeric structures of these three proteins are very similar, the crystallographic dimers (Fig. 9) show no similarity. In addition to the crystallographic dimers for HisP, MalK, and Rad50, the comparison of NBD sequences from a large number of ABC transporters has led to the development of an alternative model for the HisP dimer, aHisP (19). In Fig. 9, *A*-D, the aqua monomer (NBD1) is always in the same orientation, and the arrow indicates the orientation of the helix in NBD2 that is projecting toward the viewer in Fig. 9*A*. Epitopes from one NBD of CFTR that bind to the other NBD are indicated with a darker color. Because they are found in the interfacial region of the crystal structures for MalK (9*C*), Rad50 (9*D*), and aHisP (9*B*), our data are more consistent with these models than with the HisP crystal structure (9*A*).

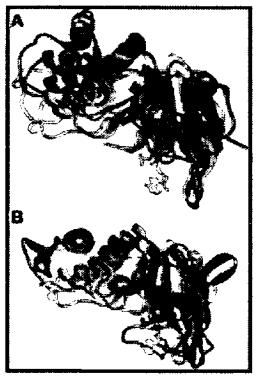

View larger version (52K):
[in this window]
[in a new window]

Fig. 7. Alignment of NBD crystal structures. *A*: the crystal structure of the HisP monomer (17) is aligned to that for MalK (7). *B*: the HisP structure is aligned with one NBD of the Rad50 dimer (15). In *A* and *B*, HisP is shown in aqua and bound ATP in green. MalK and Rad50 are indicated in purple, with 2 tints used to indicate the 2 subunits that comprise the Rad50 NBD. Bound pyrophosphate (MalK) and ATP (Rad50) pyrophosphate are shown in red. The alignments were generated by minimizing the root mean square deviation between the α-carbons of the Walker A lysine and Walker B aspartate (amino acids 45 and 178 in HisP).

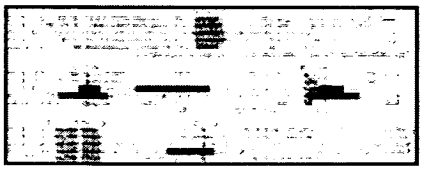

View larger version (42K):
[in this window]
[in a new window]

Fig. 8. Sequence alignment of MalK, HisP, NBD1, NBD2, and Rad50. Sequence alignments are taken from published comparisons of MalK and HisP (7); HisP, NBD1, and NBD2 (17); and Rad50, NBD1, and NBD2 (15). Two large segments of Rad50 that have no counterparts in NBDs from ABC transporters are indicated below the alignment in lower case letters. Secondary structure assignments for MalK, HisP, and Rad50 are indicated by the colored amino acids with red indicating β-sheet and aqua indicating α-helix. Walker A, B, and C motifs, as well as the Q-, D-, and H-loops, are

highlighted in yellow. Epitopes in NBD1 that bind to NBD2 are highlighted in blue. Epitopes in NBD2 that bind to NBD1 are highlighted in red. Epitopes in either NBD that bind R-domain are highlighted in green.

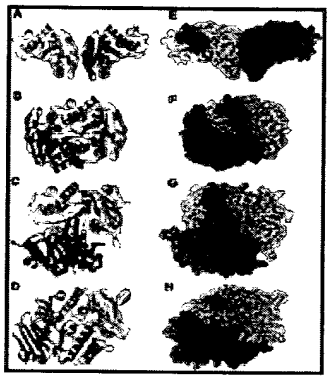

View larger version (80K): [in this window] [in a new window]

Fig. 9. Localization of peptides that bind to NBD1, NBD2, or R-domain in dimeric structures of HisP, MalK, and Rad50. Ribbon drawing for the dimeric crystal structures of HisP (17), MalK (7), and Rad50 (15) are shown in *A*, *C*, and *D*. *E*, *G*, and *H* show space-filling models of the same structures. *B* and *F* show the aHisP structure (19). In *A-H*, NBD1 (aqua) is shown in the same orientation. In *B-D*, the arrow indicates the orientation of the helix (*X*) in *A*, whose COOH-terminus is facing the viewer. In *A-D*, ATP (*A*, *B*, *D*), or pyrophosphate (*C*) is shown in yellow, epitopes in NBD1 that bind NBD2 are indicated in red, and epitopes in NBD2 that bind NBD1 are indicated in dark blue. In *E-H*, peptides in either NBD that bind to the R-domain are indicated in green.

These models can also be used to identify the location of peptides in NBD1 and NBD2 that bind to the R-domain. This is a more speculative analysis because the model proteins do not contain structures that are analogous to the R-domain. However, because CFTR is a member of the ABC transport superfamily, it is reasonable to propose that the basic alignment of NBDs and MSDs in CFTR is similar to that for other ABC transport superfamily members. If this is the case, then the R-domain should associate on the surface of the basic structure formed by the NBDs and MSDs. To test this hypothesis, we mapped epitopes in NBD1 and NBD2 that bind the R-domain onto the structures in Fig. 9, *E-H*. The HisP and MalK crystal structures (*E* and *G*) suggest that binding sites for the R-domain in NBD1 and NBD2 form two isolated patches. In contrast, the Rad50 and alternate HisP structures (*F* and *H*) suggest that R-domain binds to NBD1 and NBD2 along a long stripe. Although we do not regard this as conclusive evidence for any structure, we suggest that the data favor the Rad50 and alternate HisP structures. However, it is possible that peptides derived from regions of NBD1 and NBD2 that lie between the indicated binding sites may not be retained on our membranes.

DISCUSSION

Since the discovery of the gene for cystic fibrosis and the identification of transmembrane helices with hydropathy plots (35), there has been little success in efforts to further refine the structure of CFTR. At present, there is consensus on the domain boundaries (3).

▲ TOP
▲ ABSTRACT
▲ INTRODUCTION
▲ MATERIALS AND METHODS
▲ RESULTS

▪ DISCUSSION
▾ REFERENCES

Yeast two-hybrid studies suggest the presence of interactions between intracellular domains and intracellular loops in the transmembrane domains (22), and binding of the NH_2 and COOH termini to the intracellular domains has been proposed on the basis of functional studies (29, 32, 42). Whereas the NBDs of CFTR have been expressed and shown by various groups to bind or hydrolyze ATP (16, 23, 31) and the conformation of expressed R-domain has been shown to be altered by phosphorylation (8), there is presently no structural information for any of these domains. In a recent study, the CD spectrum of an R-domain construct (amino acids 708-831) that lacks the first 119 amino acids of our construct was analyzed and found to have little defined secondary structure (30). This construct was shown to restore kinase-dependent channel activity to a CFTR construct that lacked amino acids 708-831, but the presence of the NH_2-terminus region of the R-domain in the CFTR construct may induce bound R-domain to assume a native structure. A similar effect could occur in solution. If this were the case, results should be more consistent with earlier studies of an expressed R-domain construct from amino acids 595-831, in which considerably more secondary structure was observed and in which PKA-dependent phosphorylation caused an appreciable change in the CD spectrum (8). It has been suggested that expressed R-domain is largely unstructured in solution. Whereas an unstructured R-domain might bind to the NBDs and specific peptides, the binding data in Figs. 5 and 6 and the phosphorylation data in Fig. 3 would appear to be more consistent with an R-domain with a defined tertiary structure. We therefore suggest that the absence of amino acids from the NH_2 terminus of the R-domain peptide may in large part cause the reported absence of R-domain structure.

At present, the best structural information for CFTR comes from studies of other ABC transporters. Crystallographic structures have been reported for NBDs from two bacterial ABC transporters, the HisP subunit of the *S. typhimurium* histidine permease (17) and the MalK subunit of the *T. litoralis* maltose transporter (7). In addition, a crystal structure for Rad50 from *Pyroccus furiosus* has also been solved (15). The structures of two additional NBDs, MJ1267 and MJ0796, have recently been reported (21, 44). The monomeric structures are very similar to those of MalK and HisP, but they have not been considered in this analysis because the authors chose not to infer dimeric structures from their crystallographic data. In addition, the recent structure of the ABC transporter homolog MsbA was not considered because much of the NBD is unresolved in the crystal (4). Also, the authors' conclusion that the NBDs may not interact appears to be dependent on a series of interactions between extracellular loops in the transmembrane domains. Because these loops are considerably shorter in CFTR (see Fig. 6*A*), it is highly unlikely that CFTR could form a structure similar to that described from MsbA.

As described in RESULTS, these proteins show little sequence similarity but a great deal of structural homology. The regions with the most highly conserved sequences are those indicated in Fig. 8: the Walker A, B, and C regions and the Q-, D-, and H-loops. These regions have been linked to the binding or hydrolysis of ATP (7, 15, 17). With regard to domain-domain interactions between the NBDs, the crystallographic studies have generated vastly different dimeric structures. This is perhaps to be expected as the conditions for NBD crystallization are quite different from those found within the cell. One difference is that the MSDs are not present during crystallization, and, therefore, any effect that these domains have on interactions between the NBDs will not be reflected in the crystal structure. A

better model for the structure of the NBD dimer in CFTR may be the soluble Rad50 dimer, formed in the presence of ATP, in which alterations in structure due to the absence of MSDs should not occur. In general, there are two different models for NBD-NBD interaction. The HisP dimer places the ATP binding sites on opposite sides of the dimer (17), whereas the Rad50 and MalK structures place the ATP binding sites in a cleft formed by the NBD-NBD interface (7, 15). For both of these models, ATP binding sites are likely to be composed of residues from both NBDs. Whereas this issue may be resolved only with the crystal structure of a complete ABC transporter, cysteine mutagenesis of amino acids in the ATP binding sites of MDR allows disulfide cross-links to be generated between the NBDs (25). This result is consistent only with an interfacial model. An ATP binding site at the interface of an NBD-NBD dimer may also explain why it has been difficult to observe ATP hydrolysis by NBD constructs.

In this study, we expressed, purified, and refolded tagged NBD1, NBD2, NBD1-R, and R-domain. These expressed CFTR domains had properties that were consistent with a native-like structure. All NBD-containing proteins bound ATP. The affinities for ATP binding to his-NBD1 and his-NBD2 were similar to values reported previously. However, it is somewhat surprising that the affinity of NBD2 is greater than that of NBD1, because previous studies have suggested the opposite (23, 31). The only explanation we can offer is that, in the previous studies, NBD1 and NBD2 constructs from amino acids 433-589 and 1208-1399 were fused to the maltose binding protein, whereas our NBD1 and NBD2 constructs were His-tagged and spanned amino acids 373-589 and 1151-1476 (23, 31). Recent studies have indicated that NBD1 may extend as far as amino acid 640 (3). However, the observation that, when fused to the maltose-binding protein, an NBD1 construct that terminates at amino acid 589 can hydrolyze ATP (26) suggests that amino acids after 589 are not essential for the formation of a native-like structure. In vitro phosphorylation of NBD1-R by PKA occurred at the same sites as in situ phosphorylation of full-length CFTR. In addition, the sites of R-domain phosphorylation differed from those observed when immunoprecipitated CFTR was in vitro phosphorylated with PKA. Direct associations between the expressed domains were observed with overlay assays and by tryptophan fluorescence quenching. The dose dependence of tryptophan fluorescence quenching allowed binding to be quantified. However, since we have no data regarding homodimerization, caution must be used with regard to quantification of the association between NBD1-R and NBD2. Recently, it has been reported that dimers of NBDs are not formed in solution (21). This has been used as an argument in favor of the possibility that crystallographic NBD dimers may not reflect the structure within native ABC transporters. Although we are in agreement with this conclusion, our fluorescence quenching data indicate that NBDs can associate in solution. Perhaps the presence of the R-domain stabilizes the interaction, because an NBD1-R/NBD2 complex has been observed previously (26). We also suspect that conditions designed to precipitate NBDs may disfavor solution dimer formation, whereas ours, designed to maintain NBDs in solution, favored dimer formation. Differences in the size of the expressed domains may also affect domain-domain interactions. Lastly, we have shown that an association between NBD1-R and NBD2 alters the effects of ATP binding on tryptophan fluorescence.

The principle finding of our study is that specific epitopes in a peptide library spanning all cytoplasmic regions of CFTR bind to the expressed domains of CFTR. Epitopes from one domain that bind to another domain are likely to define sites of interaction between the two domains. Because the epitopes in one NBD that bind to the other NBD are at the interface in models that place the ATP binding sites at

the NBD-NBD interface, our data are most consistent with the crystal structures of MalK, Rad50, and the alternative structure for HisP. Our data are in agreement with crystallographic (7, 15) and cross-linking (25) studies of other ABC superfamily members. However, because there are complications with each approach, the confluence of data with three different techniques and with three different ABC superfamily members is comforting.

In the present study, care has been taken to exclude false positive results. Our ad hoc procedures for identifying false positives are described in RESULTS, but an additional test for specific binding made use of the fact that each six-amino acid sequence is expressed on three different peptides (see Fig. 6*A*). As a consequence, a series of sequential peptides that bound a domain was considered to be a stronger indication of a specific interaction than binding by a single peptide. However, since peptides may form structures that obscure the relevant epitope, strong binding by an isolated peptide cannot be ignored. Binding to sequential peptides also defines the site of interaction more precisely. In addition, the peptides that bound NBD1 and NBD2 were not the same. These observations strongly suggest that, in general, peptide binding to our expressed domains was specific.

In addition to interactions between NBD1 and NBD2, interactions between R-domain and both NBDs were observed. Previous functional studies of CFTR channel activity have suggested that the activities of the NBDs and R-domain are linked (18). In an NBD1-R-domain construct, R-domain phosphorylation inhibits nucleotide binding, and the presence of R-domain alters the kinetics of ATP hydrolysis by NBD1 (27, 43). Our results provide direct physical evidence for these interactions. The analysis of peptide binding to the R-domain in terms of NBD crystal structure is more speculative than that for NBD-NBD interaction because the model proteins do not have an R-domain. However, because we have based our analysis on the assumption that arrangement of NBDs and MSDs in ABC superfamily members are the same, regions of NBD1 and NBD2 that associate with R-domain should form a contiguous surface. Although none of the structures in Fig. 9 are entirely consistent with our assumption, the peptides that interact with the R-domain are most contiguous in the Rad50 and aHisP structures. The MalK and HisP crystals show binding of the R-domain at two distant locations. On the basis of these observations, we conclude that the Rad50 structure and the alternative aHisP (20) structures represent the most likely structures for the NBDs in CFTR.

ACKNOWLEDGEMENTS

The technical assistance of Mu-Young Kim is acknowledged.

FOOTNOTES

This work was supported by grants from the Cystic Fibrosis Foundation, Cystic Fibrosis Research, and the Nemours Foundation.

Address for reprint requests and other correspondence: W. W. Reenstra, Institute for Human Gene

Therapy, Univ. of Pennsylvania, Philadelphia, PA 19104 (E-mail: Reenstra@mail.med.upenn.edu).

The costs of publication of this article were defrayed in part by the payment of page charges. The article must therefore be hereby marked "*advertisement*" in accordance with 18 U.S.C. Section 1734 solely to indicate this fact.

First published January 2, 2002;10.1152/ajpcell.00337.2001

Received 20 July 2001; accepted in final form 27 November 2001.

REFERENCES

▲ TOP
▲ ABSTRACT
▲ INTRODUCTION
▲ MATERIALS AND METHODS
▲ RESULTS
▲ DISCUSSION
▪ REFERENCES

1. **Anderson, MP, Berger HA, Rich DR, Gregory RJ, Smith AE, and Welsh MJ.** Nucleoside triphosphates are required to open the CFTR chloride channel. *Cell* 67: 775-784, 1991[ISI][Medline].

2. **Boyle, WJ, van der Geer P, and Hunter T.** Phosphopeptide mapping and phosphoamino acid analysis by two-dimensional separation on thin-layer plates. *Methods Enzymol* 210: 110-148, 1991.

3. **Chan, KW, Csanady L, Seto-Young D, Nairn AC, and Gadsby DC.** Severed molecules functionally define the boundaries of the cystic fibrosis transmembrane conductance regulator's NH_2-terminal nucleotide binding domain. *J Gen Physiol* 116: 163-180, 2000[Abstract/Free Full Text].

4. **Chang, G, and Roth CB.** Structure of MsbA from *E. coli*: a homolog of the multidrug resistance ATP binding cassette (ABC) transporters. *Science* 293: 1793-1800, 2001[Abstract/Free Full Text].

5. **Cheng, SH, Rich DP, Marshall J, Gregory RJ, Welsh MJ, and Smith AE.** Phosphorylation of the R domain by cAMP-dependent protein kinase regulates the CFTR chloride channel. *Cell* 66: 1027-1036, 1991[ISI][Medline].

6. **Chen, JH, Chang XB, Aleksandrov AA, Hammerk MM, Shanmugam K, and Riordan JR.** Biochemical and electrophysiological evaluation of CFTR quaternary structure (Abstract). *Pediatr Pulmonol Suppl* 20: 174, 2000.

7. **Diederichs, K, Diez J, Greller G, Muller C, Breed J, Schnell C, Vonrhein C, Boos W, and Welte W.** Crystal structure of MalK, the ATPase subunit of the trehalose/maltose ABC transporter of the archaeon *Thermococcus litoralis*. *EMBO J* 19: 5951-5961, 2000[Abstract/Free Full Text].

8. **Dulhanty, AM, and Riordan JR.** Phosphorylation by cAMP-dependent protein kinase causes a conformational change in the R-domain of the cystic fibrosis conductance transmembrane regulator. *Biochemistry* 33: 4072-4079, 1994[ISI][Medline].

9. **Eskandari, S, Wright EM, Kreman M, Starace DM, and Zampighi GA.** Structural analysis of cloned plasma membrane proteins by freeze-fracture electron microscopy. *Proc Natl Sci USA* 95: 11235-11240, 1998[Abstract/Free Full Text].

10. **Frangioni, JV, and Neel BG.** Solubilization and purification of enzymatically active glutathione *S*-transferase (pGEX) fusion proteins. *Anal Biochem* 210: 179-187, 1993[ISI][Medline].

11. **Gadsby, DC, and Nairn AC.** Control of CFTR channel gating by phosphorylation and nucleotide hydrolysis. *Physiol Rev* 79: S77-S107, 1999[Medline].

12. **Hall, RA, Ostedgaard LS, Premont RT, Blitzer JT, Rahman N, Welch MJ, and Lefkowitz RJ.** A C-terminal motif found in the beta2-adrenergic receptor, P2Y1 receptor, and cystic fibrosis transmembrane conductance regulator determines binding to the Na+/H+ exchanger regulatory factor family of PDZ proteins. *Proc Natl Acad Sci USA* 95: 8496-8501, 1998[Abstract/Free Full Text].

13. **Hallows, KR, Raghuram V, Kemp BE, Witters LA, and Foskett JK.** Inhibition of cystic fibrosis transmembrane conductance regulator by novel interaction with the metabolic sensor AMP-activated protein kinase. *J Clin Invest* 105: 1711-1721, 2000[Abstract/Free Full Text].

14. **Higgins, CF.** ABC transporters: from microorganisms to man. *Annu Rev Cell Biol* 8: 67-113, 1992 [ISI].

15. **Hopfner, KP, Karcher A, Shin DS, Craig L, Arthur LM, Carney JP, and Tainer JA.** Structural biology of Rad50 ATPase: ATP-driven conformational control in DNA double-strand break repair and the ABC-ATPase superfamily. *Cell* 101: 789-800, 2000[ISI][Medline].

16. **Howell, LD, Borchardt R, and Cohn JA.** ATP hydrolysis by a CFTR domain: pharmacology and effects of G551D mutation. *Biochem Biophys Res Commun* 271: 518-525, 2000[ISI][Medline].

17. **Huang, LW, Wang IX, Nikaido K, Liu PQ, Ames GFL, and Kim SH.** Crystal structure of the ATP-binding subunit of an ABC transporter. *Nature* 396: 703-707, 1998[ISI][Medline].

18. **Hwang, TC, Wang F, Yang CH, and Reenstra WW.** Potentiation of ΔF508 channel function by genistein binding to CFTR. *Am J Physiol Cell Physiol* 273: C988-C998, 1997[Abstract/Free Full Text].

19. **Jones, PM, and George AM.** Subunit interactions in ABC transporters: towards a functional architecture. *FEMS Microbiol Lett* 179: 187-200, 1999[ISI][Medline].

20. **Joseph, G, and Pick E.** "Peptide walking" is a novel method for mapping functional domains in proteins. Its application to the Rac1-dependent activation of NADPH oxidase. *J Biol Chem* 270: 29079-29082, 1995[Abstract/Free Full Text].

21. **Karpowich, N, Martsinkevich O, L, Millen Yuan YR, Dei PL, MacVey K, Thomas P, and Hunt JF.** Crystal structures of the MJ1267 ATP-binding cassette reveal an induced-fit effect at the ATPase active site of an ABC transporter. *Structure* 9: 571-586, 2001[ISI][Medline].

22. **Kiser, GL, Chang XB, and Riordan JR.** Two-hybrid analysis of CFTR domain interactions (Abstract). *Pediatr Pulmonol Suppl* 13: 213, 1996.

23. **Ko, YH, and Pedersen PL.** The first nucleotide binding fold of the cystic fibrosis transmembrane conductance regulator can function as an active ATPase. *J Biol Chem* 270: 22093-22096, 1995 [Abstract/Free Full Text].

24. **Kyte, J, and Doolittle RF.** A simple method for displaying the hydropathic character of a protein. *J Mol Biol* 157: 105-132, 1982[ISI][Medline].

25. **Loo, TW, and Clarke DM.** Covalent modification of human P-glycoprotein mutants containing a single cysteine in either nucleotide-binding fold abolishes drug-stimulated ATPase activity. *J Biol Chem* 270: 22957-22961, 1995[Abstract/Free Full Text].

26. **Lu, NT, and Pedersen PL.** Cystic fibrosis transmembrane conductance regulator: the purified NBF1+R protein interacts with the purified NBF2 domain to form a stable NBF+R/NBF2 complex while inducing a conformational change transmitted to the C-terminal region. *Arch Biochem Biophys* 375: 7-20, 2000[ISI][Medline].

27. **Ma, J, Zhao J, Drumm ML, Xie J, and Davis PB.** Function of the R-domain in the cystic fibrosis transmembrane conductance regulator chloride channel. *J Biol Chem* 272: 28133-28141, 1997 [Abstract/Free Full Text].

28. **Marshall, J, Fang S, Ostedgaard LS, O'Riordan CR, Ferrara D, Amara JF, Hoppe H, Scheule RK, Welsh MJ, and Smith AE.** Stoichiometry of recombinant cystic fibrosis transmembrane conductance regulator in epithelial cells and its functional reconstitution into cells in vitro *J. Biol Chem* 269: 2987-2995, 1994[Abstract/Free Full Text].

29. **Naren, AP, Quick MW, Collawn JF, Nelson DJ, and Kirk KL.** Syntaxin 1A inhibits CFTR chloride channels by means of domain-specific protein-protein interactions. *Proc Natl Acad Sci USA* 95: 10972-10977, 1998[Abstract/Free Full Text].

30. **Ostedgaard, LS, Baldursson O, Vermeer DW, Welsh MJ, and Robertson AD.** A functional R-domain from cystic fibrosis transmembrane conductance regulator is predominantly unstructured in solution. *Proc Natl Acad Sci USA* 97: 5657-5662, 2000[Abstract/Free Full Text].

31. **Randak, C, Neth P, Auerswald EA, Eckerskorn C, Assfalg-Machleidt I, and Machleidt W.** A recombinant polypeptide model of the second nucleotide-binding fold of the cystic fibrosis transmembrane conductance regulator functions as an active ATPase, GTPase, and adenylate kinase. *FEBS Lett* 410: 180-186, 1997[ISI][Medline].

32. **Raghuram, V, Mak DD, and Foskett JK.** Regulation of cystic fibrosis transmembrane conductance regulator single-channel gating by bivalent PDZ-domain-mediated interaction. *Proc Natl Acad Sci USA* 98: 1300-1305, 2001[Abstract/Free Full Text].

33. **Reenstra, WW, Yurko-Mauro K, Dam A, Raman S, and Shorten S.** CFTR chloride channel activation by genistein: the role of serine/threonine protein phosphatases. *Am J Physiol Cell Physiol* 271: C650-C657, 1996[Abstract/Free Full Text].

34. **Rich, DP, Berger HA, Cheng SH, Travis SM, Saxena M, Smith AE, and Welsh MJ.** Regulation of the cystic fibrosis transmembrane conductance regulator Cl^- channel by negative charge in the R-domain. *J Biol Chem* 268: 20259-20267, 1993[Abstract/Free Full Text].

35. **Riordan, JR, Rommens JM, Kerem B, Alon N, Rozmahel R, Grzelczak Z, Zielenski J, Lok S, Plavsic N, Chou JL, Drumm ML, Iannuzzi MC, Collins FS, and Tsui LC.** Identification of the cystic fibrosis gene: cloning and characterization of complementary DNA. *Science* 245: 1066-1073, 1989[ISI] [Medline].

36. **Seibert, FS, Chang XB, Aleksandrov AA, Clarke DM, Hanrahan JW, and Riordan JR.** Influence of phosphorylation by protein kinase A on CFTR at the cell surface and endoplasmic

reticulum. *Biochem Biophys Acta* 1461: 275-283, 1999[ISI][Medline].

37. **Sheppard, D, and Welsh MJ.** Structure and function of the CFTR chloride channel. *Physiol Rev* 79: S23-S45, 1999[Medline].

38. **Shindyalov, IN, and Bourne PE.** Protein structure alignment by incremental combinatorial extension (CE) of the optimal path. *Protein Eng* 11: 739-747, 1998[Abstract].

39. **Short, DB, Trotter KW, Reczek D, Kreda SM, Bretscher A, Boucher RC, Stutts MJ, and Milgram SL.** An apical PDZ protein anchors the cystic fibrosis transmembrane conductance regulator to the cytoskeleton. *J Biol Chem* 273: 19797-19801, 1998[Abstract/Free Full Text].

40. **Smith, PK, Krohn RI, Hermanson GT, Mallia AK, Gartner FH, Provenzano MD, Fujimoto EK, Goeke NM, Olson BJ, and Klenk DC, DC** Measurement of protein using bicinchoninic acid. *Anal Biochem* 150: 76-85, 1985[ISI][Medline].

41. **Valerio, RM, Benstead M, Bray AM, Campbell RA, and Maeji NJ.** Synthesis of peptide analogs using the multipin peptide synthesis method. *Anal Biochem* 197: 168-177, 1991[ISI][Medline].

42. **Wang, S, Yue H, Derin RB, Guggino WB, and Li M.** Accessory protein facilitated CFTR-CFTR interaction, a molecular mechanism to potentiate the chloride channel activity. *Cell* 103: 169-179, 2000 [ISI][Medline].

43. **Winter, MC, and Welsh MJ.** Stimulation of CFTR activity by its phosphorylated R-domain. *Nature* 389: 294-296, 1997[ISI][Medline].

44. **Yuan, YR, Blecker S, Martsinkevich O, Millen L, Thomas PL, and Hunt JF.** The crystal structure of the MJ0796 ATP-binding cassette: implications for the structural consequences of ATP hydrolysis in the active site of an ABC-transporter. *J Biol Chem* 276: 32313-32321, 2001 [Abstract/Free Full Text].

45. **Yurko-Mauro, KA, and Reenstra WW.** Prostaglandin F_2alpha stimulates CFTR activity by PKA and PKC-dependent phosphorylation. *Am J Physiol Cell Physiol* 275: C653-C660, 1998[Abstract].

46. **Zeltwanger, S, Wang F, Wang GT, Gillis KD, and Hwang TC.** Gating of cystic fibrosis transmembrane conductance regulator chloride channels by adenosine triphosphate hydrolysis. Quantitative analysis of a cyclic gating scheme. *J Gen Physiol* 113: 541-554, 1999 [Abstract/Free Full Text].

47. **Zerhusen, B, Zhao J, Xie J, Davis PB, and Ma J.** A single conductance pore for chloride ions formed by two cystic fibrosis transmembrane conductance regulator molecules. *J Biol Chem* 274: 7627-7630, 1999[Abstract/Free Full Text].

Am J Physiol Cell Physiol 282(5):C1170-C1180
0363-6143/02 $5.00

C. H. Gross, N. Abdul-Manan, J. Fulghum, J. Lippke, X. Liu, P. Prabhakar, D. Brennan, M. S. Willis, C. Faerman, P. Connelly, S. Raybuck, and J. Moore

Nucleotide-binding Domains of Cystic Fibrosis Transmembrane Conductance Regulator, an ABC Transporter, Catalyze Adenylate Kinase Activity but Not ATP Hydrolysis

J. Biol. Chem., February 17, 2006; 281(7): 4058 - 4068.